Solar Agribots

Project Professors:

Mehul Bhatia, Department of Mechanical Engineering

Nicholas Bertozzi, Department of Robotics Engineering

Kaveh Pahlavan, Department of Electrical & Computer Engineering

Submitted By:

John Benoit, ME

Raymond Carter, RBE

Nicholas Hudgins, RBE

Stephen Kendrish, RBE & ME

Nathan Maldonado, ME

Samuel Ng, ECE

John Pattinson, ME

Calvin Thomas, ME

Calvin Zhang, ME

Date:

28th of April 2022

Table of Contents

List of Figures

List of Tables

Abstract

As populations rise and the agriculture industry takes on more demand for increased crop yields, farmers find themselves strained. The insertion of robotics and autonomous technology into farming is a solution that supplements the work and exertion of the farmers. The purpose of this project is to combine maneuverable drivetrain technology, base station capability, water deployment hardware, and autonomy into an individual robot designed to navigate and irrigate crop fields while being independent and reliable on solar power.

Introduction

In the modern age, population growth and increasingly scarce labor forces in the agriculture industry pose an issue for large scale farms and crop holders who find themselves being stretched thin in both directions. This lack of solutions will inevitably result in failures and farm turnovers. A growing industry with less and less people to tend it is a waning model that could lead to an inevitable food scarcity. Without adequate and efficient solutions soon, shortages are bound to occur. In order to curb this decay in production, a few things need to happen; either labor must be found to accommodate the growing needs or a scalable system for crops without increase in labor is utilized. However, rethinking and revolutionizing the current agriculture landscape requires an increase in technology implementation (Jin, 2021).

Recent data gathered by the United States Department of Agriculture (USDA) showed that the number of farmers has steadily decreased from 6.8 million farmers in the 1970s to just over 2 million in 2020. Due to this shortage and increasing demand for produce, a gap in the labor force was created. To fill this gap, industrial agriculture has invested in higher-technology production practices such as advanced heavy machinery and vertically-integrated agricultural firms that have increased efficiency while also filling the labor shortage. While this has benefited large-scale farms that have the capital to invest in these expenditures, local farmers are unable to compete due to constraints on justifying these large expenses. These small farms (i.e., those grossing under $250,000) represent 91 percent of farms in the United States (Hoppe et al., 2010). Those small farms are exactly the target audience for this Major Qualifying Project (MQP), with the objective of designing and building a rover to help fill the labor gap for smaller farm operations at an affordable price.

The goal of this project is to provide a solution to the lack of autonomous robotics applications in the agriculture industry in order to increase efficiency of growing and harvesting crops. Solving this problem greatly benefits the stakeholders at play, who may be burdened by heavy labor loads and minimal access to large pools of laborers. These issues will be addressed in a sustainable manner through the use of renewable resources in an effort to reduce agriculture's contribution towards pollution and climate change.

This project aims to brainstorm, design, and prototype methods to replace the tedious and repetitive labor required to work crop fields. The solutions to this issue are in the form of a swarm proof of concept. In swarm robotics, multiple robots collectively solve complex issues by forming advantageous structures and behaviors. This is similar to the ones observed in nature, such as swarms of bees, birds, or fish. Swarm bots usually have a hive and worker structure in which individual robots leave a central location or hub and perform their required tasks. From there they will then return to their home base to refuel, resupply, repair, etc. The process is then repeated until the overarching goal is completed. In this case, swarm robotics would be used to maintain crops and take various metrics using real-time environmental analysis.

Description of Work

Objectives

This project has 5 goals that together create a proof of concept agricultural swarm rover for commercial farm use. The five goals are:

1. To develop a rover capable of high weight carrying capacity.
2. To have field irrigation capabilities onboard the rover to deliver fluid efficiently over a large space.
3. To equip the rover with sensors and controllers to allow for autonomous navigation through a crop field.
4. To utilize a sensor array on the rover and the base station to conduct soil testing, atmospheric conditions monitoring, and rover-hub communication.
5. To refuel and recharge the rover at a central base station.

To accomplish these goals, the system will consist of two main components. The first component of the system is the rover, which will spray fluid and use a robotic arm to test for water hydration, pH levels, nutrient content, and ground temperature. The second component of the system is the hub station, which serves as a base station for the rover. In the event of low charge or low resources, the vehicle will return to the hub where it will resupply and recharge. The hub comes equipped with a solar array and battery station for charging. These components make the system more sustainable and independent of a preexisting grid which is not as green conscious. The hub also has a roof-mounted tank for refilling the rover, which is the primary source of the vehicles' supply. Positioned in the middle of the farm, the hub allows for minimum distance of travel for the rover. The central location was determined as the best compromise for saving energy and time when the swarm is performing its tasks.

Background

Prior MQPs

Many previous MQPs at Worcester Polytechnic Institute provide valuable methods and considerations for applications such as those stated in the requirements of application. In the MQP "Modular Environmental Controller for Sustainable Agriculture," the team designed and built a control system involving a network of sensors for CO_2 concentration, relative humidity, temperature, pH, and conductivity. Applications of such systems involve controlling actuators and pumps in greenhouses and concisely communicating the status of the environment. The project was motivated as a means of managing and conserving resources. This was done by reducing the pesticides, herbicides, and water used to save energy by applying them only where needed. If scaled appropriately, systems like this could reduce overall CO_2 emissions from the agricultural industry and minimize byproducts of excess fertilizer and pesticide use that may have detrimental effects on nearby environments. (Bitar and Padir, 2013) The full system makes use of a CAN (controller area network) that utilizes serial communications. PID (proportional integral derivative) loops are the main control mechanism for the output nodes of the system. Additionally, to support a diverse array of sensors with varying voltage inputs, a Buck converter, LM2671, was used for its high efficiency and low cost. The team designed a custom PCB to handle connections between the electronics reducing the size of the system. Although pH and EC sensors were not included in the final design, the finalized product cost only $400 in parts indicating that full feature greenhouse controllers available on the market for ~$3000 are overpriced. Much of the work done in the above MQP is applicable in the requirement of sensors which help in evaluating the surrounding environment for agriculture health.

Working with a subsidiary of iRobot, the "Lionfish 2.0" MQP improved upon the pre-existing lionfish capturing robot that serves to limit the invasive species in the Indo-Pacific region. (Antaya et al, 2019) Much of this project involved creating a unique intake system for a submersible robot and generating a detection model for finding lionfish through video. The relevance of this project to Solar Agribots relates to the potential for the rover to be able to detect certain plant life or the condition of plant life for the purposes of watering, pruning, fertilizing, and herbicide/pesticide. Other considerations from this project in regards to the Solar Agribots is how the lionfish team weatherproofed their robot for aquatic conditions. The Solar Agribot does not need the same level of water protection, however some of this methodology can be used for making the agribot rover resistant to dirt, rain, wind, etc.

The "Agricultural SWARM Robotic System" MQP looked to help farmers collect data on their field and make informed decisions based on this data. This data is collected by using a rover to autonomously place nodes around the field to collect data that the farmer would like to record in certain places. Different sensors could be installed in the nodes based on what the farmer would like to know about their farm. The rover could then autonomously place and retrieve these nodes in locations designated by the user (Stegman and Shen, 2018). Some of the practices used in this MQP can be used to help the team make decisions for autonomous missions in crop fields.

The "Car-Snow Clearing Drone MQP" aimed to remove excess snow in freezing-cold conditions from vehicles using a spraying system for de-icing liquid mounted to a drone. Their spraying system could be utilized in an agricultural application towards the deployment of pesticides, herbicides, fertilizer (liquid, powder & granular), and water, seen in Figure 1 and Figure 2.

Figure 1: Snow-Clearing MQP Drone

Figure 2: Snow-Clearing MQP Spraying System

Commercial Agricultural Robots

The team looked at previous designs and models of agricultural robots to garner ideas and identify gaps in their designs that could in turn be implemented in this project. The first robot that was looked at was the Rantizo DJI Agras MG-1P Drone, which features an eight rotor design, a 10L tank paired to a single-phase flow spraying system, and a first-person view (FPV) camera to allow manual control and autonomous capabilities (GPS mapping, collision avoidance, and terrain mapping). They offer a complete system designed specifically for commercial drone spraying. Their starter package begins at $47,000 and includes an RTK drone with base station and tripod, Rantizo Upgrade Kit, dry spreader, battery charger, batteries, Mix & Fill Station and support and training.

Rantizo Elevation Precision A.G. is a U.S.-based company that offers a complete drone system with a combination of autonomous hardware and software for commercial agricultural solutions. Its DJI Agras MG-1P Drone in Figure 3 is built specifically for agriculture spraying and its technical specifications include an eight rotor design with a 10 liter tank, first-person view (FPV) camera, GPS tracking, autonomous terrain follow, collision avoidance and mission mapping ("Rantizo System Products," 2021).

Figure 3: Rantizo DJI Agras MG-1P Drone

The spraying system in their drone influenced the rovers' design, since it features carbon fiber booms with multiple nozzles that are able to spray both wet and dry fluids (such as water, pellet fertilizer, natural wet fertilizer, pesticide and herbicide).

The Fendt Xaver agricultural robot was also examined for this project. Fendt is a tractor manufacturer that has committed themselves to creating autonomous and smart agricultural solutions. One of these solutions was their concept Xaver system (Figure 4), which consists of a series of small robots linked with cloud based systems to collectively monitor and document the process of corn production.

Figure 4: Fendt Xaver Robot

The Xaver robot prototype is a relatively small four wheel robot with the ability to carry out a variety of different functions. The robot is currently being designed to document the exact location of each seed and seed patterns in their Xaver app (Fendt, n.d). The hope is for this robot to analyze and execute more operations as further developments are implemented. Some of these operations could potentially include seed planting, watering and harvesting. This system is still currently being designed and tested, but the future of these large scale agriculture robots are very promising.

Constraints

Farming Logistics

Crops are the main focus and subject for this autonomous vehicle. Crops require frequent and tedious maintenance in farming. They are to be watered and treated with fertilizers or herbicide/pesticide when deemed necessary. This ensures that the yield and health of the crops are acceptable for production and quality. The crops of interest in this project are plants that have a relatively low profile, meaning the stalks and leaves do not extend more than about one to two feet off the ground. This ensures that a small vehicle can pass over the selected plant and deliver the desired resource without interference. The design for the rover relies entirely on this fact. In light of this, the crop layout that best benefits the rover's responsibilities is a plot of land in which the crops are all young and recently planted or small in general, such as carrots, beets, and broccoli. Carrots are used as the ideal plant for this rover's future calculations and design choices because they have a low profile and can be driven over relatively easily. The spacing of the crop rows is an important metric as well. In order for the rover to best perform its duties, the crops are spaced in a manner that corresponds to the width of the rover and its transmission system. One of the considerations for the rover is that it does not damage surrounding crops by driving over them. A plot of crops that is around 1,000 square feet will be the area for testing throughout this project. This was decided as the sample to ensure simplicity and ease. Larger scale farms that utilize land in the magnitude of square miles, are far too large for the logistics of just one rover unless the "swarm" of rovers can be a value that accounts for one rover per a few thousand square feet. Exact values for rover coverage range depending on terrain and rover loads.

Autonomous Considerations

Autonomy is an essential aspect of self-sustaining systems such as the one explored in this project. Although much of the complex software required for this is beyond the scope of the project, the design of the rover intends to incorporate sensors, microcontrollers, and a robust control system for the mechanisms that are compatible with future implementations of smart behavior. Autonomous behavior is characterized by the relationship between the robot's perception of itself and surroundings, ability to make decisions, and interact with its surroundings through actuation. For the agribot, this can be split into a few tasks such as planting, fertilizing, watering, and taking soil data. At a high level, a sufficient autonomous system should dictate the behavior of the rover at all times answering questions such as "When should the rover leave the hub?", "What type of main task should it be completing?", "Where should it be completing them?", as well as sub-tasks such as "Which plants should the rover prioritize interaction with?" and "How will the rover navigate to the target location?". Many of these tasks are prevalent in technologies that are well studied and as such, multiple technical approaches and solutions for them can be analyzed. Systems and applications relevant include small-scale robotic lawn mowers and snow blowers, large-scale autonomous farm equipment, and self-sustaining greenhouses that make use of smart farming.

A challenge that commercially available home robots face involves building a model of the zones off limits to the robot and ensuring that they do not navigate into them. Additionally, an internal model of the space can increase effectiveness and pathfinding with a limited battery capacity. While determining a robot's position in space, the process of localization can be solved through GPS and odometry, understanding its position relative to hazards and objects in the environment is an additional complexity that must be tackled. There are two main ways to achieve this behavior through either building a map prior to the robot working or through building a map on the fly. While pre-determining the map simplifies the development of software and minimizes the number and sophistication of the sensors, it makes the robot vulnerable to unpredictable behavior if the environment is changed. The Husqvarna Automower, a commercially available autonomous lawnmower, runs the risk of accidentally mowing flowerbeds or getting stuck on out-of-yard terrain and uses a low voltage perimeter wire embedded in the ground to detect boundaries and determine position using GPS. (Lemcke, 2021) On the contrary Kobi, an all-season garden robot evaluates pathways using machine vision and does not rely on absolute location to plan paths. Similarly, iRobot's Roomba uses SLAM (Simultaneous Localization and Mapping) to know its position in a house by targeting unique landmarks in a room and calculating its orientation relative to them (Karsai, 2020). Lastly, an MQP "Autonomous Snowblower" allows the user to outline the workspace visually with a GUI relying on satellite imagery. Lidar and Gmapping are used for obstacle avoidance while the main boundaries are determined by an array of latitude and longitude values. All of these designs offer unique solutions for localization, mapping, and pathing that should be considered as case studies to inform the development of the Agribot.

Methodology

Rover Design

The rover and its structural components were designed using various engineering methods such as stress analysis, statics engineering, and kinematics. These methods help to provide optimal performance. In designing the rover, considerations for size, shape, and clearance were assessed in order to determine material selection and on board capacities. The mechanical aspect of the rover was manufactured by the team after long periods of research and consideration. First, the rover design was started with the basic requirements and estimations of the space for these requirements. From here, a loose geometry of the rover was used to determine the remaining designs of the chassis and drivetrain. This geometry was laid out in the SolidWorks models touched upon in the Statement of Work. Small changes were made to certain design elements such as dimensions of the length and width as well as the overall clearance that the rover would have with the given parts acquired.

The team came to the conclusion that the rover will be approximately three feet wide by three feet long by two feet tall. This was determined through the analysis of crop rows and the average width of a carrot crop layout. Typically, carrot rows are two feet apart and having a rover that is three feet wide is perfect considering the rover will travel over the row itself (Seed Saver 2022). One side of the rover will protrude a foot and a half from the center of a row which means the rover will not touch the adjacent row when operating. The square design allows for maximized balance and rigidity when taking on uneven or rough terrain. On top of this design parameter, the team chose to make the rover have just over a foot of ground clearance to once again make the rover have adequate stability while being able to clear obstacles. Having the rover with these dimensions makes it very stable and the critical tipping angles were calculated given the potential center of mass locations that cover the most likely scenarios given assumed weight distribution of the frame and its accessories. Much of the rover's weight is located within the upper foot of the frame and the transmission hardware is located in the legs of the rover. It is very unlikely that the center of mass of the rover would be below the M_{min} and above the M_{max} seen as the orange circles in Figure 5 below. The range of tipping angles is between 26.56 degrees (worst case scenario) and 36.87 degrees. These are similar to that of the critical angles for commercial trucks and automotive vehicles (27-32 degrees) (Hutterer, 2020). Figure 5 shows a front view with the estimated tipping angles and body diagram for the rover. Since the rover is not going to be moving very fast, this range of tipping angles is even more acceptable.

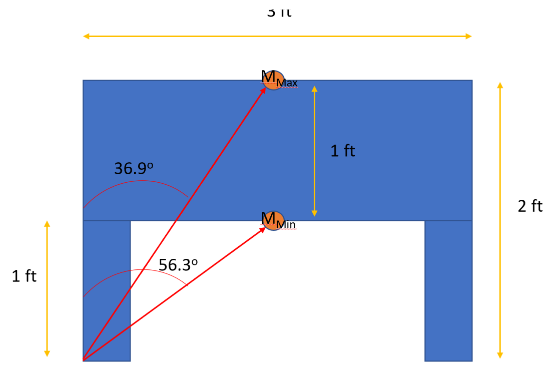

Figure 5: Rover Tipping Angle Estimation (given dimensions and estimated weight distributions)

The static structure of the chassis itself is a network of square beams that acts as the skeleton of the rover. This frame saves money through weight reduction, as having a solid body would be more expensive. The rover chassis frame was welded together, which is strong enough to withstand forces and moments on the frame within the magnitude of a few hundred pounds. This is ideal for the rover as it moves itself and the cargo it carries (such as water, electronics, housings, etc.). After coming up with a general design for the rover chassis, a hypothetical weight of the rover and its load could be assumed. The team determined that the metal chassis weighs around 50 pounds, and the remaining hardware weighed around 60 pounds, and the weight of the water load is around 50 pounds. In total, the rover has a hypothetical weight of 160 pounds. The team used a value of 200 pounds to plan the motor selection and further physics to create enough tolerance in calculations. Knowing this weight of the rover, the team started procuring other parts such as motors and other parts for the transmission. Besides the metal framed chassis, the rover includes the housing, which is a wooden cover on the top of the rover. This part was chosen as a simple and easy way to accommodate for debris interference and keep the electronics safe from weather. The exploded CAD model in Figure 6 shows the mechanical aspects of the rover, these do not include the electronic components or the sprockets and chains. Figure 7 shows another CAD view without the lid to what is underneath. The lid that was fabricated as the substitute for the white cover seen can be seen in Figure 8. Additional CAD models can be found in Appendix G as drawings as well as in the attached materials.

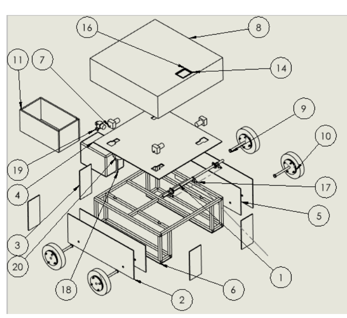

ITEM NO.	PART NUMBER	DESCRIPTION	QTY.
1	frame		1
2	acrylic siding		2
3	acrylic siding		4
4	acrylic siding		1
5	acrylic siding		2
6	acrylic siding		2
7	motor		4
8	Rover Top		1
9	washer		4
10	wheel and axel		4
11	Enclosure		1
12	gear & pinion mechanism		1
13	hatch assembly		1
14	rail		2
15	rack key		1
16	rail		2
17	spraybar assembly		1
18	Tank		1
19	Pump		1
20	tank elbow		1

Figure 6: Exploded View of Rover Assembly (including the chassis, motors, cover, and internal housing/tanks)

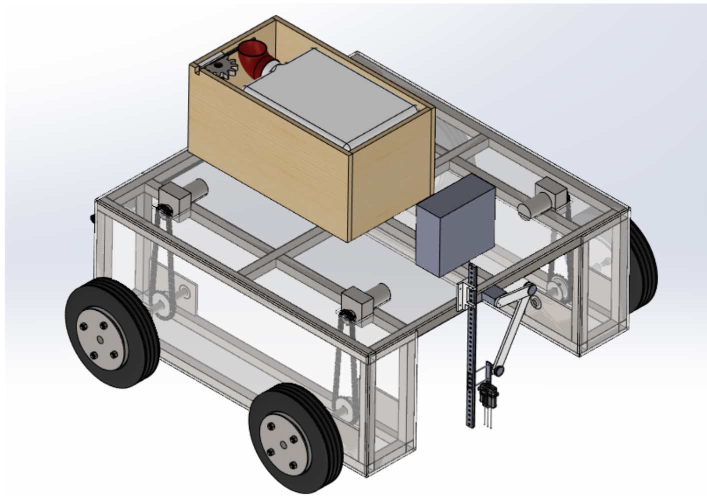

Figure 7: Lidless CAD model to see under the hood

Figure 8: Rover Lid

Chassis

The design process for the platform base section of the rover ensured that the space provided can accommodate room for the water/fertilizer tank, electronics housing, battery, and motors. This platform base does not need as much stiffness or bending strength as it is supported by other metal structures. The platform base's main purpose is to keep debris out of the undercarriage in the same manner as the plastic cover.

For the chassis of the rover, the team chose to use one inch by one inch square steel tubing. There were multiple considerations taken into account when choosing the steel. The material for the chassis had to be relatively lightweight, strong, and capable of being welding together easily. The team's first thought was to utilize aluminum as this material is both strong and lightweight. However, the team quickly realized that aluminum would not work as it is not an easy metal to weld given the equipment available at hand and is more malleable. Aluminum was also too expensive for the amount that was needed. The next option the team looked into was steel, which was chosen as it fit all three parameters and could be purchased for a relatively low price in large quantities. Figure 9 below shows the welded chassis of the rover.

Figure 9: Welded Steel Chassis

The next material that the team had to identify was the outer shell that wraps around the rovers legs and serves as the exterior layer. This material would have to be very light, strong, cheap, and easy to work with. Similar to the shell the first material looked at was aluminum. Aluminum fit the bill in terms of being lightweight and strong, however the team quickly realized that aluminum was not the material to go with. Using a sheet of aluminum would not only be far over the budget expectations, but it would also weigh far more than anticipated. The team then looked into utilizing plastic as the primary material for the exterior of the rover. Acrylic was chosen as the ideal material for the rover exterior, as it is far lighter than aluminum and easy to work with. Additionally, acrylic is see-through allowing for visibility of the interior components to ensure proper functionality and improve problem diagnosis. To allow for acrylic to be utilized, the frame was extended downwards such that the shape of the legs was formed by the steel tubing. This allows for acrylic to simply be used to cover the sides while maintaining the strength and rigidity necessary in the design.

Additionally, all 3D printed parts will be made of PLA plastic, as it is inexpensive while still providing the necessary structural rigidity. Additionally, PLA is a readily available material, meaning that there will not be any issues in the manufacturing of the components. The parts made of PLA include the actuated arm, axle shaft supports, and the supports holding the cover. Other 3D printing material was considered, including carbon reinforced plastic, however they were all deemed to be unnecessary as the parts that were printed are not being subjected to large loads.

The chassis was simulated in SolidWorks using the static analysis tool, as seen in Figures 10A and 10B. The simulation was conducted with the chassis as well as the axels to simulate the load being transferred through the wheels to the ground. The simulation was run with a load three times that of the maximum expected load giving the chassis a safety factor of two. This safety factor is acceptable at the current time however additional simulations will continue to be run to ensure that additional loading can be handled up to a safety factor of three, a standard that will allow for most unforeseen loads to be managed. A safety factor of three is common and ideal for many larger vehicles such as cars, so for a small rover this is above expectations (Burr and Cheatham 1995). The loading was applied as a vertical distributed load on the center beams of the chassis as the battery and water system sit on this beam. Additionally, the gravitational force acting on the chassis itself was taken into account in the simulation. The ends of the axles were modeled as fixed as in a static setting these points will be supported by the wheels and would stay still even if other parts of the chassis began to deform.

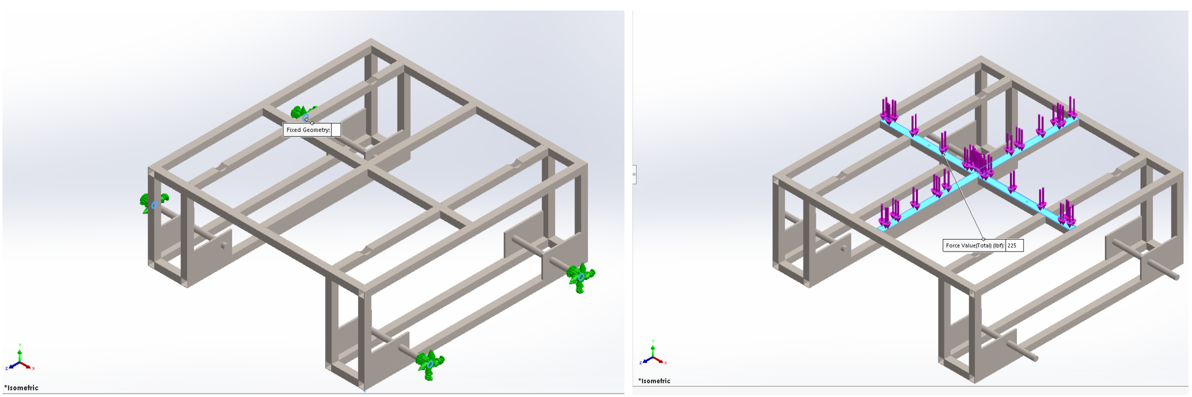

Figures 10 and 10A: Setup of static simulation with fixed surfaces and applied loads shown

While creating the simulations several issues did arise, including the extreme complexity of the wheel system which was not able to correctly form a mesh and as such did not allow for the simulation to be correctly run. This is the reason that the wheels were ultimately omitted from the simulation as they made it such that the needed details could not be evaluated. Other issues included ensuring the welds created in the simulation would accurately represent the welds on the model as SolidWorks assumes that all welds made are machine welds and as such are more precise and consistent than the welds that were able to be performed on the prototype. As such, the welds had to be created in a way that best represented the actual welds in the system, to do this, different levels of welds were used on various systems to best represent the welds that were expected on the final prototype.

Once the solid model mesh had been created, the simulation was run. The simulation showed the expected levels of stress, strain, and deformation for the structure. There were increased deformation in the areas closest to the center of applied force however all values were within the acceptable ranges for our materials. The max deformation seen was a millimeter and due to the size of the chassis this level of deformation was deemed acceptable and largely negligible. This deformation can be seen in Figure 11. Additionally, an area of concern before running the simulation was bending in the axels however due to the three points of support as well as how much the loading had dissipated throughout the structure. As such all deformation within the chassis system is acceptable.

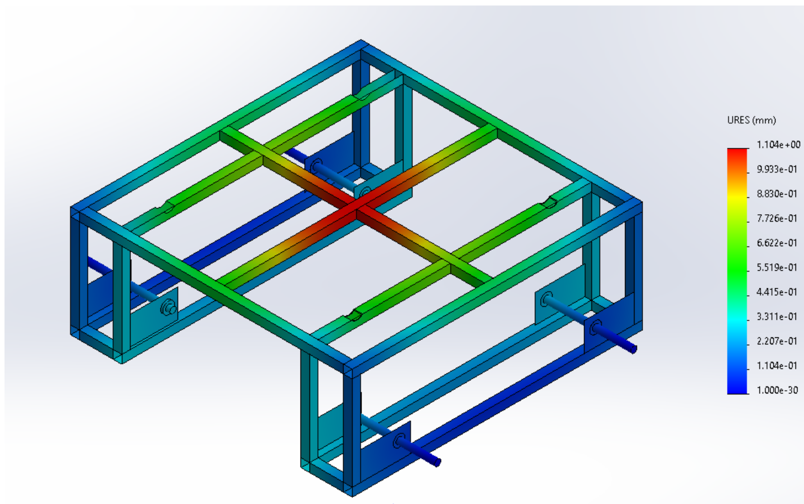

Figure 11: Chassis Displacement Propagation (225 lb. force)

The stresses observed also followed the expected pattern with higher levels of stress on the two central beams concentrated at the center of the applied force that then dissipated to a negligible level as it moved farther along the main level and down the support beams. This can be seen in Figure 12. This is as expected as stress is directly proportional to the force acting on the cross section being examined. These stresses are well within the listed yield stress of the steel used. Additionally, the stress at the welded joints was well within the threshold that the welds are able to support without any concern.

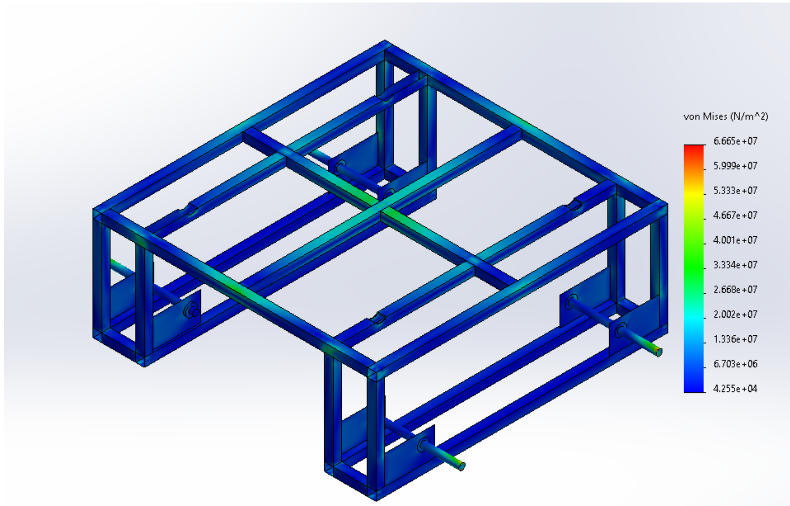

Figure 12: Chassis Stress Propagation (225 lb. force)

The strain data, shown in Figure 13, within the simulation also supports the fact that the loads applied are within the acceptable range for the chassis as the displacement was so low.

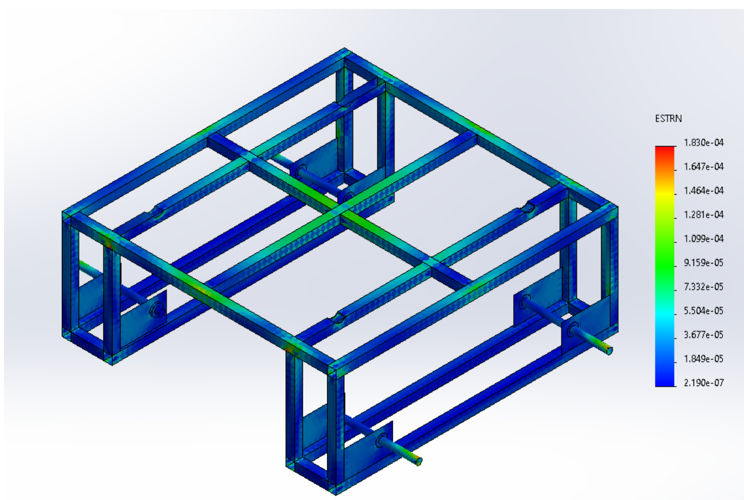

Figure 13: Chassis Strain Propagation (225 lb. force)

Based on the simulations performed, the chassis is able to support three times the necessary load. Therefore, the chassis design has been deemed acceptable based on loading characteristics.

Drive System

For the drivetrain and steering system of the rover, several different systems were considered. For this project, a system with all wheel drive capabilities to maneuver through various agricultural species was needed. Along with that, the system had to have a compact drivetrain to minimize the size of the rover. With this in mind, four different types of all-wheel drive (AWD) systems were considered.

The most commonly used system is a four-wheel drive system that can be seen on many modern-day vehicles. It is composed of two steerable wheels located at the front of the vehicle and two fixed wheels at the rear of the vehicle. Each wheel delivers power to the ground. An image of the system is shown in Figure 14. For the sake of this project, the all-wheel drive system was considered for its superior performance on rough terrains (Hojin Jung and Seibum Choi). The benefits of this system include high maneuverability with a small footprint for minimal damage to the ground. The downside to this system was its large spatial requirements for both the steerable wheels and the powertrain.

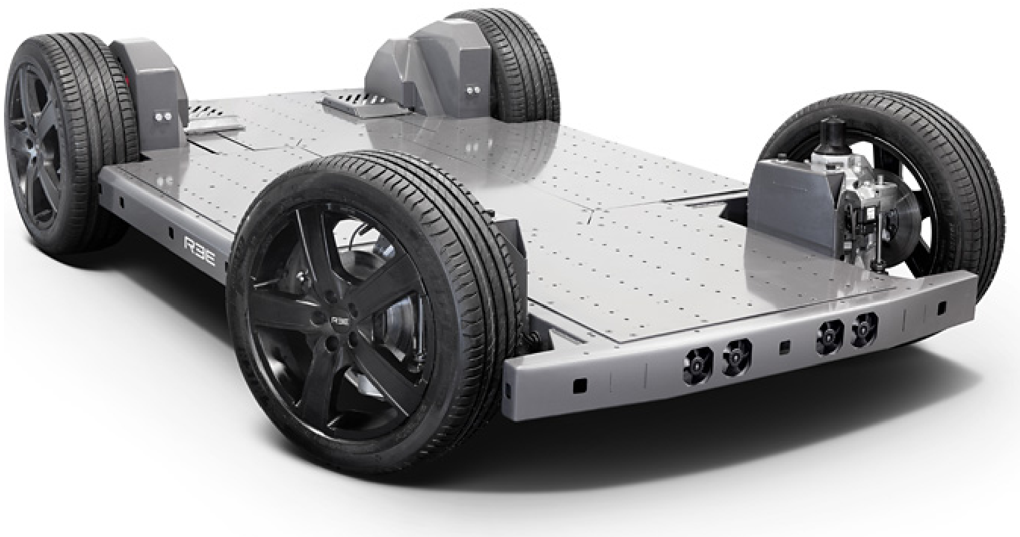

Figure 14: AWD System with 2 Steerable Front Wheels

A trike system with 1 steerable wheel in the rear is another system considered for this rover. This system has been used in several agricultural rover startups, such as the Fendt Xaver's seeding unit (Fendt, n.d). An image of this seeding unit is shown in Figure 15. Some of the benefits of this system include a more compact design with high maneuverability. Along with that, this system would have a smaller footprint compared to 4-wheel drive systems. On the other hand, due to the smaller footprint, the system required more weight to have the same amount of traction as a 4wd system.

Figure 15: Trike System with One Steerable Wheel

A dual tread system was also considered for this project. This system would consist of a dual motor setup with treads on opposite sides of the vehicle. This system is very commonly used in tanks. The benefits of this system would include enhanced traction and extreme mobility. On the other hand, this system involves a very complicated drivetrain that would require modified treads and tension springs. A dual-motor tread system has also been known to create a large amount of deformation to the floor.

The final drivetrain system considered was a four wheel drive system that does not have steering wheels, but relies on individual wheel speed and power to steer the vehicle. This system would have a 4-wheel drive system but with no extra steering mechanism. This would work by either activating both sides to move forwards or one of the sides to turn. Compared to other drivetrains discussed, this system is a lot less complex and expensive. It would also be able to fit in a very compact drivetrain.

Making a system that delivers enough power while also allowing for precise steering is a difficult process that requires gear and torque analysis. The drivetrain of the rover utilizes sprockets and chains to deliver power from the motors to the wheels located lower on the rover. One of the main requirements was to have 4 wheel drive to ensure that the rover could maneuver through farmland and any other obstacles in its way.

With a general design in mind, the next step was selecting the right motors for the designed operation. To do so, a motor torque analysis was conducted to determine the required output torque from each motor in order to move the weight of the rover and its cargo without damaging the motors. Along with that, the team conducted several iterations of motor and torque calculations to determine the most efficient combination between the required motor torque and the transmission gear ratio. A free-body diagram of the forces acting on the wheels is shown in Figure 16.

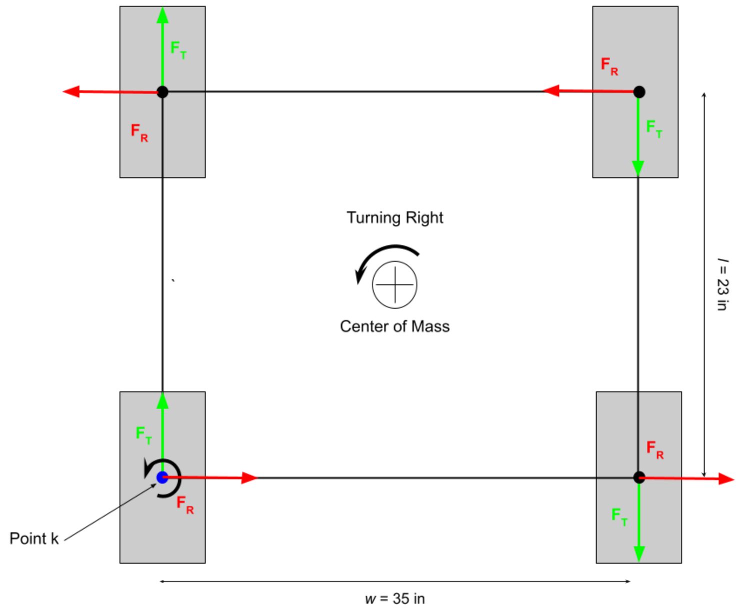

Figure 16: Skid Steering Free-Body diagram

To calculate the required turning force needed from the motors the simplified net moment equation (1) was used to determine the minimum overall torque required from the transmission system.

$$(1)\ M_k = 2F_T w - 2F_R l = 0$$

Where M_k is the moment about point k shown on the free-body diagram. F_T and F_R are the force traction and force resistance from the wheels. And finally, *w* and *l* are the widths and the length of the rover wheelbase (takeda et al., 2019). After further simplification of the net moment equation by simplifying the forces along a single wheel, equation (2) is derived. The free body diagram for the forces acting along a single wheel is also shown in Figure 17.

$$(2)\ F_T = F_f\, sin(\theta)$$

$$(3)\ F_T = \mu \frac{W_t}{4}\, sin(\theta)$$

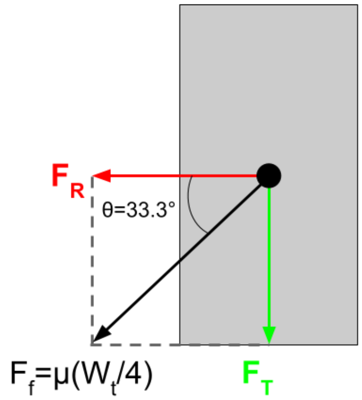

Figure 17: Free-Body Diagram of a Single Wheel

From equation 2, F_f is the force of friction and θ is the angle between the F_f and the F_T. Equation 3 further expands the Friction force, where μ is the coefficient of friction between the wheel and the dirt and W_t is the total weight of the rover (takeda et al., 2019). From these two equations, the two main factors affecting the required traction force are the coefficients of friction and the total mass of the rover. The coefficient of friction of the wheel was calculated by placing the wheel in a dirt like environment that would best stimulate the worst conditions that the rover would have to drive through. To do this, the wheel is positioned so that it has roughly 0.5 inch of dirt surrounding it. Then attached is an electronic spring force measuring tool to the center of the axel and pulled horizontally and measured the force required. From these measurements the coefficient of friction was determined using this equation.

$$(4)\ F = \mu * N$$

Where F is the force required to pull the wheel out of the dirt, μ is the coefficient of friction and N is the normal force the wheel exerts on the ground. From the calculations, the coefficient of friction of the wheel was determined to be 0.39. Using the cad models, a rough weight estimate of 200lb for the rover was also determined. From these calculations, a F_T value of 10.62 lbf was determined for each motor. Equation 4 was then used to calculate the T_T, traction torque required.

$$(5)\ T_T = F_T * r$$

Using this equation where r is the radius of the wheel, the minimum motor torque required was 4. 425 ft-lb or 6 N-m of torque. A more detailed step by step torque force calculation can be found in the appendix A. With these force calculations the desired gear ratio could be chosen. To accommodate unforeseen loads and other environmental disruptions a safety factor of 1.5 was to choose for the final output torque of the rover. This was chosen primarily due to budget limitations. A higher safety factor could have been chosen but the cost to benefit ratio was not needed for the purpose of the project. A 10 N-m final output torque per wheel was accomplished with motors that can withstand 5 N-m of torque under continuous load and a 2:1 ratio transmission. The transmission system consisted of an independent transmission for each motor. Each transmission would have a 2:1 chain and sprocket system to drive the wheels. The driving sprocket will be directly attached to the drive shaft of the motors, and the driven sprocket will be welded to the axle so that it is held in place to prevent slipping. This independent transmission system was chosen so that each motor could be operated independently from the others. This will serve to improve handling of the rover while also improving more accurate location sensing since each wheel would have its own motor sensor. Figure 19 shows the completed chain and sprocket assembly.

In order to hold the axles in place and institute support from the chassis, axle support plates made of steel were plasma cut and welded to the frame with axle size holes in them that will hold a bearing around the axle. The Figures below show the CAD model of the axle support and the actual picture of the axle support attached to the frame.

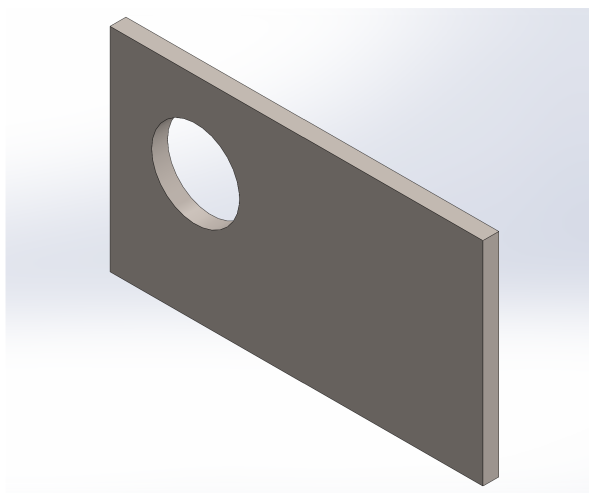

Figure 18: Axle Support made of steel

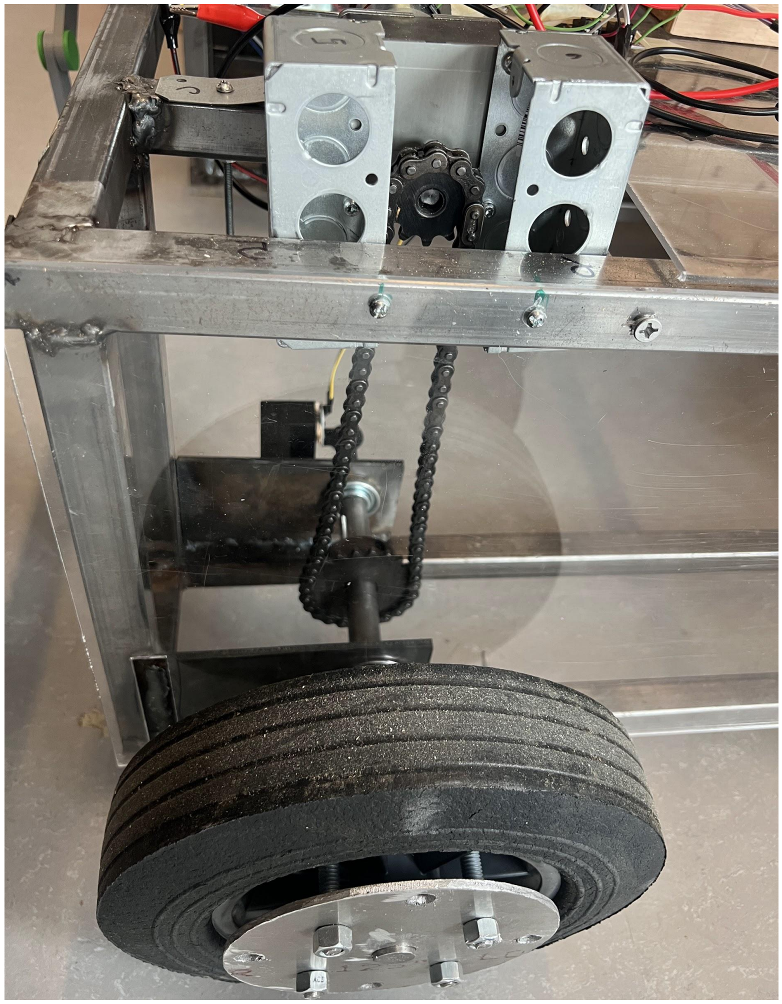

Figure 19: Completed 2:1 Ratio Chain and Sprocket Transmission System

To calculate the tension in the chain system it is necessary to know the weight of the chain, the force applied by the motor, the gear ratio between the sprockets, and the weight acting on the chain due to the rover. For this calculation it is assumed that there is no tension in the chain at rest since it is supported on both ends due to the sprockets being mounted to the motor shaft and wheel axle. The weight of the rover is estimated to be about 115 lbs, the weight of each chain is .66 lbs, the force of the motor acting on the chain is .0143 lbs, the weight of the rover acting on each chain is 28.75 lbs, and the gear ratio is 2. To calculate the tension in the chain all of the the forces are added together and multiplied by the gear ratio to find the instantaneous tension in the chain. The total force acting on the chain is 29.424 lbs and after multiplying this by the gear ratio the instantaneous tension in the chain is 58.85 lbs. With the working load of the chain being 560 lbs this gives a safety factor of 9.5.

Wheels

The wheels used to transfer the power from the motors to the ground was an integral part of the rovers' overall design. Without the proper wheel size and composition, the rover could become unbalanced and therefore would not be able to move as it is designed. Choosing the correct wheel ultimately involved 3 major factors: cost, size and carrying capacity. With these factors in mind, the team decided upon a 10" Rubber solid tread flat free wheel with internal bearing from Mcmaster, seen in Figure 20.

Figure 20: Solid-Tread Flat-Free Wheels (from McMaster-Carr)

These specific wheels were chosen because they had a high carry capacity of 550 lb and were extremely affordable for this project. However, since the wheels aren't designed to be driven (i.e. non-motorized use), a hub locking mechanism was designed to transfer the motor power, rather than buying wheels that were suitable for this purpose. The design for the wheel hub locking mechanism revolved around manufacturability and cost. Ensuring that the design could easily be manufactured in the manufacturing labs while still being a cost efficient solution is a top priority. 8 steel circular plates were created and placed on the face of the wheels that allow the axle to be fused to the wheels. The wheels purchased do not have the proper fitting through the center to be anchored and therefore these metal plates were created. The wheels are prefabricated from the manufacturer. These plates will have bolts through them and the webs of the wheels. The axle, which is ¾ inch diameter steel, is then welded to the plate.

Two plasma cut steel plates are placed perpendicular to the axles on both sides of the plastic wheel and have four 3/8th inch bolts running through both the plates and the wheel hub to secure the axle to the wheel as shown in Figure 21. Along with this, the space in between the 2 inch axle shaft of the wheel and the actual ¾ inch axle is an ABS shaft collar. This is designed to minimize any vibrations and help distribute any bending forces within the axle. The majority of the torque force from the transmission will be evenly distributed between the four bolts and into the hub of the wheel.

Figure 21: Completed Wheel Hub Assembly

Force calculations were completed to determine the overall force on each rod just to ensure it was within the limits of the hub. These calculations used a similar equation as equation 4 which was used to determine the output torque of the motors.

$$(6)\quad T_R = (F_T * r_R)/4$$

Where T_R is the torque force on each rod, F_T is force traction given in equation 4 and r_R is distance from the rod to the center of the axle. Using this, it was determined that T_R would be 0.43 lb-ft or 0.58 N-m for each rod.

Rover Fluids System Design

The rover's spray system will be used to dispense fluid from the rear of the rover as it traversed the field. It was adapted and improved upon from a system that was designed and used by a previous MQP team ("Car-Snow Clearing Drone"). Their design was also modeled after agricultural drone systems but was instead used to clear snow and ice from car windshields with deicing fluid, seen in Figure 22.

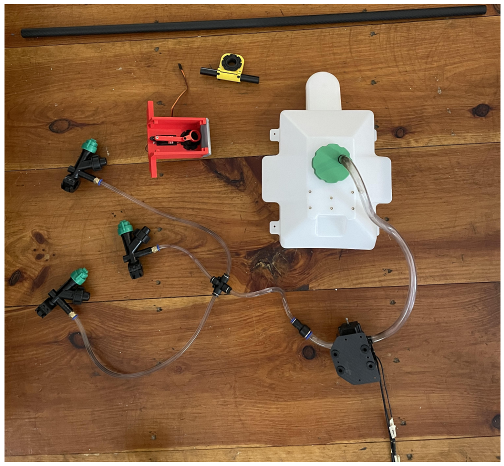

Figure 22: Spray-Bar System from "Car-Snow Clearing Drone" (5L water tank, pump, flat fan nozzles, actuated spray bar mechanism)

Originally, the spray-bar system was actuated in the drone using a servo motor and a four bar linkage that toggled 60 degrees, as seen as a CAD model in Figure 23. It worked with a stereoscopic camera and an RTK system to correctly position the boom's angle to clear snow, depending on the location of the drone. It was ultimately decided that the added cost and complexity was not needed in the final design, since the rover would not be moving vertically. However, further iterations of the rover could include this device to provide automated positioning of the spray bar, depending on the conditions.

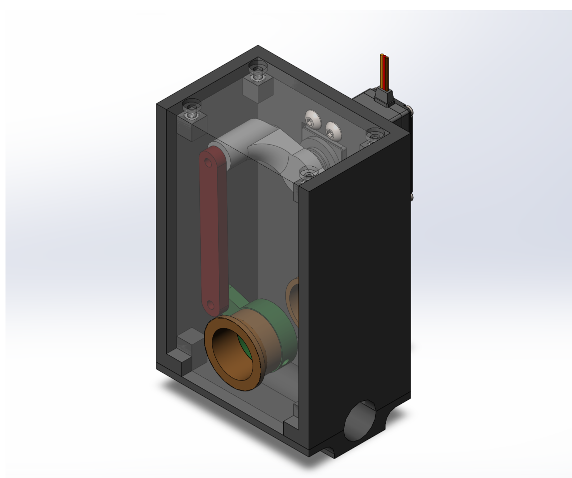

Figure 23: CAD Model of Actuated Spray-Bar Mechanism

The spray pattern of the nozzles was chosen to ensure optimal fluid coverage over the field and to prevent drift and overspray, which is common among pesticides sprayed at a height in the agricultural industry.

The final design, seen in Figure 24, drew additional inspiration from similar unmanned ground rovers that typically spray fluid out of the rear of the vehicle. A 5-Gallon high-density polyethylene (HDPE) carboy jug is located inside the main body. The fluid is then gravity-fed via an 8mm PVC spray line (connected to the jugs' spigot) to a 24V diaphragm pump that is capable of 1.5 gallons per minute. The fluid is finally directed to three flat-fan nozzles, which are mounted to a 500mm-long carbon fiber boom on the back of the rover, as seen in Figure 24. Despite being manually actuated, it offers around 75 degrees of upwards rotation from horizontal. This is an acceptable range of motion since the spray-bar will never need to move outside of a 90° range to spray.

Figure 24: Spray-Bar Attached to the Rear of the Rover

The rover filler cap mechanism was designed to allow fully automated access to a refill point for the onboard tank. The first iteration of its design featured a fourbar linkage as the driver of the hatch as it opened. However, there were multiple drawbacks that eventually led to the current design. Instead of a fourbar linkage, which provided space and manufacturing constraints, a linear actuator was ultimately decided due to its simplicity to implement into the rover design, seen during testing in Figure 25.

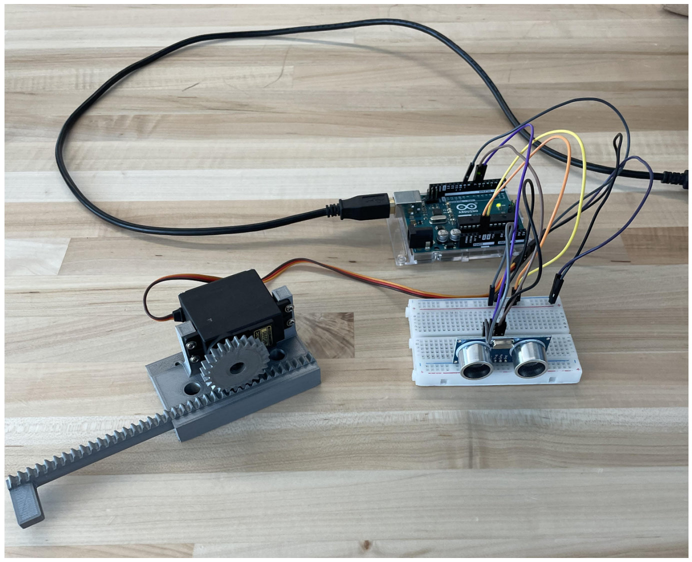

Figure 25: Actuated Hatch Mechanism

A rack and pinion is driven by a Servo motor which is all mounted to the enclosure of the rover's tank. An ultrasonic sensor mounted to the rear of the rover would provide distance detection. When the distance measured from the rear of the rover to the back interior wall of the hub is under a specified distance (as the rover enters into the hub), the rover would stop moving and the hatch would slide open, providing an opportunity for the solenoid valve to refill via the hub. Secondary manual control of the hatch is provided by a button on the rover that opens and closes the hatch. Figure 26 shows the optimal open and closed positions.

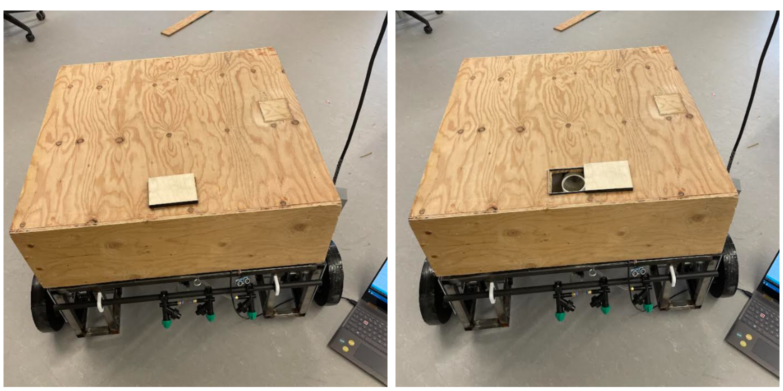

Figure 26: Closed (left) and Open (right) Configurations for Actuated Hatch

Figure 27: Testing of Spray System Outside

Considerations of high pressure loss across the fluid delivery led to the determination that a higher pressure pump should be used in the system so that a higher flow rate leaving the nozzles could be achieved. Another issue that was found while testing the spray system was that there was leaking from the nozzles. These high pressure nozzles had their check valves bypassed (permanently opened) because the pump pressure wasn't high enough to engage the valves along with the fact that the pump already leaked when connected to power. If a higher quality pump and better nozzles were used in the system (since both were inexpensive options), that would eliminate the pressure and leaking issues.

Soil Sensor Arm

The final mechanical system on the rover is a linear actuation arm. The arm is designed to allow for soil measurements to be taken using an NPK sensor. The arm consists of a servo motor, a crank and slider four bar linkage, and a custom printed housing for the NPK sensor. The arm is located on the front of the rover to allow it to have its full range of motion as well as to keep it out of the way of other systems. The arm goes through 90 degrees of motion from its up resting position to its active position at full extension as seen in Figure 28. The custom housing is designed to fit an NPK sensor and is able to be attached to a vex interior slide which runs in a vex linear motion rail. Additionally, the housing is printed as two parts so that the sensor can be removed if service is needed.

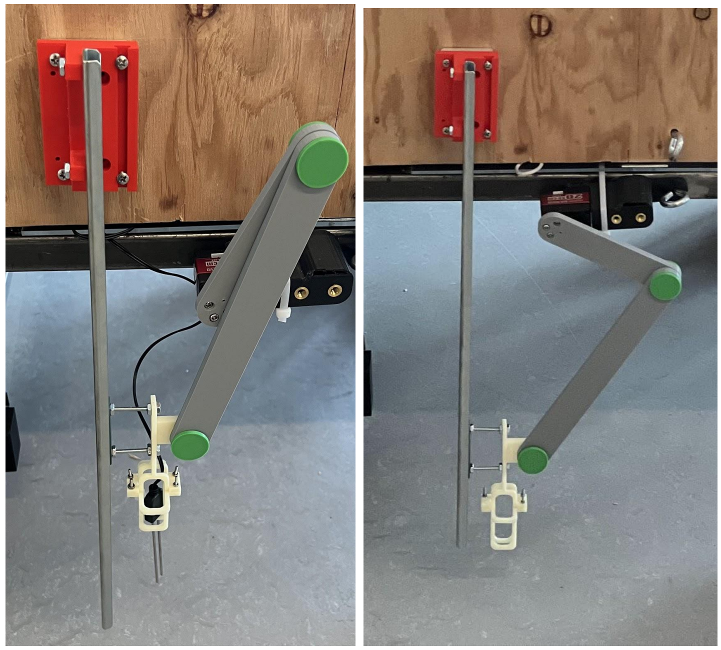

Figure 28: Linear Accusation Arm for Soil Sensor

The arm was printed out of PLA while the housing was printed out of ABS due to the need to use the Dimension SST 1200es due to geometric constraints of the design. Assembly of the arm is relatively basic with printed pin joints connecting each linkage in the mechanism, the central pin joint is able to be taken apart to allow for the top of the rover to be separated from the base as the current mounting system is not fully optimized and currently has points of contact both on the frame and the top.

Rover Hub Station

Serving as the home for the rover when not in operation the hub is a vital part of this project. The process of creating the hub started with designing and redesigning using SolidWorks. This was followed by conducting simulations on the hub design also performed in SolidWorks. The team then constructed the first iteration of the hub. This iteration was found to not have the longevity desired by the team so it was decided to reinforce the entire hub. This process involved identifying key stressors in the design to locate where to place reinforcements. Following the reinforcement the hub fluid systems were then able to be installed.

Hub Design

The hub serves as the base of operations and home for the rover while not in operation, and sits outdoors at all times. Therefore, the team had to select a material for the support frame and walls that would be largely water resistant, lightweight for transportation, could be easily worked on and manipulated, and inexpensive. The material that was eventually selected was plywood, due to its availability at hardware stores and how it is far lighter than other alternative options available to the team. The issue of waterlogged wood was solved by choosing a water-resistant lacquer that was layered onto the plywood in multiple coats. Aside from the weathering abilities of plywood, the material fit all of the other expected criteria. In a more commercial application that allows for more funding, the hub would more likely be fabricated out of plastic or acrylic for the weatherproof capabilities and lightweight benefits they provide over wood. Below an exploded view of the hub assembly can be seen in Figure 29.

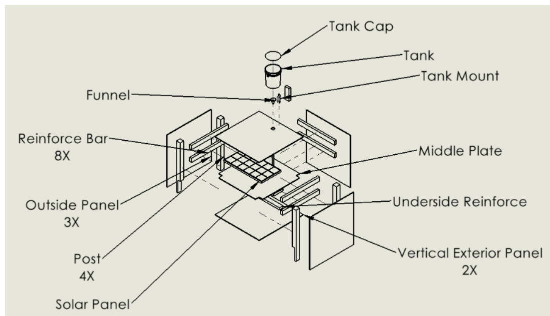

Figure 29: Exploded View of Hub Assembly

The first design of the hub consisted of three rear tank sections that are meant for various liquid storage. This design iteration was quickly scrapped as it required too much material and would be difficult to transport. The team had to modify the original design set out for the hub due to these constraints. Instead of a rectangular base shape that would require far more material, the team chose to use a square based shape. In Figure 30, you can see the original rectangular base shaped hub design. Adjacent to Figure 30, the new square base shaped hub design can be seen in Figure 31.

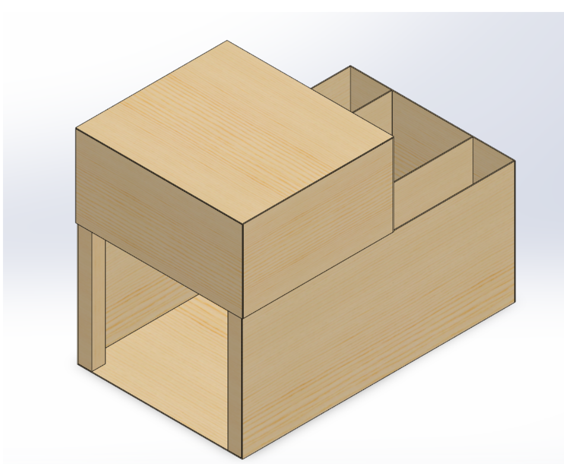
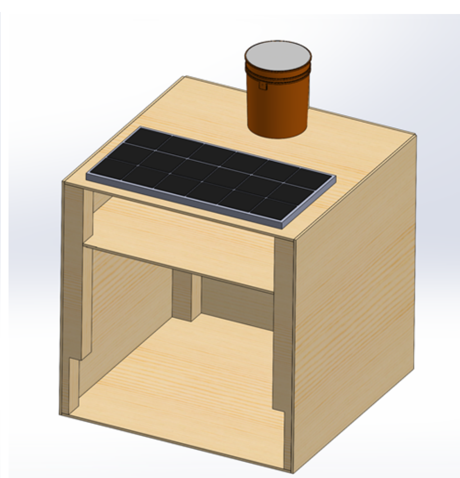

Figures 30 & 31: Rectangular Base Hub Design and Square Base Hub Design, respectively

Hub Simulations

To have a more complete understanding of the hub design and potential areas of failure, the team performed SolidWorks simulations for stress, displacement, and strain. For the simulations a factor of safety of three was used as the team believed this would cover all the bases for potential risk. A factor of safety value of three equates to approximately 600 newtons of force exerted on the top of the hub at a point close to the rear. This value comes from three times the weight of the water when the water tank is full. The simulations were performed after increased reinforcements were installed to the hub frame and have been included in this SolidWorks file used in these simulations.

As one can see in Figure 32 below, the hub stress simulation, the hub at maximum value will undergo approximately .7957 MPa in the red area. However, a majority of the hub is not red, mostly green which is half of the .7957 MPa value. Further below in Figure 33, one can see the displacement values for the hub under load. The maximum displacement seen is approximately .00003923 mm in the red portion of the hub. This fraction of a millimeter value can't even be seen by the naked eye and this is three times the expected value of the load on top of the hub. This goes to show that the additional reinforcements to the hub proved extremely beneficial in increasing the longevity and feasibility of this design. Lastly, in Figure 34 below, one can see the strain simulation on the hub. Once again the maximum value is quite small with just .00000000363 equivalent strain measured.

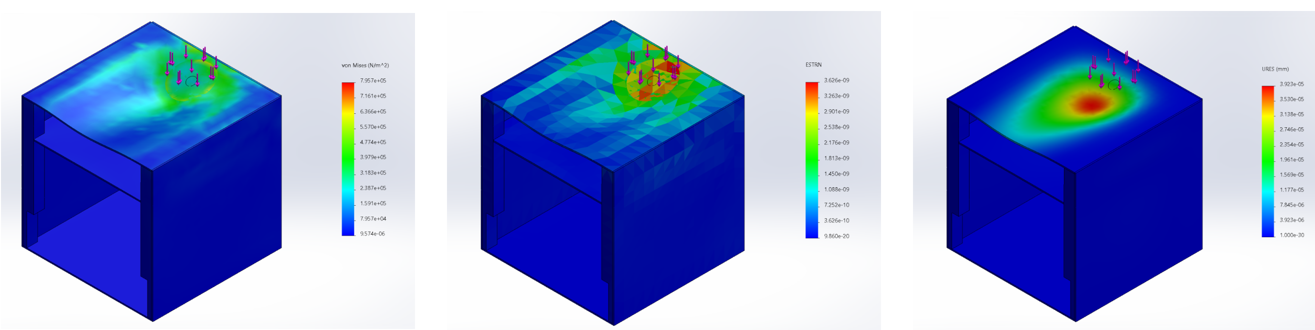

Figure 32, 33, 34: Hub Stress Simulation, Hub Displacement Simulation and Hub Strain Simulation, respectively

The stress, displacement, and strain simulations performed on SolidWorks by the team has enabled a peace of mind that the hub is structurally sound and will not collapse, displace, or elastically deform, when under loads far greater than anticipated. Additionally, the hub is designed in such a way that if modifications are required following long periods of time in the fields, such additions can be done so quickly and efficiently. Making the hub out of wood allows for easy removal of side panels and internal reinforcements as all components are held together using high strength steel screws. This modularity allows for design changes given the environment the hub is used in and any unforeseen irregularities with its working conditions. These simulations can be performed time after time as long as modifications are made to the original design used.

Hub Assembly

The square shaped hub sacrificed the three rear tanks, but reduced the overall weight of the hub and required materials. The dimensions of the hub are 4’x4’x4’. These dimensions are ideal as a sheet of plywood is 4’ x 8’ and cutting that in half is two 4’ x 4’ sheets. To build the hub, the team acquired the necessary sheets of plywood, and had them cut in half. Then built the base of the hub by taking one sheet of plywood and screwing in 4, 4” x 4” x 48” posts. The posts serve as supports for the walls and roof of the hub. Next, the team screwed three walls on the hub, exposing the front side. A middle section is then installed that is suspended 3’ from the base for electronic components. This section is supported by metal brackets that are screwed into the posts. The last major portion of the hub installed was the roof, which was screwed straight into the posts, like the base. To weather-proof the hub, a lacquer was applied to the panels. To give the best possible weather-proofing results, three layers of the lacquer were applied to all exterior sides of the hub. While the lacquer was applied, caulking was also filled in on all exterior edges and bottom edges of the hub to ensure a tight waterproof seal. The exterior and interior of the hub can be seen in Figures 35 and 36, respectively.

Figure 35 & 36: Weather-Proofed Hub and Hub Interior, respectively

Hub Reinforcement

With more available funding, the hub was able to be reinforced with wooden boards, which allowed for it to have the same overall look of the first iteration, but included necessary structural changes and removal of the brackets used for the shelf. A cross-brace two-by-four can be seen with the purpose of replacing the metal brackets used to hold up the shelf. Figure 37 below shows the hub with the added reinforcements, which proved necessary for two primary reasons. One, the hub was noticeably shaky and unstable, with the roof beginning to droop over time as it weakened. Two, the two by fours used for this purpose were cheap and easy to acquire.

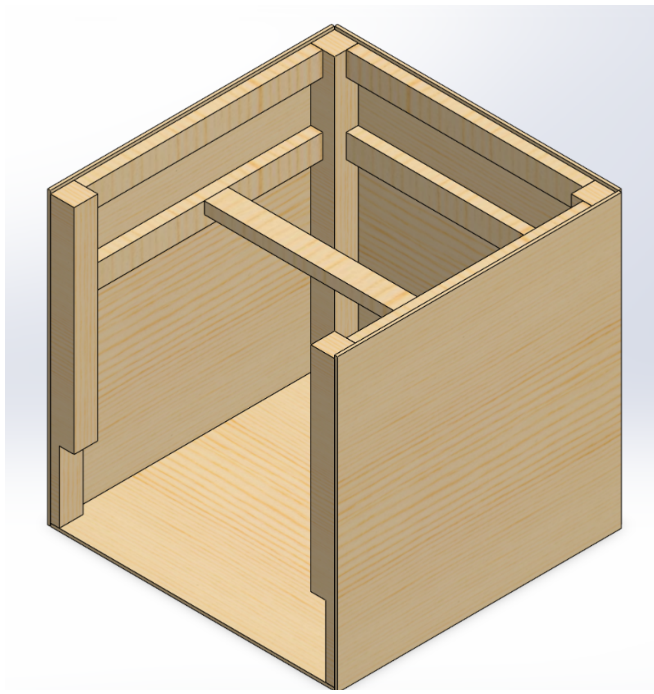

Figure 37: Hub Structure with Reinforcements

The last improvement done for the final hub iteration was the removal of wood from the two front posts.This was done to allow extra clearance for the wider-than-expected rover wheels to fit.

Hub Fluids System Design

The hub's refill station is used to fully replenish the rover's spraying system when all 5 gallons in the onboard tank have been dispensed. The hub's refill system was designed to allow safe, efficient, and automatic delivery of fluid at a constant rate to a refill point for the rover's tank. It was modeled after similar refill stations that are sold commercially in the United States farming industry, like the Rantizo Fill & Go Station. Their medium-scale agricultural drone autonomously docks and refills in their filling station to replenish its multipurpose spray system, seen in Figure 38 ("Rantizo System Products," 2021).

Figure 38: Rantizo Fill & Go Station

The design of the refill system also drew inspiration from a wall-mounted plastic water tank on McMaster Carr, as shown in Figure 39. Originally, this vertical tank was to be attached to the outside of the hub, since it would allow better access for it to be refilled. Therefore, it was decided to attach the tank to the rear wall.

Figure 39: 10-Gallon Wall-Mount Plastic Easy-Drain Tanks

Although a comparative system for this project would provide a complete method of fluid replacement, the size and cost needed to be optimized for use with the rover. Ultimately a similar refill system was developed and manufactured using much less expensive materials with the same objectives and constraints.

The refill system features a 5-gallon high-density polyethylene (HDPE) tank that is mounted to the top of the hub, to allow gravity feeding capabilities and ease of refilling. Helping in the ability for the tank to be gravity-fed is an 8 oz. polypropylene funnel attached to the bottom of the bucket. Next, clear vinyl tubing connects to a 12V actuated solenoid valve that controls fluid flow (either on/off). The tubing will lead straight down to a specified access point where it will meet the rover and its onboard water tank and spray system.

The refill system currently works by operating the solenoid valve independently to dispense water through to the access point for the rover. The valve was connected to an Arduino and a 12V car battery and was tested successfully in Figure 40. Figure 41 shows how the rover lines up with the hub tubing. This system is somewhat autonomous currently.

Figure 40: Solenoid Valve Testing

This system is supposed to work in conjunction with the rover, where these three steps would happen in succession in order to refill the rover's tank:

1. The rover drives into the hub, stopping 22 cm. from the back wall.
2. Actuated hatch moves into the "open" position, exposing the access point to the tank.

3. Solenoid valve would open, sending water into the rover's tank and beginning the refill process.

Figure 41: Hub and Rover Interaction During Refill

Solar Power

Solar Power is the power from converting the energy from solar radiation into electrical energy. The energy from solar radiation is called photovoltaic energy (PVE) and is based on a number of factors. Combining the PVE and several characteristics of the solar cell array the power output can be calculated using a series of equations. These factors are affected by both geographical and weather conditions, including latitude, climate, and weather patterns (EIA). Figure 42 and Figure 43 below show the distribution of several types of solar irradiance in the United States. Each type of solar irradiance requires different solar panel shapes and angles to maximize the amount of energy that can be harvested.

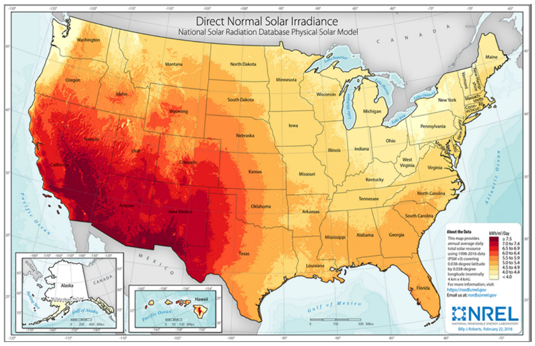

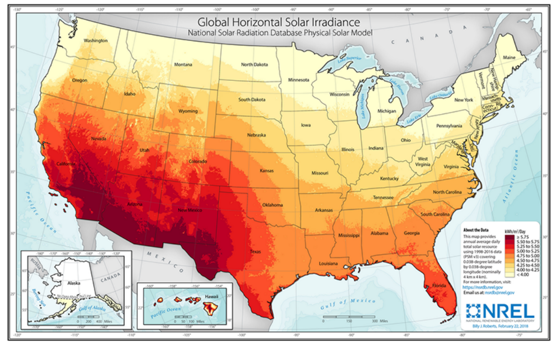

Figures 42 and 43: Solar Irradiance in the United States (EIA)

Current solar cells have an efficiency rate between 13 and 50 percent. However due to budgetary restraints, expected efficiency will be between 20 and 30 percent. Due to the lower efficiency that will be achieved by the solar cell, it is likely that measures will need to be taken to ensure that the cells are able to receive as much energy as possible. Efficiency values for PERC, monocrystalline, and polycrystalline can be seen in table 1 below.

Panel Type	**Efficiency**
PERC	Highest (5% more than monocrystalline)
Monocrystalline	20% and up
Polycrystalline	15-17%

Table 1: Solar Panel Types by Efficiency (Mcbride, 2021)

Solar panels come in different types that can each have their own benefit to fit the project's needs. These types include monocrystalline, polycrystalline, and passivated emitter and rear cell (PERC). Monocrystalline solar panels are made from a single silicon crystal that are cut into many wafers. Since this type of solar panel is made from one type of silicon crystal it allows the solar panel to be very space efficient and not wear as quickly over time. A drawback to these types of solar panels is that they can be very expensive, as seen in table 2 below, as a lot of silicon is wasted in the manufacturing process of these panels. Polycrystalline solar panels, as its name implies, is made from multiple different silicon crystals allowing it to be not as expensive as monocrystalline solar panels. However, since these panels are not as pure in silicon as monocrystalline panels, they are less efficient in energy conversion and are also not as heat tolerant in high temperature environments. PERC solar panels are a more efficient version of monocrystalline solar panels. These panels work by reflecting the solar radiation back into the cells. PERC panels are also able to absorb a broader wavelength of light than monocrystalline panels that would normally pass through them, by reflecting them back into the solar cells. Due to these panels' high efficiency compared to other types of solar panels, they are more expensive due to added material, however they have a lower cost per wattage (Mcbride, 2021).

The solar panel chosen for the hub of this project is rated for 100 Watts and 12 Volts. This selected solar panel was a part of a larger solar charging kit that also included a 30 AMP PWM charging controller, a 20 AmpHour lithium iron phosphate battery, and a 600W 12V pure sine wave inverter. With these four components working in tandem, the hub is able to charge the battery for the rover, display current power output, and invert the DC into AC. Additionally, the solar panel in this configuration is able to charge the aforementioned battery in about 6 hours of direct sunlight as calculated in the equations below.

$$100W\ /\ 12V\ =\ 8.33A\ (Max\ charge\ current\ output\ by\ controller)$$
$$8.33A\ *\ (1\ -\ 20\%)\ *\ 75\%\ =\ 5A\ (Multiply\ current\ \ by\ system\ losses\ and\ efficiency)$$
$$30Ah\ *\ (1/85\%)\ =\ 35.29Ah\ (multiply\ capacity\ by\ battery\ charge\ efficiency)$$
$$35.29Ah/5A\ =\ 7.06\ hrs\ (divide\ battery\ capacity\ by\ current)$$
$$7.06hrs\ *\ 50\%DoD\ =\ 3.53\ hrs\ (multiply\ charge\ time\ by\ battery\ depth)$$
$$3.53\ hrs\ +\ 2hrs\ =\ 5.53\ hrs\ (add\ 2\ hours\ to\ account\ for\ absorption)$$

Panel (Module) Type	**Average Cost per Watt**
PERC	\$0.32 - \$0.65
Monocrystalline	\$1.00 - \$1.50
Polycrystalline	\$0.70 - \$1.00

Table 2: Solar Panel Types by Cost per Watt (Mcbride, 2021)

Electrical Design

Two of the characteristics that were selected for in the electrical components were the price and the ease of integration into the project. Price was a priority as budgetary restrictions played a heavy role in the project. Ease of integration was important due to the time constraints as well as the importance of making the system easy to maintain for people without an engineering background.

For the microcontrollers controlling the sensor data, two Arduinos were opted for as the control unit for the basic sensors and communication. Arduinos were the best option due to the team's experience and familiarity with Arduinos, as well as members of the group having extras to lend towards this project. This saved money to be spent into other systems of the project. In terms of the data that is measured from the hub, the speed that data is read from these sensors is not a priority. This data is stored in an SD-card with the primary use to measure current environmental readings and for the user to track.

The wiring diagrams of the separate Arduinos are shown in Figure 44 and Figure 45. The hub's digital ports are used by the barometer, and the digital ports are used by the temperature/humidity sensor and anemometer. The rain sensor utilizes both analog and digital data. The soil sensor utilizes a connection through a MAX485 to connect to 4 separate digital ports on the rover's Arduino. Both the hub and have a transmitter/receiver system that use the digital ports of the Arduinos to transfer data to each other.

For the hub, a DHT22 was selected to measure the temperature and humidity of the surrounding area due to its precision and accuracy of temperature of +/-.5 degrees Celsius and its precision and accuracy of humidity of +/-5%. The DHT11 temperature sensor was an alternative that was cheaper, but we had a DHT22 available from previous courses to use. A BMP280 module was selected to measure barometric pressure for its accuracy of +/- .12 hPa, which needs to be accurate to measure changes in weather. This data and patterns of weather will also be compared to readings with a rain sensor module, which determines whether there is water on the surface, and acts as a variable resistor, whether the surface is wet. The final sensor attached to the hub's Arduino is an analog anemometer that measures the wind speed. At the worst case, it has an accuracy of +/- 1 m/s. The accuracy of these sensors is important as it informs the rover what tasks need to be carried out as well as whether or not the weather is suitable for operation. All of these specifications are broken down in Table 3, which contains the accuracy of each component and the purpose of the component.

Component	Accuracy	Purpose
DHT22	+/-5 ° C +/-5% humidity	Measures temperature and humidity
BMP280	+/- .12 hPa	Measures the air pressure
Rain sensor	N/A	Measures whether the surface is wet or dry
Adafruit Anemometer	+/- 1 m/s	Measures the wind speed
ACOUTO NPK Soil Sensor	+/- 2% NPK +/- .3 pH +/- 3% moisture	Measures the soil NPK, pH and moisture.

Table 3: Components with Accuracy and Purpose

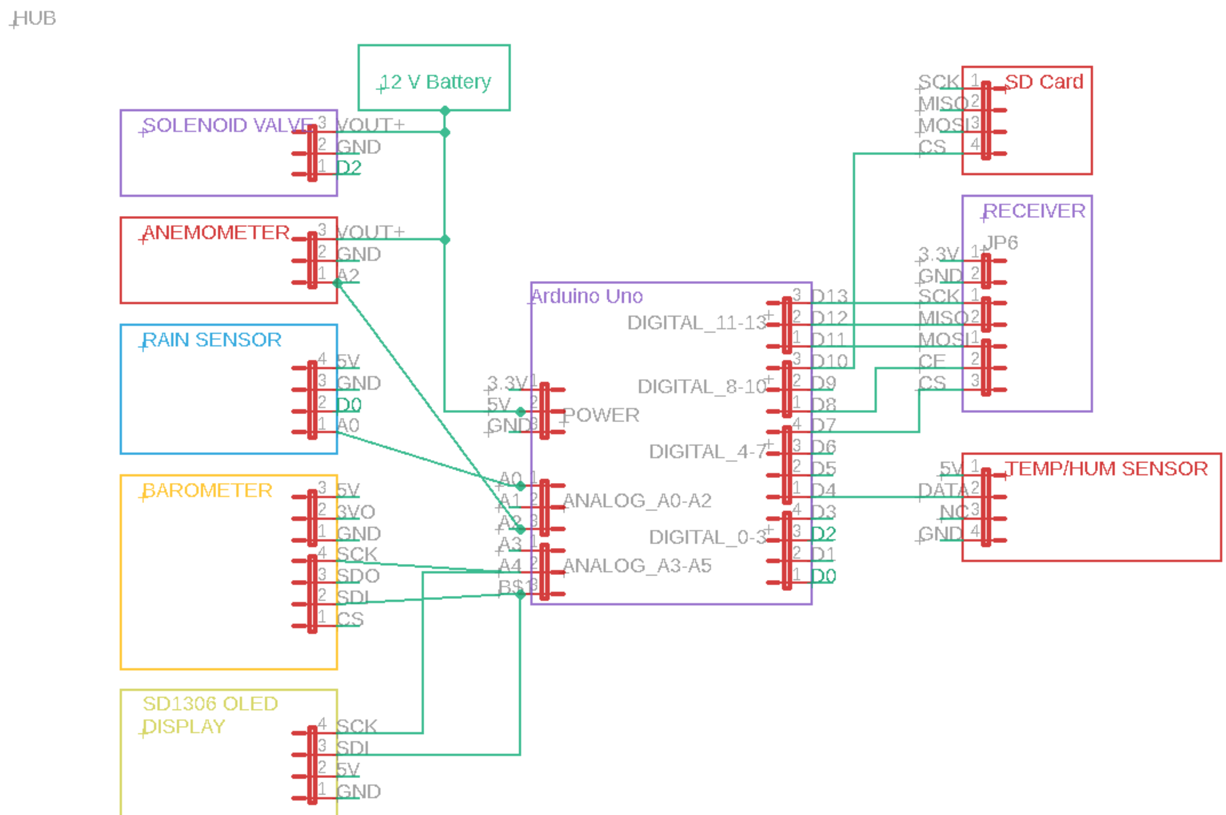

Figure 44: Hub Sensors Wiring Diagram.

The main sensor on the rover is a soil sensor. An ACOUTO Soil Tester was selected to measure the NPK (soil pH, nitrogen, phosphorus and potassium), temperature and moisture. This soil tester was selected due to its wide range of possible readings, with the cost being the same if each of these test sensors were purchased separately. Not only is it all in one form factor, but it made the integration of this sensor easier into the rover due to it being one single sensor, with multiple prongs for measurements. The precision of the pH readings are +/- .3 pH, the NPK readings are +/- 2% F.s, the temperature readings are +/- .5 degrees Celsius and the moisture readings are +/-3%. It is also rated as IP68, which makes it resistant to dust, dirt and sand, while being considered waterproof. This soil sensor utilizes inquiry frames and response frames to send and receive data from each of the prongs. The code is received as a hexadecimal code, and then is converted into decimal.

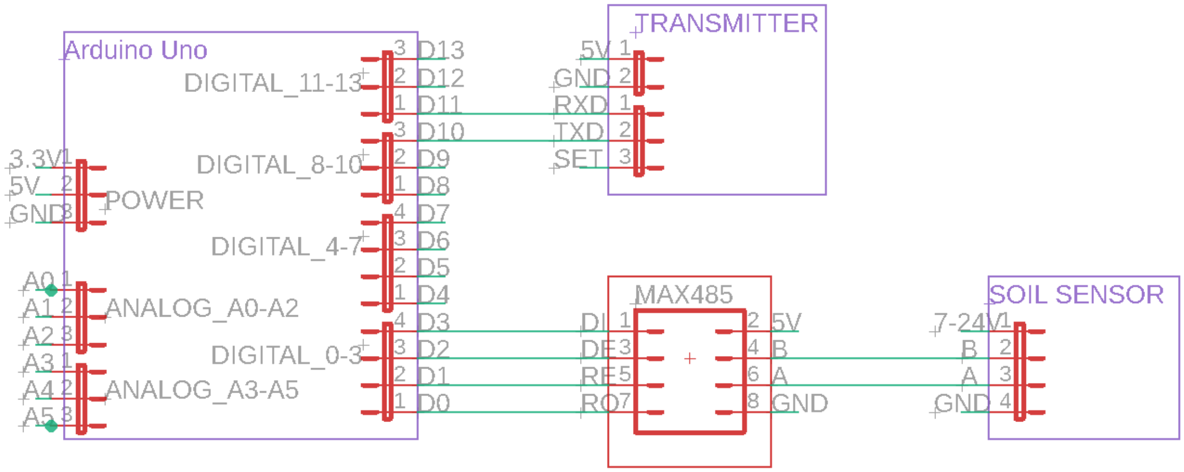

Figure 45: Rover Sensors Wiring Diagram

For the Arduino communication system between the hub and the rover, we are using an nRF24L01 digital transceiver on each end to transmit the data taken by the NPK sensor. Originally, we planned on using an HC-12 wireless serial port communication module which has a maximum range of 2 km, but had issues receiving data with the modules that we received. The nRF24L01 practically has the same communication capabilities as the HC-12, and we have had more success with communicating using the nRF24L01. Even though the range of the transceiver is less, 100 m in an open field is well within our needs to communicate between the rover and hub. The data transmitted is then sent to the receiver attached to the hub, and saved onto an SD card. The initial SD card module we received utilized a built-in level shifter at the MISO (Master-In-Slave-Out) for the SPI (Serial Port Interface), which caused the MISO line for both modules to stop running. In order to prevent this from happening, we opted to use an Adafruit SD card since it was confirmed to not have this level shifter built into it. This allowed us to utilize the same SPI on the Arduino and different chip selects for both the transceiver and SD card module without running into any issues.

Sensors

There are many considerations for this project and many different sets of data collection required to complete the required applications. One aspect that is important is GPS. Most applications of GPS, Global Positioning System, involve fast moving or larger objects and thus do not rely on extremely precise locations. The strengths of using GPS rely on the power of distributed localization, an objective reference frame, and widespread compatibility between numerous other technologies. RTK GPS, also known as Real-Time Kinematic GPS, is a means of achieving a higher accuracy position in the range of 1 cm as opposed to traditional GPS in the range of 2-5 m. This is accomplished by using a triangulation technique involving communication between GNSS (Global Navigation Satellite System), a base station of known location, and a rover station that is mobile. The range between the rover and base is calculated using carrier wavelength and communication between the rover and base station is often done through radio. While some errors and inaccuracies can propagate throughout the system, due to clock differences between satellites, a process called ambiguity resolution between multiple GNSS receivers minimizes error. Although RTK GPS has a low update frequency dependent on satellite connection strength due to the many calculations and signals that must be transmitted, it can be used in conjunction with other odometry and localization techniques with a higher update frequency, and statistical tools such as a Kalman Filter, to increase the overall accuracy of a system.

Along with positioning the rover, collecting soil data will be the next priority. Soil pH is an important metric for farmers and gardeners hoping to maximize plant health by ensuring their compatibility with the environment and balancing the chemical makeup of the soil. While pH may not have direct effects on some plants, it has a significant impact on bioavailability of nutrients and even toxins. For example, too high of a pH (alkalinity) is correlated with deficiency in iron, a nutrient, but too low of a pH (acidity) increases the availability of manganese and aluminum, both toxic to plants in high doses. Using a pH soil sensor can minimize the work and expense needed to solve plant health conflicts as the root causes of problems are addressed rather than adding an excess of nutrients. Because acidity is the concentration of hydrogen ions, soil pH meters measure conductivity to calculate pH. The meter uses two electrodes, one glass with a permeable membrane, and one a stable reference electrode. The voltage differential between these electrodes when inserted into the soil is correlated to the acidity of the soil and allows the pH to be calculated.

In addition to pH, nitrogen, phosphorus, and potassium (with chemical symbols N, P, and K) are primary nutrients in commercial fertilizers and their concentration in soil are generally indicative of plant nutrition. Nitrogen is essential in protein formation, phosphorus is responsible for plants storage and usage of energy, and potassium strengthens plants making them resistant to disease. While optical sensors and spectrometers make use of spectral analysis to determine soil content concentrations, a more accurate and cheaper technique makes use of conductivity. As an A.C. voltage is applied to a soil sample, movements of ions cause variable conductivity in which variability is correlated with ion concentration. Three electrodes embedded in the soil sensitive to specific electrical conductivity variations allow the calculation of nutrient concentration in units mg nutrient per kg of soil.

Sensor Module Design

The environmental, meteorological, and soil sensors are used to inform the rover and the hub of the local conditions. Specifically, sensors indicating metrics related to weather will be located on the hub and used to determine when the robot should be active and estimate solar energy received by the solar panel. An outline of data consolidation and use is shown in Figure 46. The soil sensors located on the rover are used to complete a control loop related to the amount of water and fertilizer applied to specific plants.

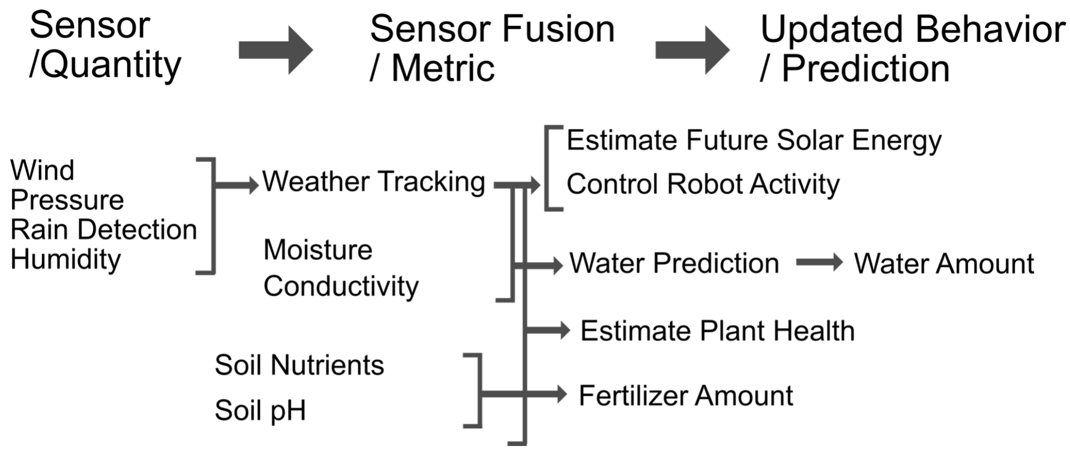

Figure 46: Sensor Impact on Robot Behavior

Sensor fusion will be utilized to improve the predictive capabilities of the control loop, which will rely on PID. Additionally, these can be used as a metric for plant health that can be monitored and documented over time. The environmental sensors provide raw voltage outputs that an Arduino on the hub will take as inputs to ADC (analog to digital converters). The soil sensor array on the rover uses the communication protocol RS485 which will be received by the Raspberry Pi. The units of each of these sensors and their communication protocols can be found below in Figure 47.

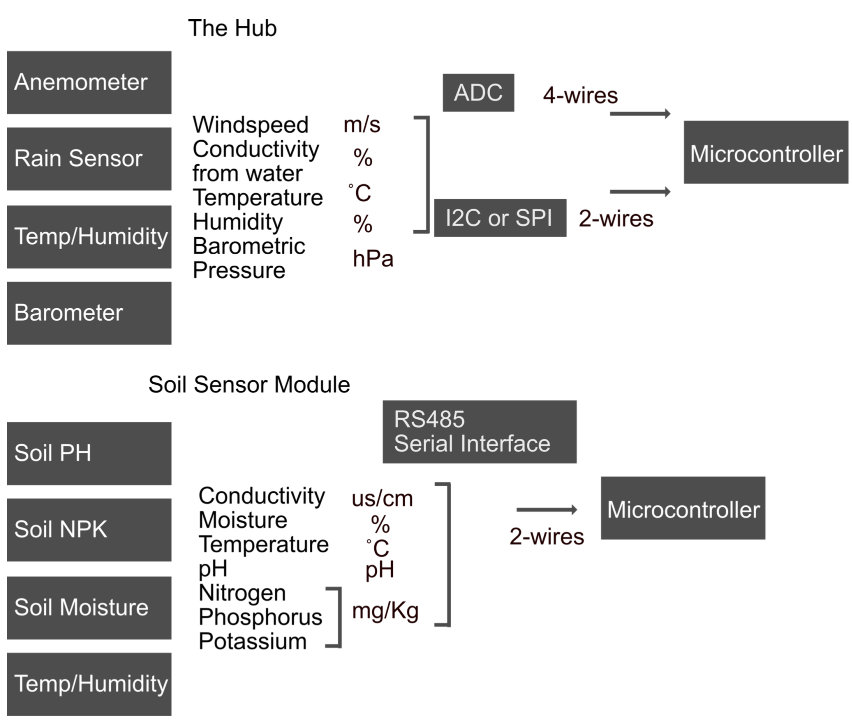

Figure 47: Sensor Measurements and Communication Protocols

Sensors and Robot Behavior

While it is important to understand which sensors and microcontrollers are being implemented on the hub and the rover, it is equally important to know how these electronics impact the behavior of the system altogether. On the hub, the data recorded from the rain and wind sensors have a large impact on the system behavior. In a scenario where the rain sensor records a reading higher than a certain threshold, the hub will indicate that the rover will not need to water the crops for a set period of time. Similarly, if the wind sensor were to read that the levels of wind are at an unsafe value, the hub will communicate to the rover that it should not leave the hub to ensure the rover stays safe. Some sensors, however, such as the temperature and humidity sensors, will simply have their values stored in the SD card for analysis from the operator.

While the sensors on the hub have a considerable influence on the decisions made by the rover, the sensors on the rover also affect the system. The main sensor on the rover, the soil sensor, has a plethora of different readings that it produces with each of which having an effect on the rover's behavior. Using the pH and NPK readings from this sensor, the rover can adjust the soil's characteristics accordingly using the fertilizer tank mentioned in the "Rover Fluids System Design" section. Additionally, using the moisture readings from this sensor will allow the rover to distribute an accurate amount of water for the crops. Ideally, a water gauge sensor in the tank of the rover will indicate to the rover that it must return to the hub for refilling. This is currently not procured in this iteration of the project but could be integrated in the future.

Localization and Control

The rover will be navigating a field of crops planted in rows such that each individual crop's GPS coordinates may be approximated. Instead of relying on machine vision to maneuver around an ever changing environment due to plant growth and unknown visibility conditions, the rover utilizes RTK GPS for lower frequency localization and a control system making use of an array of sensors. Multiple sensors of various types are used for error checking, and to obtain location approximations at a higher frequency than the limits of the RTK GPS which may have delays on the order of seconds. Specifically motor encoders located on the axle of each of the four motors and an inertial measurement unit (IMU) with a gyroscope and accelerometer are used to update location information while the RTK is communicating with Satellites and the Department of Transportation (DOT). The information from GPS, which gives an absolute position and the encoders and IMU which use immediate feedback from the motion of the rover are fused in such a way that a control loop can be formed with access to position, velocity, and acceleration data. The control unit, a Raspberry Pi, directly communicates with all three sensors and is able to log data. Recently taken data is utilized in code by a Kalman filter, a control theory approach that allows both a prediction and update step to model the state of the physical system.

The previously mentioned sensing algorithm is shown graphically in Figure 48 below and outlines half of the control system. The Raspberry Pi directly interfaces with two motor controllers each powering two motors. These possess H-bridge circuits which allows control over the direction of the motor rotation and can additionally control motor speed through PWM. These and additional components that allow monitoring current and power use over time are used to monitor the state of the motors and control them.

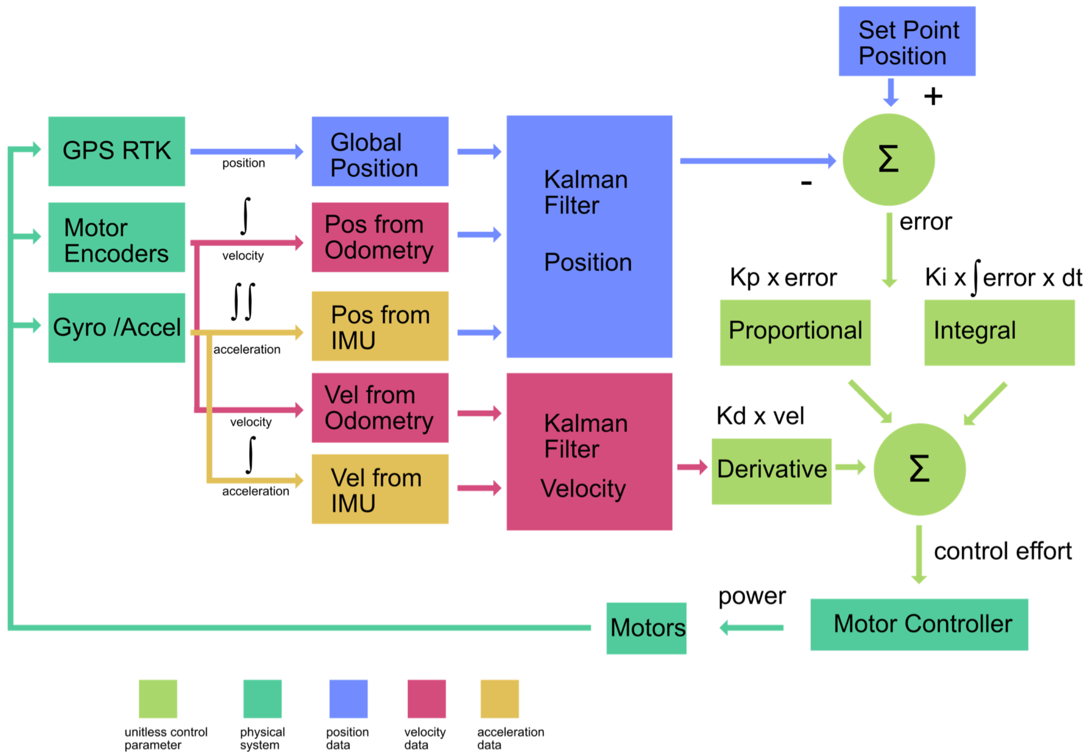

Figure 48: Localization and Position Control Diagram.

After the sensors and localization algorithm have determined a close estimate of position, and the rover has a task to accomplish at a different location, the control mechanism of proportional-integral–derivative (PID) is used to drive the motors to the location. This rover requires both position and velocity control as it must exhibit a wide variety of behaviors. While soil sensor measurements are not entirely time dependent or sensitive, the other task of carrying a water tank requires smooth movements to accommodate the dynamics of a large quantity of fluid. Through experimentation with the tank at various fill levels, and different magnitudes of traction for differing soil conditions, PID parameters can be tuned and substituted for any situation that may occur. For example, the dynamics of driving on wet loose soil may have an impact on maximum speed to not spin out which may vastly differ from driving on compact dry soil where overshooting location may pose a problem. For these reasons, computationally redundant sensor systems, as well as physical bump sensors and distance sensors not only allow precise position prediction and control, but also act as fail safes in scenarios such as spin-outs, undetected obstacles, and performance at low battery.

Electrical Systems and Communication

Computation occurs between the Raspberry Pis, which acts as the brain and interface of the high level robot behavior, localization and position control, and the two Arduino Unos that operate sensors and simpler mechanisms that require less feedback. One Arduino is stationed on the rover with the main purpose of soil conditions measurements and error checking while the other provides weather and environmental data on the hub. The Arduino on the rover interacts with the Raspberry Pi via serial communication receiving the signal of when to take data and sending data points as well as informing the controller of emergencies such as low battery or rain. The two Arduinos also utilize serial communication but through a pair of long range radio transmitters and receivers, instead of being directly connected. The range of the transmitters and receivers has a maximum of 100 m, which is well within the space of a 1000 square foot field. The Raspberry Pi can be controlled or monitored with a laptop at close ranges through Bluetooth and SSH; it also saves all data (weather, soil, and location records) on a micro SD card in a MySQL database. For redundancy some of this data as well as debugging logs are also directed recorded on a different micro SD card with one of the Arduinos. The Raspberry Pi runs off of Python due ease of use and the numerous libraries of code appropriate for GPS, sensing, motor control, and database storage. The Arduinos both run a simplified version of C/C++ and in most instances have a simpler software design as most of their behavior involves interfacing with sensors and peripherals.

While many of the weather sensors including the temperature and humidity sensor, anemometer, and rain sensor, are interacted with through voltage readings on the Arduino's ADC, the soil condition sensor uses a RS485, a type of serial communication. To take readings, the Arduino requests a specific value in an inquiry and receives packets of values to be decoded into the correct units. Additionally, the barometer uses I2C, a synchronous communication protocol. On the other system, the Raspberry Pi, the IMU also uses I2C while the RTK GPS uses an asynchronous communication called UART. Understanding the details and limits of these communication protocols is essential to the various microcontrollers and sensors functioning together correctly. Many of them involve error checking which will make the systems resilient from unpreventable transmission issues. These systems form a strong basis for complex software utilizing environmental feedback and redundant controls for the rover's actuated mechanisms.

Manufacturing

Several different manufacturing techniques were used in the creation of the prototype. Both traditional and additive methods were used. This section will discuss the various methods used, why they were used and how they were carried out. Additionally, the purchasing of raw materials as well as prefabricated components will be discussed.

Machining

There were three major parts that were machined, they are all a part of the wheel subassembly and were machined to precisely fit together. These parts were the wheel hub, the wheel covers, and the driven axle. Each part was machined on a Haas MiniMill using basic drilling and pocketing operations.

The first parts machined were the wheel hubs. While the wheel itself was purchased it needed to be modified to suit the needs of the project. Changes that needed to be made included the drilling of four additional holes into the hub to allow for supports to be added. The decision to machine these holes was made due to the fact that a high level of uniformity was needed and the most reliable way to create a repeatable process is using a computer aided drilling process. The wheel hubs presented a unique set of challenges when machining due to their irregular shape, large size, and non-standard material for the process. To combat these difficulties several steps were taken. To combat the issues presented by the size and shape of the hubs, a special fixturing was devised to clamp the hub at four evenly spaced points along the other section of the hub. Additionally due to the irregular geometry, ensuring that the hub was aligned presented its own challenges. To ensure that the hub was properly aligned, in addition to the standard probing required to successfully run a computer aided machining process, several extra steps were taken to ensure that the part was fastened in the correct position. Measures were taken to ensure that the spokes of the hub were properly aligned along the x and y axises of the mill including using a sensitive probe to measure the distance away from straight of the spoke. By getting the measurements of the probe within the determined acceptable range, plus or minus 5 nm of change from one end of the spoke to the other, the proper alignment of the hub was able to be ensured. Once fixtured, the machining process on the wheels was still non-standard as the hubs are made of high density polyurethane plastic, a material not often used in milling procedures. As such precautions needed to be taken in the feed rates and spindle speeds selected for the process. Based on information presented by the faculty in charge of running the machine shop, appropriate feed rates and spindle speeds were selected. Once the unique material had been accounted for the actual process carried out on the mill was fairly standard as it was a single step drilling operation using a 3/8ths inch drill bit.

The second set of parts machined were the wheel covers. These are metal plates used to help transmit torque from the axle to the wheel. They are designed to reduce the amount of tangential force needed to apply sufficient torque to move the rover. They needed holes drilled in them to match the holes in the wheel hub so that a shaft could be passed through both to complete the torque transfer from the axle to the wheel. These parts presented significantly fewer issues when compared to the hubs as they had a smooth surface profile that allowed for much simpler fixturing and didn’t require the additional steps to ensure proper alignment. As with the milling process for the wheel hubs the operation for the wheel covers was also a single step drilling operation using a 3/8ths inch drill bit to make through holes in the covers.

The final machined parts were the axles. In order for the axels to be keyed to properly fixture the sprocket on them a pocketing operation was needed. To perform this operation the axel was fixtured in a vice in the mill. This was the most standard fixturing as it is often used to fixture stock in the mill for machining. The pocketing procedure used was also a standard procedure and was a single tool process however due to the size of the end mill used (1/8th inch) it required multiple passes to successfully complete.

Welding

The rover design consists of multiple welded parts. The welding method of choice was MIG (Metal Inert Gas) welding. MIG welding “is an arc welding process that uses a continuous solid wire electrode heated and fed into the weld pool from a welding gun. The two base materials are melted together forming a join. The gun feeds a shielding gas alongside the electrode helping protect the weld pool from airborne contaminants” (Metal Inert Gas (MIG) Welding - Process and Applications). The chassis of the rover is made up of steel square tubing that is welded together for structural support. Other parts of the design that were welded include the wheel hub design. The wheel hub design consists of two metal plates for each of the four wheels, an axle, and a key and sprocket. The axle is to be welded to the inner facing metal plate that clamps the wheel so that the rotational force of the axle can be transmitted to the wheels.

Printing

Many of the components in the rover were 3D-printed, due to the rapid prototyping and flexibility available at a decreased cost. Also, the design could be modified and a new iteration could be manufactured without adversely affecting the length of time. One of the critical components of the rover that was decided to be printed were the collars that connect the axels to the wheels. The dimensions were customized to allow a tight fit between the axles and wheels such that slipping was minimized. The material was selected to be PLA due to its strength compared to its low cost, see in Figure 49.

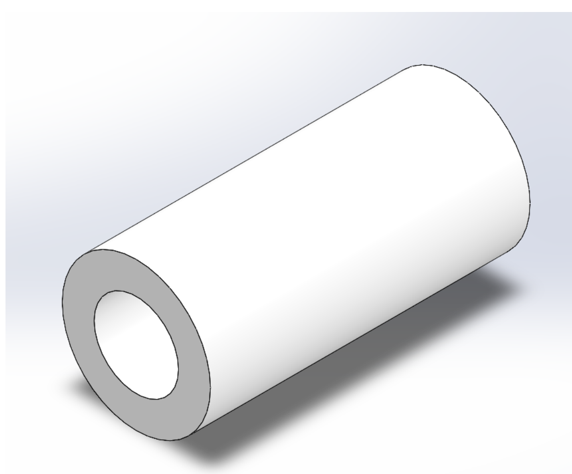

Figure 49: Model of Axle Collars

Also, the gear and pinion for the actuated filler cap mechanism was printed, since it allowed customizable dimensions to fit the goals and constraints. Since there wouldn't be a lot of stresses on the components, low infill PLA was selected as the material. The model of the final design can be seen in Figure 50.

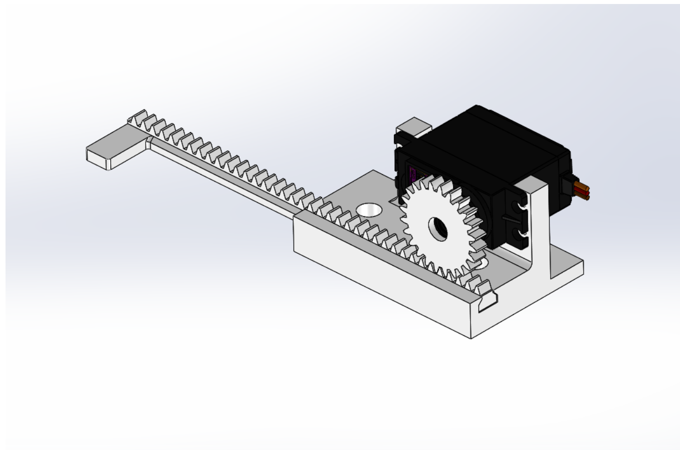

Figure 50: Model of Rack and Pinion Mechanism

A plastic mount for the motor encoders was also printed so that the axle holds a plastic rod which has the motor encoder wheel glued to it, and then a block that holds the actual encoder in position. The mount was printed out of black PLA. The rod was glued to the end of the axle on the interior of the rover and the larger block piece was glued to the axle support plate.

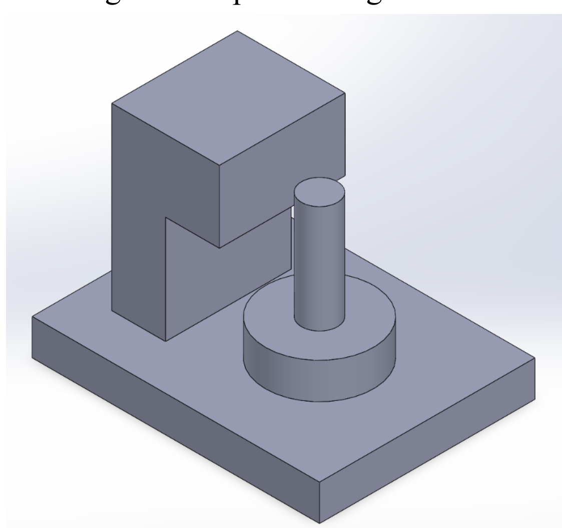

Figure 51: Encoder Mount Assembly

Testing & Results

Testing Structure

To understand if the rover and hub are fulfilling their purposes, qualitative and quantitative tests must be performed. Fundamental systems like power and fluid delivery systems on both the rover and the hub were the focus of the testing in addition to motion and autonomous behavior testing. To test these systems, the team decomposed the major objectives of the project into smaller subsequent tests that together fulfill them. The original objectives of this project were as follows:

1. To develop a rover capable of high weight carrying capacity.
2. To have field irrigation capabilities on board the rover to deliver fluid efficiently over a large space.
3. To equip the rover with sensors and controllers to allow for autonomous navigation through a crop field.
4. To utilize a sensor array on the rover and the baes station to conduct soil testing, atmospheric conditions monitoring, and rover-hub communication.
5. To refuel and recharge the rover at a central base station.

The decomposition of these objectives into smaller goals are as follows:

1. To develop a rover capable of high weight carrying capacity.
    a. Move linearly
    b. Skid turn
2. To have field irrigation capabilities on board the rover to deliver fluid efficiently over a large space.
    a. Hold water
    b. Move water to spray bar
    c. Allow refilling
3. To equip the rover with sensors and controllers to allow for autonomous navigation through a crop field.
    a. Receive localization information from RTK GPS
    b. Process encoder values
    c. Process IMU values
4. To utilize a sensor array on the rover and the base station to conduct soil testing, atmospheric conditions monitoring, and rover-hub communication.
    a. Actuate sensor
    b. Relay sensor data
    c. Collect motion data
    d. Relay to RTK GPS

    e. Communicate data between rover and hub
5. Create solar base station hub for rover to resupply
    a. Charge battery using solar energy
    b. Hold water
    c. Dispense water
    d. House the rover

Ideally, the testing structure of this project contains a full course that mimics a plot of crops. The layout of this test is depicted in Figure 52. This test would require the rover to leave the hub and follow the crop lines while watering. It would then reach the end of the crop and turn onto the next line of crops and continue. After running low on water or power, the rover would find the shortest path to return to the hub without destroying crops, and refill/recharge itself. In reality, the group did not have access to a location that could fulfill the proper space to perform this full-on test. Therefore, this situation was turned into several smaller tests that would prove the project's capabilities.

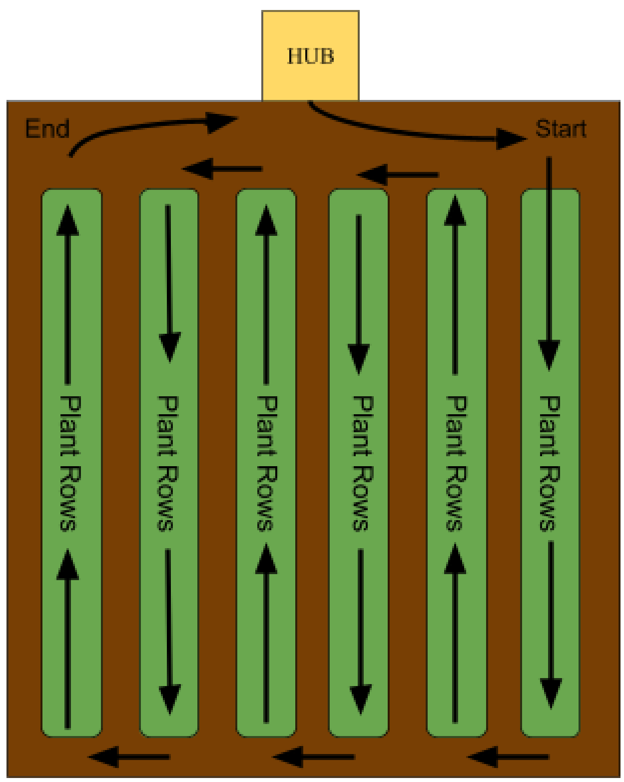

Figure 52: Rover Testing Route

For the rover specifically, there are six tests that fulfill the five decomposed objectives and the ideal situation. The tests are located below.

Rover Testing Goals:

1. Forward and backward locomotion
2. Skid turning
3. Water spraying
4. Docking with hub
5. Soil sensor insertion
6. Autonomous navigation

For the hub specifically, there are three tests that fulfill the five decomposed objectives and the ideal situation. The tests are located below.

Hub Testing Goals:

1. Dispense water into rover
2. Obtain atmospheric data
3. Protect rover

The results of these tests are located in the tables below as well as relevant notes on the tests regarding its success level.

Rover Testing Results

Test	Result	Note
Forward/Backward moving	Successful	Stable and straight
Skid turning	Semi-Successful	Internal friction and sprocket security hinders adequate motion
Water spraying	Semi-Successful	Low pressure, stronger pump needed
Docking with hub	Successful	Lining up can be difficult but still works as intended
Soil sensor insertion	Successful	Works as intended, sturdy linear motion
Autonomous navigation	Semi-Successful	Needs improvement and further development

Table 4: Rover testing results

It was determined through testing that the spray time of the rover was around 22 minutes, and had a flow rate of about 0.42 gallons per minute (GPM). The pressure loss across all of the tubing and fittings was significant enough to cause the 1-GPM pump to lose a flow rate of about 0.58 GPM as it traveled from the pump to the outlet of the nozzles. The rover tests did not accrue any other quantitative data besides fluid flow.

Figure 53: Rover parked in hub

The testing process for the rover's spray system began with spraying water from the three rear-mounted nozzles, as seen in Figure 54. As the rover drove straight in a field, water was sprayed out of the nozzles to simulate dispensing water over rows of crops. From the test, a constant spray velocity out of all three nozzles was achieved.

Figure 54: Testing of Spray System Outside

Hub Testing Results

Test	Result	Note
Dispense water into rover	Semi-Successful	Works as intended (0.42 GPM and 22 minute spray time)
Obtain weather data	Successful	Sensors work as intended and can relay data
Protect rover	Successful	Limits weather contact of rover
Weatherproofing	Successful	Water does not soak wood

Table 5: Hub testing results

The hub tests obtained some sensor data from the mounted atmospheric/meteorological apparatus and the specific quantitative information is located in the data collection section in table six.

Data Collection

Besides the charging aspect of the hub, the other purpose of the hub was to store soil data collected by the rover. For the soil data, a transceiver system was utilized to send data wirelessly to the hub. This data is used to see the current readings of the soil and to see what could be improved in the soil based on the readings. The range of the nRF transceiver system is around 100 m, which is sufficient for a farmspace of 1,000 square feet. Field data is being transmitted which includes soil temperature readings, moisture levels, pH measurements, and NPK readings. On board the hub, there are multiple sensors which give readings of the current environment and weather in the area. In order to achieve this, an anemometer, barometer, rain sensor and temperature/humidity sensor is placed onto the hub to collect data. This data is used to record wind speeds, barometric pressure, whether it is raining, degrees in Celsius and Fahrenheit, and the amount of humidity in the air. From this data, any patterns involving these metrics are stored. The format and code for all of this data is seen in Appendix C. All these sensors are operated through an Arduino which sends the data directly to another Arduino on the hub for it to be stored onto an SD card. This can be viewed on a computer as a text file and the data format is displayed as seen in Table 6.

Temperature	20.80 C
Humidity	39.30%
Wind Speed	156.78 mph
Pressure	983.87 hPa
Soil Moisture	50%

Table 6: Example of Displayed Sensor Readings

To ensure that the sensors were functioning properly, we tested the readings in different environments to see whether the readings changed as expected. All the sensors functioned correctly, besides the NPK sensor. The NPK sensor was operational earlier on in the year, but suddenly broke. In order to keep a soil sensor as a part of our project, we changed out the NPK sensor with a soil moisture sensor. This new sensor only measures the amount of moisture in the soil, and this data can be used to determine whether a plant needs to be watered. Along with testing the weather array sensors, the range of the nRF transceiver system was tested to ensure the range was suitable for our needs. Although it is listed to have a range of 100 m, our results showed that the nRF's range capabilities were closer to 30 m in an open space. This is significantly lower than the expected range; however, 30 m is well within our needs to communicate data over a 1,000 square foot field.

Recommendations & Discussion

From the testing and results section of this project, the team developed a set of recommendations that aligned with the objectives that were created at the beginning of the project. These were compiled in response to the objectives that were either partially or not met. This section has been split up into three categories; mechanical, electrical, and future iterations. The mechanical section goes in depth into the transmission, drivetrain, and fluids systems. The electrical section will discuss further development of localization control methods, along with autonomous charging and soil sensor options. Lastly, there is a discussion of potential iterations of this project that could be added in future years.

Mechanical

The mechanical testing of the rover led the team to both positive and negative results based on the objectives that were laid out. The team found that the locomotion of the rover forward and backwards worked as expected, with the spray system working as intended to dispense water. The ability to dock with the hub and soil sensor insertion ability were also successful and worked as intended. However, the skid turning and autonomous navigation fell below the team's expectations.

The skid turning worked improperly due to unexpected friction values that led to slipping on the tires and increased loading on the smaller structural components of the sprocket assembly. The team recommends adding a higher gear ratio in the sprocket and chain system, as the 2:1 ratio cannot handle higher-end friction forces when skid steering. An additional fix to this issue would be to implement a full suspension system that would give enough vertical travel to maintain contact on rough terrain on all four tires. Lastly, a more capable all-terrain tire with increased surface contact would be prudent to solve the rough terrain traction issue.

Considerations of high pressure loss across the fluid delivery led to the determination that a higher pressure pump should be used in the system so that a higher flow rate leaving the nozzles could be achieved. Another issue that was found while testing the spray system was that there was leaking from the nozzles. These high pressure nozzles had their check valves bypassed (permanently opened) because the pump pressure wasn't high enough to engage the valves, along with the fact that the pump already leaked when connected to power. If a higher pressure pump and better nozzles were used in the system (since both were inexpensive options), that would eliminate the pressure and leaking issues.

Electrical

Some recommendations for the electrical system of this project would include further developing the localization and control systems; implementing fully autonomous charging of the hub and rover batteries, and replacing the soil moisture sensor on the actuated arm with a new NPK soil sensor.

In order for the rover to navigate the field and localize itself in reference to the hub, the RTK GPS was implemented with the base station located on the hub and the mobile unit on the rover. However, this localization and control system could be further developed as, in this iteration, information from the GPS is available but is not being processed. The team recommends processing the data gathered from the RTK GPS to create paths for the rover to travel along autonomously to avoid damaging the crops.

Next, along with the autonomy of the control system, the hub should act as an autonomous recharging station to refuel the battery of the rover after driving around the crops. The current iteration requires the battery to be taken out of the hub and manually plugged into the solar panel for charging. Along with autonomous charging, a future implementation would be to monitor the battery life of the rover, and return it back to the hub after the battery goes below a certain threshold. This would prevent the rover from getting stuck in the fields and losing its charge before returning back to the hub for charging.

While testing the original NPK soil sensor for the actuated sensor arm on the rover, the sensor malfunctioned and was no longer usable for this current iteration of the project. Although this sensor was replaced, its replacement was only capable of recording soil moisture levels. While knowing the moisture level of the soil near crops is quite valuable and can be processed to determine if the crops need watering, knowing the soil nutrients such as potassium, nitrates, etc. provides much more insight into the health of the plants. Because of this, the team recommends incorporating a higher quality NPK soil sensor to be used in conjunction with the arm on the rover. Additionally, knowing the nutrients in the soil could also allow, in a future iteration, for the distribution of fertilizer from the onboard spraying system to alter the soil characteristics accordingly.

Future Iterations

The intention of this project was to prototype an autonomous agricultural robot with scale, ease of use, and feasible price in mind. Through developing and attempting to meet objectives outlined in the description of work and comprehensive research in the field of agricultural robotics, the team has come to the conclusion that future iterations should focus on three main concepts: scaling the rover down and implementing swarm robotics coordination, making use of machine-vision to monitor plant health and unwanted weed growth, and emphasizing long term data collection which will allow deeper analysis of patterns and causal relationships between crop health and environmental conditions. The work done thus far has focused on mechanical actuation and lower level capabilities such as navigation and data collection. As such, the project would benefit from a team more oriented and capable of software development, which could implement more complex behavior in the rover and hub.

The task of watering and fertilizing a large field of plants efficiently can be seen as a delivery problem located on a cartesian grid. Large scale problems such as these have been solved efficiently with the use of swarm robotics. For example, the robots in an Ocado owned supermarket in Britain process orders and maneuver groceries at very high efficiency and speed by utilizing swarm robotics algorithms. Moving groceries on a grid with multiple robots is much like moving fluids like fertilizer and water to various plants on a field. Both systems are redundant and resilient to the failure of a single robot and maximize efficiency through optimal path planning. The rovers additionally have the potential to tailor fertilization and watering to specific plants that may have varying health and needs through coordination and sensor fusion. While the team focused on the use of a single rover tending to a small field of 1000 square feet, this may be better suited to multiple smaller scale rovers covering a greater area. The hub remains inactive, besides solar charging, much of the day and could most likely support more than one rover. Additionally, multiple lighter rovers with tanks better suited to their size would be more efficient. These smaller designs would not only be faster, but would also require lower torque motors and less complex gearing and therefore would be cheaper to manufacture. The rovers would each be outfitted with GPS and the ability to communicate with each other over RF and therefore they would all have access to the same sensor data. Connecting these robots in a swarm system along with the hub could assist with the task of localization by increasing accuracy, and frequency of location data. There are many strengths to moving from a model utilizing a single large rover to one involving many smaller ones. Although it would include many new challenges, this would be an exciting direction for the solar agribots project that may be more applicable for use on small farms.

The rover's action and information processing currently occurs on a Raspberry Pi, which has the potential for extensive optical sensor integration. While navigation is dependent on the attached IMU, encoders, and GPS, its capabilities could be expanded with cameras to track and detect crops, adding an extra layer of safety feature preventing damage. More interestingly, the Raspberry Pi runs Python which offers many libraries for machine vision. With the priority of the rover being plant health, cameras could be used to classify instances of plant disease and weed growth. The chain of actions necessary to diagnose plant disease are as follows: identify the location and therefore, the specific plant, analyze the quality of the image and retake if it is subpar, crop the image, use a pre-trained neural network to classify plant type and health, save the data and send over RF to the hub. Large datasets of crops labeled by health are available as well as open source image processing neural networks, thus training a machine learning algorithm would not be necessary. While this task would require a solid understanding of AI and programming, it would add behavior to the rover that more closely emulates the actions a farmer might take while inspecting crops.

In terms of data collection and analysis, future iterations could collect data that further alters the actions of the rover, as well as analyze different aspects of the environment over a period of time. An example of altering the rover from the weather array would be by using the rain sensor and barometer to determine whether it is currently raining, thus stopping the rover from going out for the day to water. Along with this, further analysis of the weather array's data can be taken from the SD card and plotted to see trends in the weather.

Broader Impact

To fully understand the potential impact and implications of our project, the team put together this section that is split up into four categories: Engineering Ethics, Societal and Global Impacts, Environmental Impacts, and Economic Factors. Each of these sections culminate in a conclusive look at how this project could have a real world impact.

In developing this project, the team had to keep the engineering code of ethics at the forefront of the design constraints. Each code of ethics was examined and their respective affect on the project accounted for. The first code of ethics, as stated by the National Society for Professional Engineers, says "Hold paramount the safety, health, and welfare of the public" (NSPE 2022). This project sits in the real world so there is always potential danger to those using it. The rover is designed to move so slowly that it is virtually impossible to be a health concern, but in the future, implementing an ocular safety net around the rover that would have it stop before it ran into a person would be smart. The second code of ethics says "Perform services only in areas of their competence" (NSPE 2022). To stay in line with this, the rover should only be used for agricultural purposes as that is the core design of the project. The third code of ethics states "Issue public statements only in an objective and truthful manner" (NSPE 2022). This code of ethics pertains directly to this report, which has been written in a manner in direct accordance with this code of ethics. In writing this report, proper research was conducted, proper citations given, and only honest content included. The fourth code of ethics reads "Act for each employer or client as faithful agents or trustees" (NSPE 2022). As this project is only acting for the school, the team has taken into account all necessary requirements from the school to correctly fulfill completion. The fifth code of ethics asserts "avoid deceptive acts" (NSPE 2022). This code of ethics is fairly self-explanatory to follow which the team has done. In no part of this project did the team lie, deceive, or otherwise misdirect anyone involved. The last code of ethics declares "Conduct themselves honorably, responsibly, ethically, and lawfully so as to enhance the honor, reputation, and usefulness of the profession" (NSPE 2022). This last code of ethics serves as the most important and will guide the team into their respective professional engineering lives. Following this last code was fundamental in making this project work.

This project, and its implications towards the target audience, impacts the daily lives of small to medium sized farm owners and those subsequently impacted by them. The farmer demographic is impacted in a beneficial manner that aids their efforts regarding labor. The project saves farmers time by taking over tasks that they would normally spend a few hours on everyday or every other day depending on their schedule. This trend allows farmers to fit more into their schedule, which could expand their career or farm. The rover is meant to supplement labor that is not there, not replace existing laborers. However, in the event that a farmer places human workers with the rover, some negative impacts can come of this. Individuals may lose their jobs, which could potentially disrupt families and lives. This is hopefully not a recurring theme with the deployment of this project and it is not the intended impact given the labor issues that we researched in the agricultural industry. Positive impacts of this project for other groups of people could include better production yields for farmers, which means communities have access to more food and resources. The overall health and safety of those impacted by this project are not greatly affected as this project does not play an interactive role with humans or the quality of the food produced. Cultural impacts are under the umbrella of cultural trends regarding autonomy and the internet of things. The solar agribot is culturally to the increase in tech-savvy mindsets that are becoming more commonplace. Globally, the solar agribot is doing nothing new or groundbreaking besides translating existing technologies into agriculture. There are existing swarm robots in agriculture, but not many.

The concept for this project took environmental impacts into consideration when designing the rover and the hub. These systems are able to be completely sustainable in multiple ways. The rover and the hub are designed to be powered by solar panels and the irrigation system is equipped with rain collection capabilities. The rover does have potentially negative effects on animals that are along the path of the rover. Currently, the rover does not have the ability to detect obstacles around it. This is an upgrade that future interactions of the project should include to reduce the environmental impacts of the rover. Another potential environmental impact is the use of lithium ion batteries and lead-acid batteries that are harmful to the environment if not handled properly or if not properly disposed of.

The economic factors that could impact a potential buyer are the cost of our project. This project costs between 2500 to 3000 dollars. When compared to existing robots with similar capabilities, such as the Xavier robot, that has a price tag in the tens of thousands. The solar agribot comes at a much more affordable price range. With that being said, this is the cost of the robot without the cost of labor and research. These two factors played a large role in the affordable cost of our rover. This was the intent of our project as it was aimed towards smaller scale farmers who could not afford the expensive prices of industrial agricultural machines. As for our competitors, we occupy a niche part of the market as previously mentioned. Their main focus is on developing heavy machinery to assist large scale companies and is intended to operate within a much larger scale than our project intents. Thus, we have no economic impact on them.

References

Antaya, Alexander Antonio, et al. *Lionfish Bot 2.0.* : Worcester Polytechnic Institute, 2019.

Best Research-Cell Efficiency Chart - Nrel.gov.

Burr, A and Cheatham, J: Mechanical Design and Analysis, 2nd edition, section 5.2. Prentice-Hall, 1995.https://www.nrel.gov/pv/assets/pdfs/best-research-cell-efficiencies-rev210726.pdf.

Carr. McMaster. (n.d.). Retrieved December 16, 2021, from https://www.mcmaster.com/tanks/material~plastic/wall-mount-plastic-easy-drain-tanks/

Cantelli, Bonaccorso, Longo, Melita, Schillaci, & Muscato. (2019). A Small Versatile Electrical Robot for Autonomous Spraying in Agriculture. *AgriEngineering*, *1*(3), 391–402. MDPI AG. Retrieved from http://dx.doi.org/10.3390/agriengineering1030029

Caproni, William Bryson, and Erik Richard Dahlinghaus. *Modular Environmental Controller for Sustainable Agriculture.* : Worcester Polytechnic Institute, 2013.

Center for agroecology: Growing sustainable food systems. Center for Agroecology: Growing sustainable food systems. (n.d.). Retrieved December 16, 2021, from https://agroecology.ucsc.edu/

Correll, Nikolaus, et al. “Building a Distributed Robot Garden.” *2009 IEEE/RSJ International Conference on Intelligent Robots and Systems*, 2009, https://doi.org/10.1109/iros.2009.5354261.

Farming and farm income. USDA ERS - Farming and Farm Income. (n.d.). Retrieved December 16, 2021, from https://www.ers.usda.gov/data-products/ag-and-food-statistics-charting-the-essentials/farming-and-farm-income/#:~:text=The%20number%20of%20U.S.%20farms,sharply%20until%20the%20early%201970s.&text=In%20the%20most%20recent%20survey,from%202.20%20million%20in%202007.

Fendt, AGCO. “Mars: Robot System for Planting and Accurate Documentation.” *Fendt*, Fendt, 8 Sept. 2017, https://www.fendt.com/int/fendt-mars.

Fendt, A. G. C. O. (n.d.). Fendt puts the new robot 'xaver' to use. Fendt. Retrieved March 5, 2022, from https://www.fendt.com/int/fendt-xaver

Hoppe, Robert A., James MacDonald and Penni Korb. 2010. Small Farms in the United States: Persistence Under Pressure, EIB-63, U.S. Department of Agriculture, Economic Research Service, February 2010.

Hutterer, P. (2020, November 3). It's all about physics: Tipping. Rosenbauer Blog. Retrieved February 24, 2022, from https://www.rosenbauer.com/blog/en/driving-safety-tipping/

Jin, Yucheng, et al. “Development Status and Trend of Agricultural Robot Technology.” *International Journal of Agricultural and Biological Engineering*, vol. 14, no. 3, 2021, pp. 1–19., https://doi.org/10.25165/j.ijabe.20211404.6821.

Lowenberg‐DeBoer, James, et al. “Lessons to Be Learned in Adoption of Autonomous Equipment for Field Crops.” *Applied Economic Perspectives and Policy*, 2021, https://doi.org/10.1002/aepp.13177.

McBride Author, Ali. “Comprehensive Guide to Solar Panel Types.” *Aurora Solar*, 27 Aug. 2021, https://www.aurorasolar.com/blog/solar-panel-types-guide/.

“National Soil Health Measurements to Accelerate Agricultural Transformation.” *Soil Health Institute*, 8 Oct. 2018, https://soilhealthinstitute.org/national-soil-health-measurements-accelerate-agricultural-transformation/.

N. S. Naik, V. V. Shete and S. R. Danve, "Precision agriculture robot for seeding function," 2016 International Conference on Inventive Computation Technologies (ICICT), 2016, pp. 1-3, doi: 10.1109/INVENTIVE.2016.7824880.

“Our Project .” *Rowesys*, Robotic System Labs, 2020, https://rowesys.ethz.ch/our-project/.

Pongratz, Daniel Joseph, Nicholas Tyler Rowles, and Harrison Louis Vaporciyan. *Autonomous Snowblower.* : Worcester Polytechnic Institute, 2017.

Proskokov, A V, et al. “Software and Hardware Control Robotic Lawnmowers.” *Journal of Physics: Conference Series*, vol. 1059, 2018, p. 012018., https://doi.org/10.1088/1742-6596/1059/1/012018.

“Rantizo System Products.” *Rantizo*, 26 Aug. 2021, https://www.rantizo.com/drone-spraying-equipment/.

Seed Saver. (2022). How to grow carrots. Seed Savers. Retrieved April 26, 2022, from https://www.seedsavers.org/grow-carrot#:~:text=Spacing%20Requirements,rows%2016%2D24%20inches%20apart.

Stegeman, John Thomas, and Anqi Shen. *Agricultural Swarm Robotic System.* : Worcester Polytechnic Institute, 2018.

Takeda, & Shimoyama, I. (2019). Slip and Magnetic Attraction Effects in a Microrobot with Magnetic-Wheels and Skid-Steering. Micromachines (Basel), 10(6), 379–. https://doi.org/10.3390/mi10060379

T. Blender, T. Buchner, B. Fernandez, B. Pichlmaier and C. Schlegel, "Managing a Mobile Agricultural Robot Swarm for a seeding task," IECON 2016 - 42nd Annual Conference of the IEEE Industrial Electronics Society, 2016, pp. 6879-6886, doi: 10.1109/IECON.2016.7793638.

Tu, Xuyong, et al. “Robust Navigation Control of a 4WD/4ws Agricultural Robotic Vehicle.” *Computers and Electronics in Agriculture*, vol. 164, 2019, p. 104892., https://doi.org/10.1016/j.compag.2019.104892.

“U.S. Energy Information Administration - EIA - Independent Statistics and Analysis.” Where Solar Is Found - U.S. Energy Information Administration (EIA), https://www.eia.gov/energyexplained/solar/where-solar-is-found.php.

Ye B, Jiang J, Miao L, Yang P, Li J, Shen B. Feasibility Study of a Solar-Powered Electric Vehicle Charging Station Model. *Energies*. 2015; 8(11):13265-13283. https://doi.org/10.3390/en8111236

"Metal Inert Gas (MIG) Welding - Process and Applications." *TWI*, https://www.twi-global.com/technical-knowledge/job-knowledge/mig-welding-004#:~:text=What%20is%20Metal%20Inert%20Gas,melted%20together%20forming%20a%20join.

Appendix

Appendix A: Motor Torque Calculations

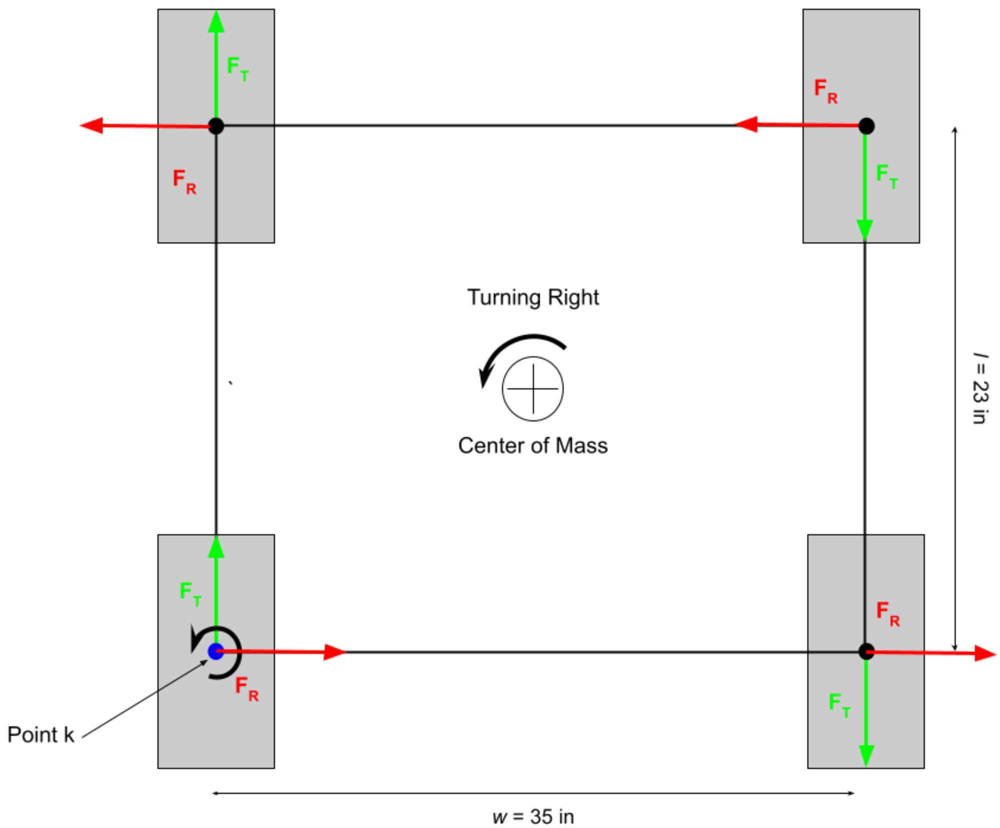

Variables: w=35in; l=23in; μ=0.39; W_t=200lb; r=5in

Moment about Point K clockwise

$$(1)\ M_k = F_T w + F_T w - F_R l - F_R l = 0$$

$$(2)\ M_k = 2F_T w - 2F_R l = 0$$

$$(3)\ 35F_T = 23F_R$$

$$(4)\ F_T = 23F_R/35$$

(5) ArcTan(23/35)=33°

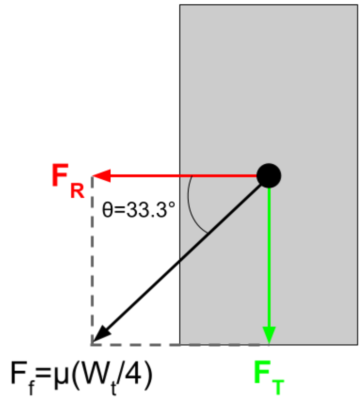

$$(6)\ F_T = F_f\, sin(\theta)$$

$$(7)\ F_f = \mu * N$$

$$(8)\ F_T = \mu \frac{W_t}{4}\, sin(\theta)$$

$$(9)\ F_T = 0.39 \frac{200}{4}\, sin(30°) = 10.62 lbf$$

$$(10)\quad T_T = F_T * r$$

$$(11)\quad T_T = 10.62 * 5/12 ft = 4.425 lbf * ft$$

$$(12)\quad T_T = 4.425 lbf * ft = 6\ Nm$$

Appendix B: Fluid Calculations for Estimated Spray Velocity

Goals	
Pressure & head loss over length of tube	
v_final out of sprayer nozzles	
HP required (head>25ft?)	

Assumptions	
h_drone (ft)	10
A_tube (in^2)	0.02761165418
L_tube (ft)	1
Water (Gal)	1
Flowrate (L/min	3.5
Flowrate (Gal/mi	0.924
Kinematic Visco:	0.000001047
laminar flow	yes
Max current (A)	2
Max Pressure (M	0.48

$Q = VA$

$m = \rho Q = \rho VA$

$\eta_{pump} = \frac{\dot{W}_{water\ horsepower}}{\dot{W}_{shaft}} = \frac{\dot{W}_{water\ horsepower}}{bhp} = \frac{\rho g \dot{V} H}{\omega T_{shaft}}$

$h_{L\text{-}Major} = f \frac{(L)(V^2)}{2(g)(D)}$

Where

$h_{L\text{-}Major}$ = head loss in ft or m.
f = Darcy-Weisbach friction factor
D= Diameter of pipe (ft or m)
L= Length of pipe (ft or m)
v= flow velocity (fps or mps)
g= gravitational acceleration

Reynold's number from kinematic viscosity:

$Re = \frac{V.d}{v}$

where:
Re is the Reynolds number
V is the pipe velocity (m/s)
d is the pipe diameter (m)
v is the kinematic viscosity (m²/s)

Reynold's number from absolute (dynamic) viscosity:

$Re = \frac{V.d.\rho}{\mu}$

where:
Re is the Reynolds number
V is the pipe velocity (m/s)
d is the pipe diameter (m)
ρ is the fluid density (kg/m³)
μ is the dynamic viscosity (Ns/m²)

$\Delta p = \rho g \Delta h,$

where:

Δh = The head loss due to pipe friction over the given length of pipe (SI units: m);[b]
g = The local acceleration due to gravity (m/s²).

Pipe ID (in)	Wall thickness (in)	Pipe OD (in)	Pipe ID (m)	Flowrate (m^3/s)	A_tube (m^2)	Reynolds Number	Relative Roughness	Friction Factor	L_tube (m)	Density of Water (kg/m^2)	Pressure Loss (N/m^2)
0.1875	0.125	0.3125	0.0047625	0.00005829516	0.000017813934	14885.41499	0.002099737533	0.031787	0.3048	997	10860.25339

Velocity (m/s)	Major Headloss (m)	Pressure Loss (MPa)
3.27	1.11	0.0109

	Velocity (m/s)
-> accounting for bends & connections between components	2.84

Appendix C: Hub Weather Data with Transmitter and Receiver Arduino Code

```
#include <SPI.h>
#include <nRF24L01.h>
#include <RF24.h>

RF24 radio(7, 8); // CE, CSN

const byte address[6] = "00001";
const int numReadings = 10;
int sensorPort = A0;
int sensorValue = 0;
float readings[numReadings];
int readIndex = 0;              // the index of the current reading
float total = 0;                  // the running total
float average = 0;                // the average
float averageFloat = 0;
struct MyData {
  byte averageFloat;
};
MyData data;

void setup() {
  radio.begin();
  radio.openWritingPipe(address);
  radio.setPALevel(RF24_PA_MIN);
  radio.stopListening();
  for (int thisReading = 0; thisReading < numReadings; thisReading++) {
    readings[thisReading] = 0;
  }
}

void loop() {
  total = total - readings[readIndex];
  // read from the sensor:
  sensorValue = analogRead(sensorPort);
  readings[readIndex] = sensorValue;
  // add the reading to the total:
  total = total + readings[readIndex];
```

```

#include <SPI.h>
#include <SD.h>
#include <Wire.h>
#include <Adafruit_Sensor.h>
#include "DHT.h"
#include <Adafruit_BMP280.h>
#include <Adafruit_GFX.h>
#include <nRF24L01.h>
#include <RF24.h>


#define DHTPIN 4
#define DHTTYPE DHT22
#define csPin 10 // chip select for SDCard
#define CE_PIN 7 //
#define CSN_PIN 8 //chip select for rf
#define BMP280_I2C_ADDRESS  0x76


RF24 radio(CE_PIN, CSN_PIN); // rf ce,cs
Adafruit_BMP280 bmp; // I2C
const int capteur_D = 3;       //Rain Sensor
const int capteur_A = A0;       //Rain Sensor
const byte address[6] = "00001";  //Address for receiver
int val_analogique;


DHT dht(DHTPIN, DHTTYPE);
File myFile;
struct MyData{
  byte averageFloat;
};
MyData data;
void setup() {

  Serial.begin(9600);
  radio.begin();
  radio.openReadingPipe(0, address);
  radio.setPALevel(RF24_PA_MIN);
```

```
  radio.startListening();
  bmp.begin();        //Begin the sensor
  pinMode(capteur_D, INPUT);
  pinMode(capteur_A, INPUT);
// Open serial communications and wait for port to open:
  dht.begin();

  while (!Serial) {
; // wait for serial port to connect. Needed for native USB
port only
}
  Serial.print("Initializing SD card...");
  if (!SD.begin(10)) {
    Serial.println("initialization failed!");
    return;
  }
  Serial.println("initialization done.");

}

void loop() {
    float sensorValue = analogRead(A2);
    float voltage = (sensorValue / 1023) * 5;
    float wind_speed = mapfloat(voltage, 0.4, 2, 0, 32.4);
    float speed_mph = ((wind_speed *3600)/1609.344);

    delay(1000);

    myFile = SD.open("test10.txt", FILE_WRITE);


    if (myFile) {
      Serial.println("************************************")
      ;
      Serial.println("Sample Start");
      Serial.print("Pressure = ");
      Serial.print(bmp.readPressure()/100);
      Serial.println(" hPa");
      myFile.print("Pressure = ");
      myFile.print(bmp.readPressure()/100);   //Save
      altitude into SD card
```

```
        altitude into SD card
        myFile.println(" hPa");
        Serial.print("Temperature = ");
        myFile.print("Temperature = ");
        Serial.print(dht.readTemperature());
        Serial.println(" C");
        myFile.print(dht.readTemperature());    //Save temp into SD card
        myFile.println(" C");
        Serial.print("Humidity = ");
        Serial.print(dht.readHumidity());
        Serial.println("%");
//        myFile.print("Humidity = ");
//        myFile.print(dht.readHumidity());     //Save humidity into SD card
//        myFile.println("%");
        Serial.print("Wind Speed =");
        Serial.print(wind_speed);
        Serial.print("m/s");
        Serial.print(" or ");
        Serial.print(speed_mph);
        Serial.println("mph");
//        myFile.print("Wind Speed =");
//        myFile.print(wind_speed);             //Save wind m/s to SD card
//        myFile.print("m/s");
//        myFile.print(" or ");
//        myFile.print(speed_mph);              //Save wind mph to SD card
//        myFile.println("mph");
       if(digitalRead(capteur_D) == LOW)
         {
           Serial.println("Digital value : wet");
           myFile.println("Digital value : wet");
           delay(10);
         }
        else
         {
           Serial.println("Digital value : dry");
           myFile.println("Digital value : dry");
           delay(10);
```

```
        }
        val_analogique=analogRead(capteur_A);
         Serial.print("Analog value : ");
         Serial.println(val_analogique);
//          Serial.print("Writing to test.txt...");
        Serial.println(myFile);
        Serial.println("first if");
      //  myFile.println("first if");
          if (radio.available()) {
            Serial.println("second if");
            myFile.println("second if");
//              char text[32] = "";
//              Serial.print(text);
            radio.read(&data, sizeof(MyData));
            Serial.print("Soil Moisture : ");
            Serial.print(data.averageFloat);
            Serial.println("%");
            myFile.print("Soil Moisture : ");
            myFile.print(data.averageFloat);
            myFile.print("%");
      }
      // close the file:
        myFile.close();
        Serial.println("************************************");
      } else {
        // if the file didn't open, print an error:
        Serial.println(myFile);
        Serial.println("error opening test.txt");
      }
     delay(1000);
}
float mapfloat(float x, float in_min, float in_max, float out_min, float out_max)
{
  return (x - in_min) * (out_max - out_min) / (in_max - in_min) + out_min;
}
```

```
  // advance to the next position in the array:
  readIndex = readIndex + 1;

    // if we're at the end of the array...
  if (readIndex >= numReadings) {
    // ...wrap around to the beginning:
    readIndex = 0;
  }

  // calculate the average:
  average = total / numReadings;
  data.averageFloat = 100 - ((average/1023) * 100);

//  const char text[] = "1 5 1 5";
//  radio.write(&text, sizeof(text));
  radio.write(&data, sizeof(MyData));
  Serial.print(averageFloat);
//  delay(1);
}
```

Appendix D: Test Code for Actuated Filler Cap Mechanism

```
#include <Wire.h>
#include <Adafruit_MLX90614.h>
#include <Servo.h>
float sum;
int dt=10;
int angle = 0.0;
Adafruit_MLX90614 mlx = Adafruit_MLX90614();
const int trig = 6;
const int echo = 7;

long duration;
int distance;
Servo myServo;

void setup(){
  pinMode(trig, OUTPUT);
  pinMode(echo, INPUT);
  Serial.begin(9600);
  myServo.attach(9);
  mlx.begin();
}

void loop(){
  int duration,distance;
  digitalWrite(trig,HIGH);
  delay(dt);
  digitalWrite(trig,LOW);
  duration = pulseIn(echo,HIGH);
  distance = duration*0.034/2;
  Serial.print("Distance: "); Serial.println(distance);
  return distance;

  myServo.write(0);
  if (distance <= 10)
  { myServo.write(360);
  }
  else
  { myServo.write(0);
  }
}

```

Appendix E: Soil NPK Sensor Arduino Code

```
#include <SoftwareSerial.h>

const int RO = 2; //RX
const int RE = 8; //Receiver
const int DE = 7; //Driver
const int DI = 3; //TX

const byte ph_inquiry[]= {0x01,0x03,0x00, 0x06, 0x00, 0x01, 0x64, 0x0B};
const byte moisture_inquiry[]= {0x01,0x03,0x00, 0x12, 0x00, 0x01, 0x24, 0x0f};
const byte temp_inquiry[]= {0x01,0x03,0x00, 0x13, 0x00, 0x01, 0x75, 0xcf};
const byte conduct_inquiry[]= {0x01,0x03,0x00, 0x15, 0x00, 0x01, 0x95, 0xce};
const byte npk_inquiry[]= {0x01,0x03,0x00, 0x1e, 0x00, 0x03, 0x65, 0xcd};

const float max_ph = 14.0;
const float min_ph = 0.0;
const float max_temp = 100.0;
const float min_temp = -20.0;
const float max_moisture = 100.0;
const float min_moisture = 0.0;
const float max_conduct = 8000.0;
const float min_conduct = 0.0;
const float max_n = 1000.0;
const float min_n = 0.0;
const float max_p = 1000.0;
const float min_p = 0.0;
const float max_k = 1000.0;
const float min_k = 0.0;

const int error_delay = 50;
const int max_errored_attempts = 5;

float a = -1.0; //pH
float t = -1.0; //˚C
float m = -1.0; //%
float c = -1.0; //US/cm
float n = -1.0; //mg/Kg
```

```
float p = -1.0; //mg/Kg
float k = -1.0; //mg/Kg

SoftwareSerial soil_sensor(RO,DI);

void setup() {
  Serial.begin(9600);
  soil_sensor.begin(9600);
  //  soil_sensor.setTimeout(100);
  pinMode(RE, OUTPUT);
  pinMode(DE, OUTPUT);

}

void Inquiry_Request()
{
  digitalWrite(DE, HIGH);
  digitalWrite(RE, HIGH);
  delay(30);
}

void Read_Request()
{
  digitalWrite(DE,LOW);
  digitalWrite(RE,LOW);
}

bool PH() // pH
{
  Inquiry_Request();
  byte response[] = {0x00,0x00,0x00,0x00,0x00,0x00,0x00};
  if(soil_sensor.write(ph_inquiry,sizeof(ph_inquiry))==8){
    Read_Request();
    for(int i=0;i<7;i++){
      response[i] = soil_sensor.read();
    }
  }

  float return_ph = (((float) response[3])*256 + (float) response[4])/100.0;
  if(return_ph > max_ph || return_ph < min_ph)
```

```
  {
    delay(error_delay);
    Serial.print("Incorrect pH Measurement: ");
    Serial.print(return_ph);
    Serial.println("pH");
    return false;
  }
  else
  {
    a = return_ph;
    return true;
  }
}

bool Temp() // ˚C
{
  Inquiry_Request();
  byte response[] = {0x00,0x00,0x00,0x00,0x00,0x00,0x00};
  if(soil_sensor.write(temp_inquiry,sizeof(temp_inquiry))==8
  ){
    Read_Request();
    for(int i=0;i<7;i++){
      response[i] = soil_sensor.read();
    }
  }

  float return_temp = (((float) response[3])*256 + (float)
  response[4])/10.0;
  if(return_temp > max_temp || return_temp < min_temp)
  {
    delay(error_delay);
    Serial.print("Incorrect Temp Measurement: ");
    Serial.print(return_temp);
    Serial.println("˚C");
    return false;
  }
  else
  {
    t = return_temp;
    return true;
  }
```

```
}

bool Moisture()  //% moisture
{
  Inquiry_Request();
  byte response[] = {0x00,0x00,0x00,0x00,0x00,0x00,0x00};
  if(soil_sensor.write(moisture_inquiry,sizeof(moisture_inquiry))==8){
    Read_Request();
    for(int i=0;i<7;i++){
      response[i] = soil_sensor.read();
    }
  }

  float return_moisture = (((float) response[3])*256 + (float) response[4])/10.0;
  if(return_moisture > max_moisture || return_moisture < min_moisture)
  {
    delay(error_delay);
    Serial.print("Incorrect Moisture Measurement: ");
    Serial.print(return_moisture);
    Serial.println("%");
    return false;
  }
  else
  {
    m = return_moisture;
    return true;
  }

}

bool Conduct()  //uS/cm
{
  Inquiry_Request();
  byte response[] = {0x00,0x00,0x00,0x00,0x00,0x00,0x00};
  if(soil_sensor.write(conduct_inquiry,sizeof(conduct_inquiry))==8){
    Read_Request();
    for(int i=0;i<7;i++){
```

```
    for(int i=0;i<7;i++){
      response[i] = soil_sensor.read();
    }
  }

  float return_conduct = (((float) response[3])*256 + (float) response[4]);
  if(return_conduct > max_conduct || return_conduct < min_conduct)
  {
    delay(error_delay);
    Serial.print("Incorrect Conductivity Measurement: ");
    Serial.print(return_conduct);
    Serial.println("uS/cm");
    return false;
  }
  else
  {
    c = return_conduct;
    return true;
  }

}

bool NPK()   //mg/Kg
{
  Inquiry_Request();
  byte response[] = {0x00,0x00,0x00,0x00,0x00,0x00,0x00,0x00,0x00,0x00,0x00};
  if(soil_sensor.write(npk_inquiry,sizeof(npk_inquiry))==8){
    Read_Request();
    for(int i=0;i<11;i++){
      response[i] = soil_sensor.read();
    }
  }
  float return_n = (((float) response[3])*256 + (float) response[4]);
  float return_p = (((float) response[5])*256 + (float) response[6]);
  float return_k = (((float) response[7])*256 + (float) response[8]);
```

```
  if(return_n > max_n || return_p > max_p || return_k > max_k || return_n < min_n || return_p < min_p || return_k > min_k)
  {
    delay(error_delay);
    Serial.println("Incorrect Measurement in one of the three following: ");
    Serial.print("N: ");
    Serial.print(return_n);
    Serial.println("mg/Kg");
    Serial.print("P: ");
    Serial.print(return_p);
    Serial.println("mg/Kg");
    Serial.print("K: ");
    Serial.print(return_k);
    Serial.println("mg/Kg");
    return false;
  }
  else
  {
    n = return_n;
    p = return_p;
    k = return_k;
    return true;
  }
}

float Get_Data(char data_code, int attempt)
{
  if(attempt > max_errored_attempts)
  {
    Serial.println("Max attempts failed, check sensor");
    return -1.0;
  }
  else
  {

  }
  switch(data_code)
  {
```

```
    case 'A':
      if(PH())
      {
        Serial.print("Acidity: ");
        Serial.print(a);
        Serial.println(" pH");
        return a;
      }
      else
      {
        Get_Data(data_code,attempt+1);
      }
      break;
    case 'T':
      if(PH())
      {
        Serial.print("Temperature: ");
        Serial.print(t);
        Serial.println(" °C");
        return t;
      }
      else
      {
        Get_Data(data_code,attempt+1);
      }
      break;
    case 'M':
      if(PH())
      {
        Serial.print("Moisture: ");
        Serial.print(m);
        Serial.println(" %");
        return m;
      }
      else
      {
        Get_Data(data_code,attempt+1);
      }
      break;
    case 'C':
      if(PH())
```

```
      {
        Serial.print("Conductivity: ");
        Serial.print(c);
        Serial.println(" uS/cm");
        return c;
      }
      else
      {
        Get_Data(data_code,attempt+1);
      }
      break;
    case 'N':
      if(PH())
      {
        Serial.print("Nitrogen: ");
        Serial.print(n);
        Serial.println(" mg/Kg");
        return n;
      }
      else
      {
        Get_Data(data_code,attempt+1);
      }
      break;
    case 'P':
      if(PH())
      {
        Serial.print("Phosphorus: ");
        Serial.print(p);
        Serial.println(" mg/Kg");
        return p;
      }
      else
      {
        Get_Data(data_code,attempt+1);
      }
      break;
    case 'K':
      if(PH())
      {
        Serial.print("Potassium: ");
```

```
        Serial.print(k);
        Serial.println(" mg/Kg");
        return k;
      }
      else
      {
        Get_Data(data_code,attempt+1);
      }
      break;
    default:
      Serial.print("Incorrect input");
      return -1.0;
  }
}

float Sample_Data(char data_code, int times, float interval)
{
  float sum = 0.0;
  for(int i = 0; i < times; i++)
  {
    float data_point = Get_Data(data_code,0);
    if(data_point = -1.0)
    {
      Serial.println("Failed Data Reading");
      return -1.0;
    }
    sum += data_point;
    delay(interval);
  }
  return sum/(float) times;
}
```

Appendix F: GPS Coordinate System and Time Initialization Code

```
from datetime import datetime
import math

# Test locations must be obtained with RTK base configuration
hub_origin_ll = (42.274315,-71.8084567)
hub_origin_deg = 34.35103851903750 #deg

def rad2deg(rad):
    return rad*(180/math.pi)

def deg2rad(deg):
    return deg*(math.pi/180)

def deg2m(pos_gps):
    mu = deg2rad(pos_gps[0])
    lat = 111132.92 - 559.82 * math.cos(2*mu) + 1.175 * math.cos(4*mu) -0.0023 * math.cos(6*mu)
    lon = 111412.84 * math.cos(mu) -93.5* math.cos(3*mu) + 0.118 * math.cos(5*mu)
    return (lat,lon)

def ll2xy(ll,origin_ll,origin_deg,scalers):
    NE = ((ll[0]-origin_ll[0])*scalers[0],(ll[1]-origin_ll[1])*scalers[1])
    psi = deg2rad(-origin_deg)
    x = math.sin(psi)*NE[0] + math.cos(psi)*NE[1]
    y = math.cos(psi)*NE[0] - math.sin(psi)*NE[1]
    return (x,y)

def xy2ll(xy,origin_ll,origin_deg,scalers):
    psi = deg2rad(origin_deg)
    N = math.cos(psi)*xy[1]- math.sin(psi)*xy[1]
    E = math.sin(psi)*xy[1]+ math.cos(psi)*xy[1]
    return (origin_ll[0] + (N/scalers[0]),origin_ll[1] + (E/scalers[1]))

def decode_GPS_RMC(str):
    data = str.split(',')
    header = data[0]
    str_UTC_time = data[1]
    str_time_valid = data[2]
```

```
    str_latitude = data[3]
    str_latitude_north = data[4]
    str_longitude = data[5]
    str_longitude_east = data[6]
    str_ground_speed = data[7]
    str_ground_course = data[8]
    str_UTC_date = data[9]

    # assuming UTC date is valid from error check bit
    str_datetime = str_UTC_time+'0000'+str_UTC_date
    datetime_obj = datetime.strptime(str_datetime,'%H%M%S.%f%d%m%y')

    latitude_north = str_latitude_north == 'N'
    longitude_east = str_longitude_east == 'E'

    latitude = float(str_latitude[0:2])+(float(str_latitude[2:])/60.0)
    if not latitude_north:
        latitude *= -1

    longitude = float(str_longitude[0:3])+(float(str_longitude[3:])/60.0)
    if not longitude_east:
        longitude *= -1
    GPS_pos = (latitude,longitude)

    return (datetime_obj,GPS_pos)
    # indicator for correct UTC_data
    # checksum thing


# toget decimal degrees take digits after first 2 and divide by 60
# an example message from the RTK is parsed, resulting value should
# be a position in meters
out = decode_GPS_RMC('$GNRMC,233205.00,A,4216.35728,N,07148.56841,W,0.025,,210222,,,A*71')
scalers = deg2m(hub_origin_ll)
```

```python
xy = ll2xy(out[1],hub_origin_ll,hub_origin_deg,scalers)
print(xy)

```

Appendix G: Link to Github Repository

The remainder of the code for this project can be found at: https://github.com/rpcarterwpi/agribots. The purpose of each file is described in README.md and code submissions are separated by their programming languages Python and Arduino.

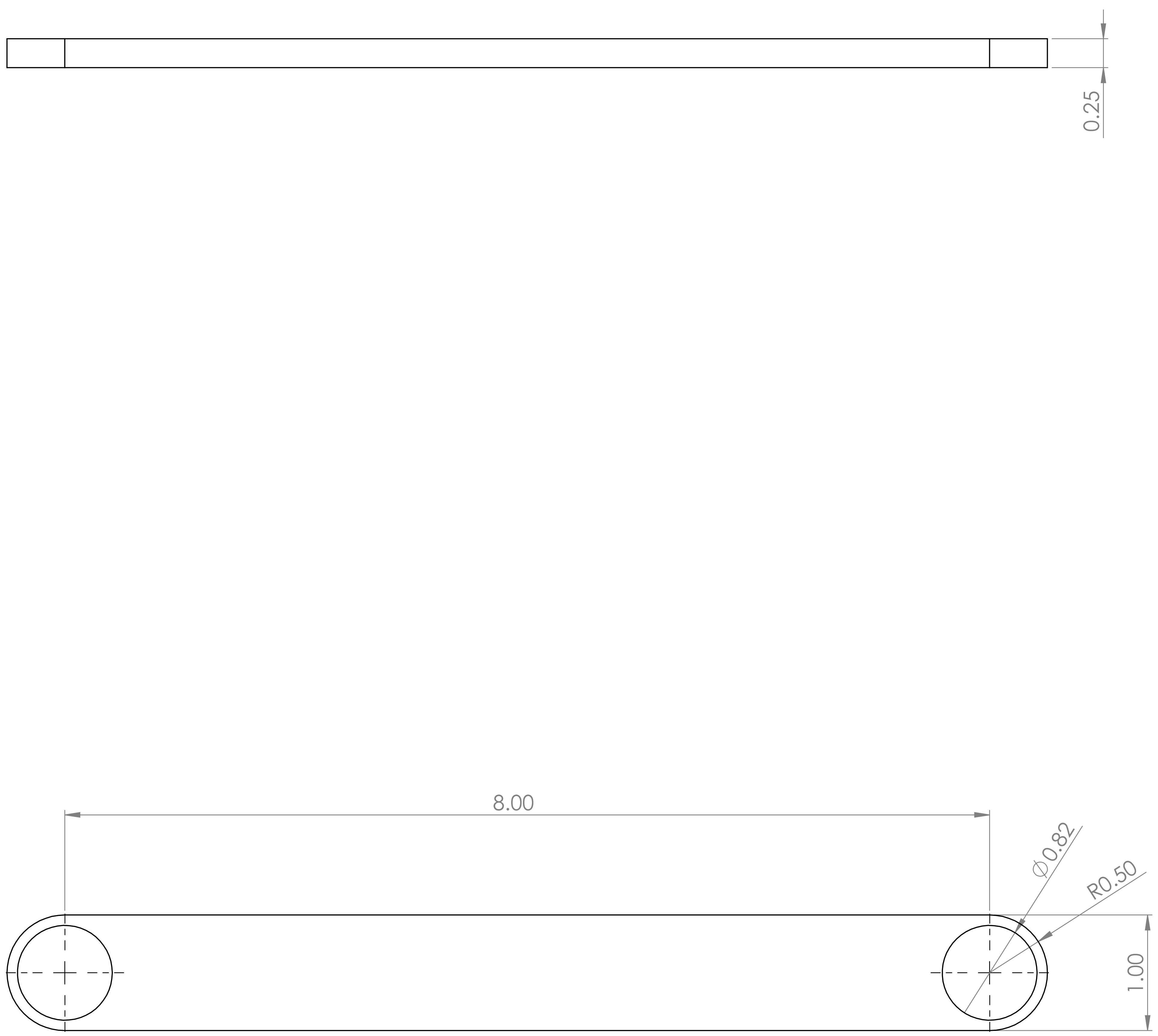

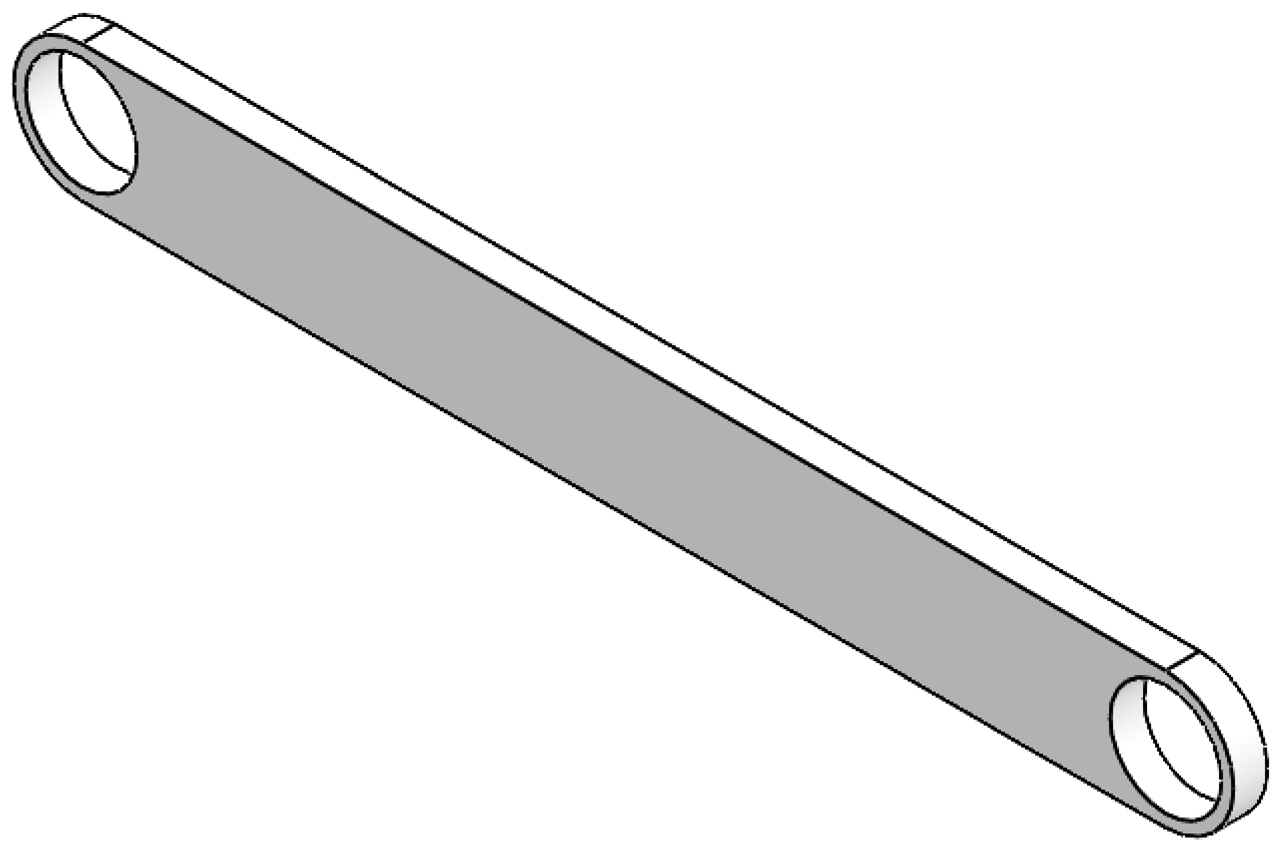

UNLESS OTHERWISE SPECIFIED: DIMENSIONS ARE IN MILLIMETERS SURFACE FINISH: TOLERANCES: LINEAR: ANGULAR:	FINISH:	DEBURR AND BREAK SHARP EDGES	DO NOT SCALE DRAWING	REVISION	
	NAME	SIGNATURE	DATE	TITLE:	Link
DRAWN	JB		04/06/22		
CHK'D	JP		4/27/22		
APPV'D					
MFG					
Q.A				MATERIAL: ABS	DWG NO. Arm Assem 01 — A2
				WEIGHT:	SCALE:1:1 — SHEET 1 OF 1

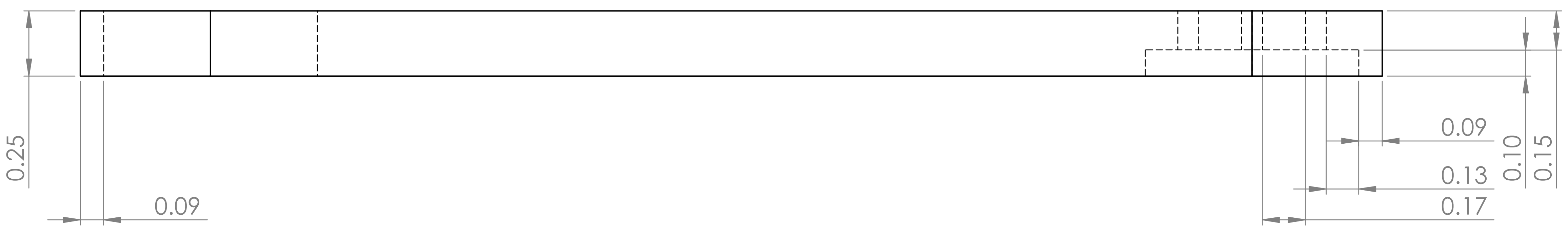

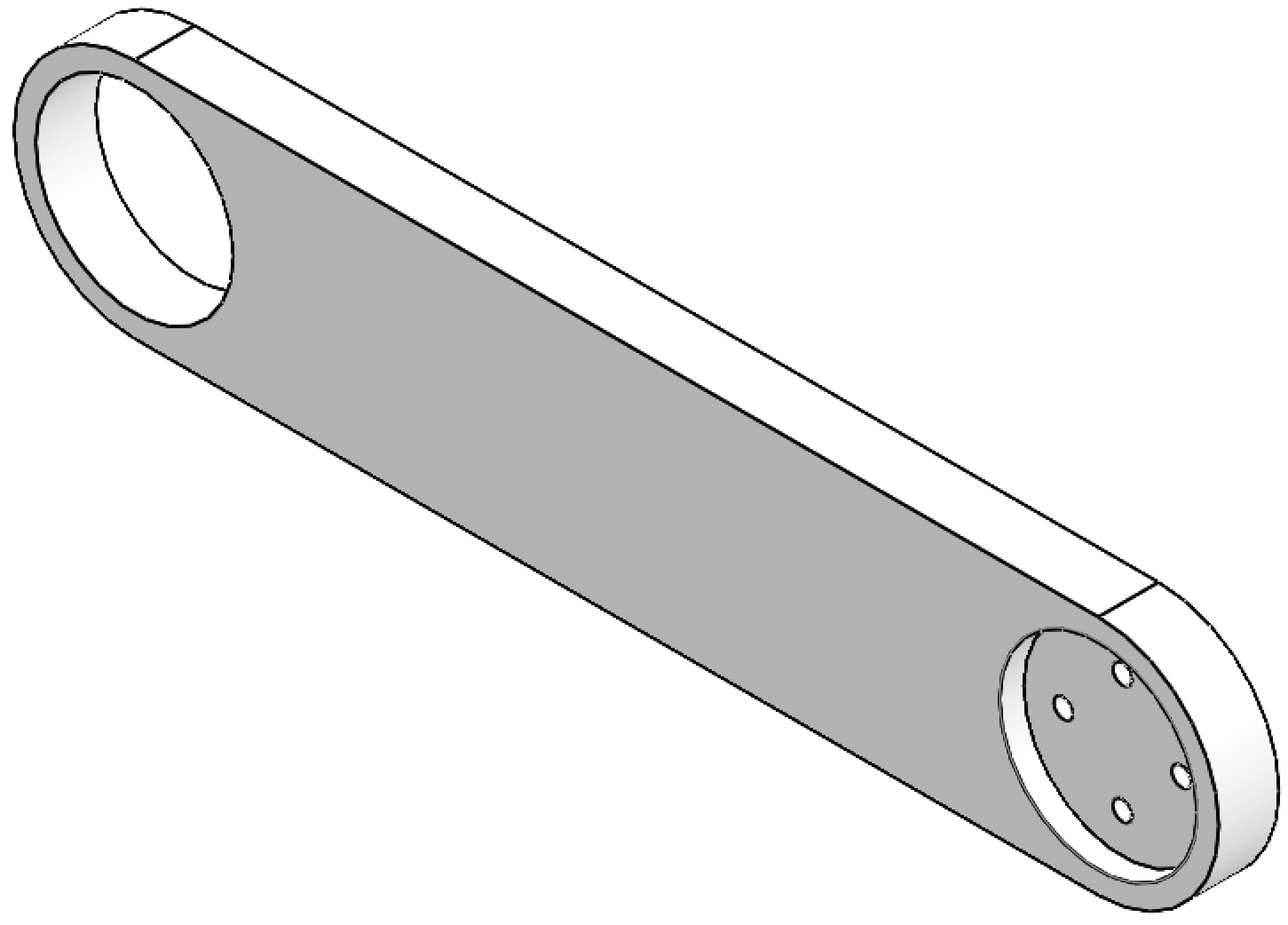

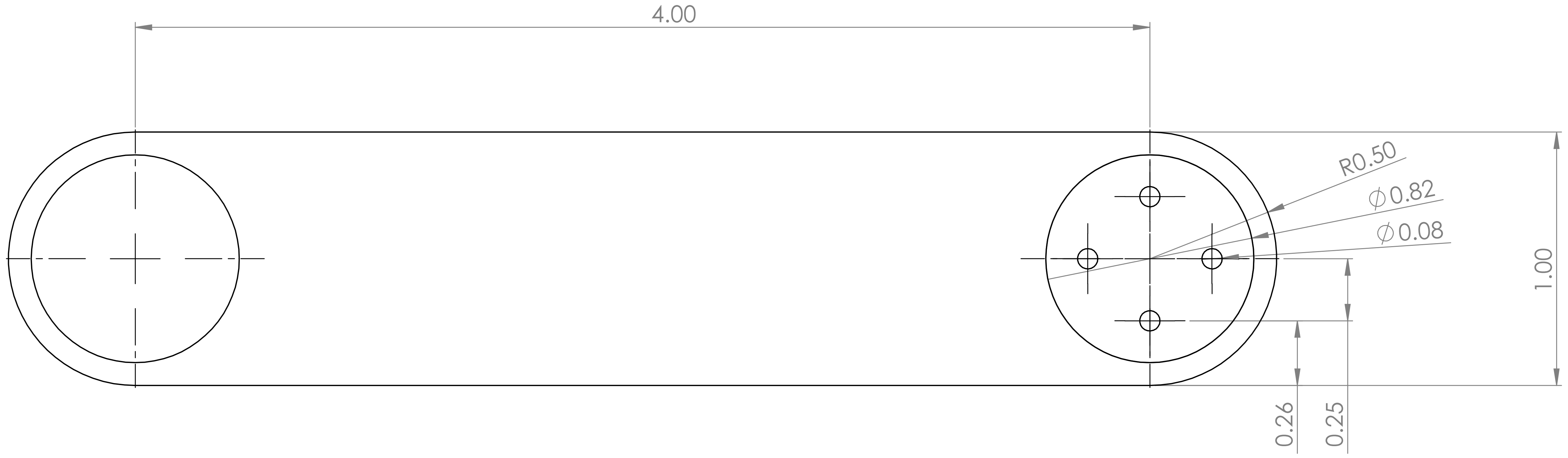

UNLESS OTHERWISE SPECIFIED: DIMENSIONS ARE IN MILLIMETERS SURFACE FINISH: TOLERANCES: LINEAR: ANGULAR:		FINISH:		DEBURR AND BREAK SHARP EDGES		DO NOT SCALE DRAWING	REVISION
	NAME	SIGNATURE	DATE			TITLE: Crank	
DRAWN	JB		04/07/22				
CHK'D	JP		4/27/22				
APPV'D							
MFG							
Q.A				MATERIAL: ABS		DWG NO. Arm Assem 02	A2
				WEIGHT:		SCALE:2:1	SHEET 1 OF 1

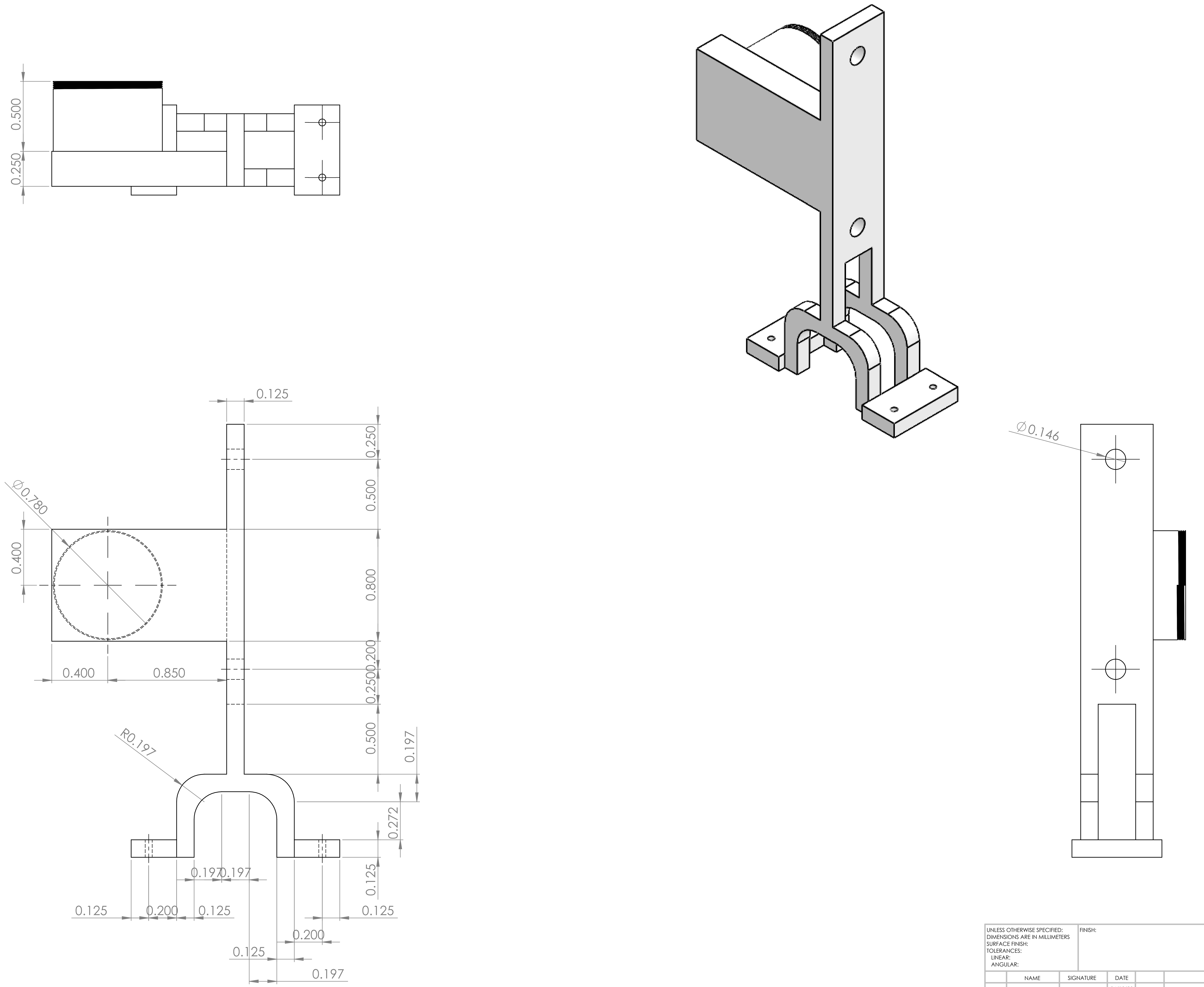

UNLESS OTHERWISE SPECIFIED: DIMENSIONS ARE IN MILLIMETERS SURFACE FINISH: TOLERANCES: LINEAR: ANGULAR:	FINISH:		DEBURR AND BREAK SHARP EDGES	DO NOT SCALE DRAWING	REVISION
	NAME	SIGNATURE	DATE	TITLE:	Slider
DRAWN	JB		04/18/22		
CHK'D	JP		4/27/22		
APPV'D					
MFG					
Q.A			MATERIAL: ABS	DWG NO. Arm Assem 03	A2
			WEIGHT:	SCALE:2:1	SHEET 1 OF 1

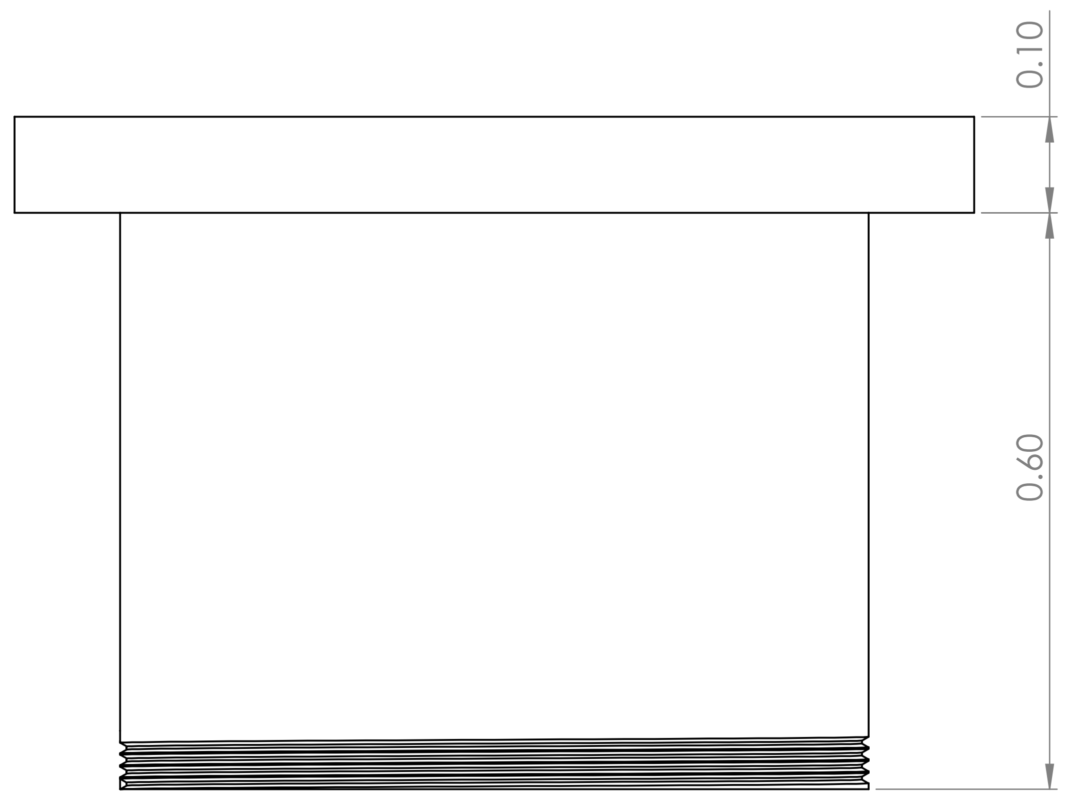

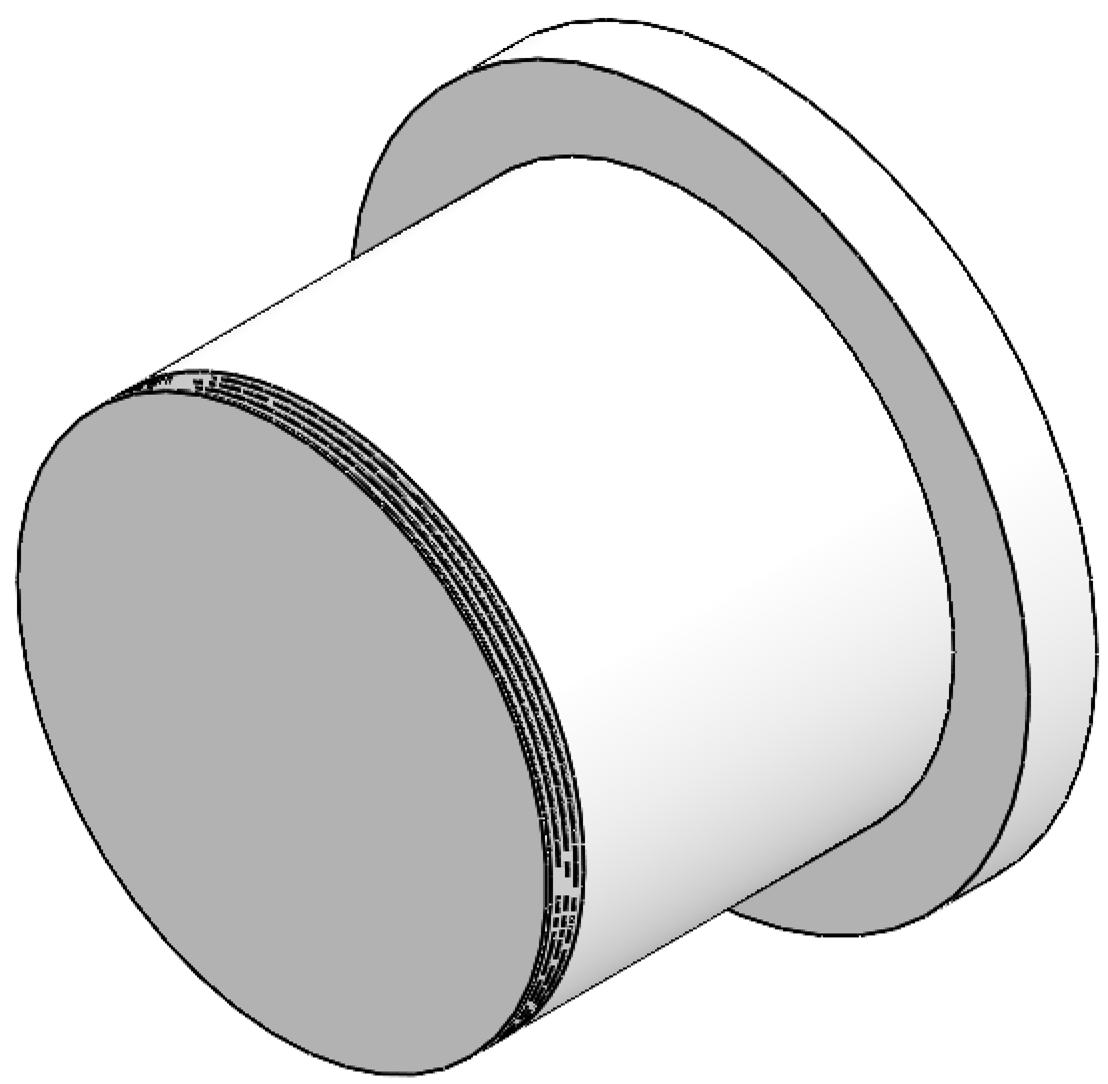

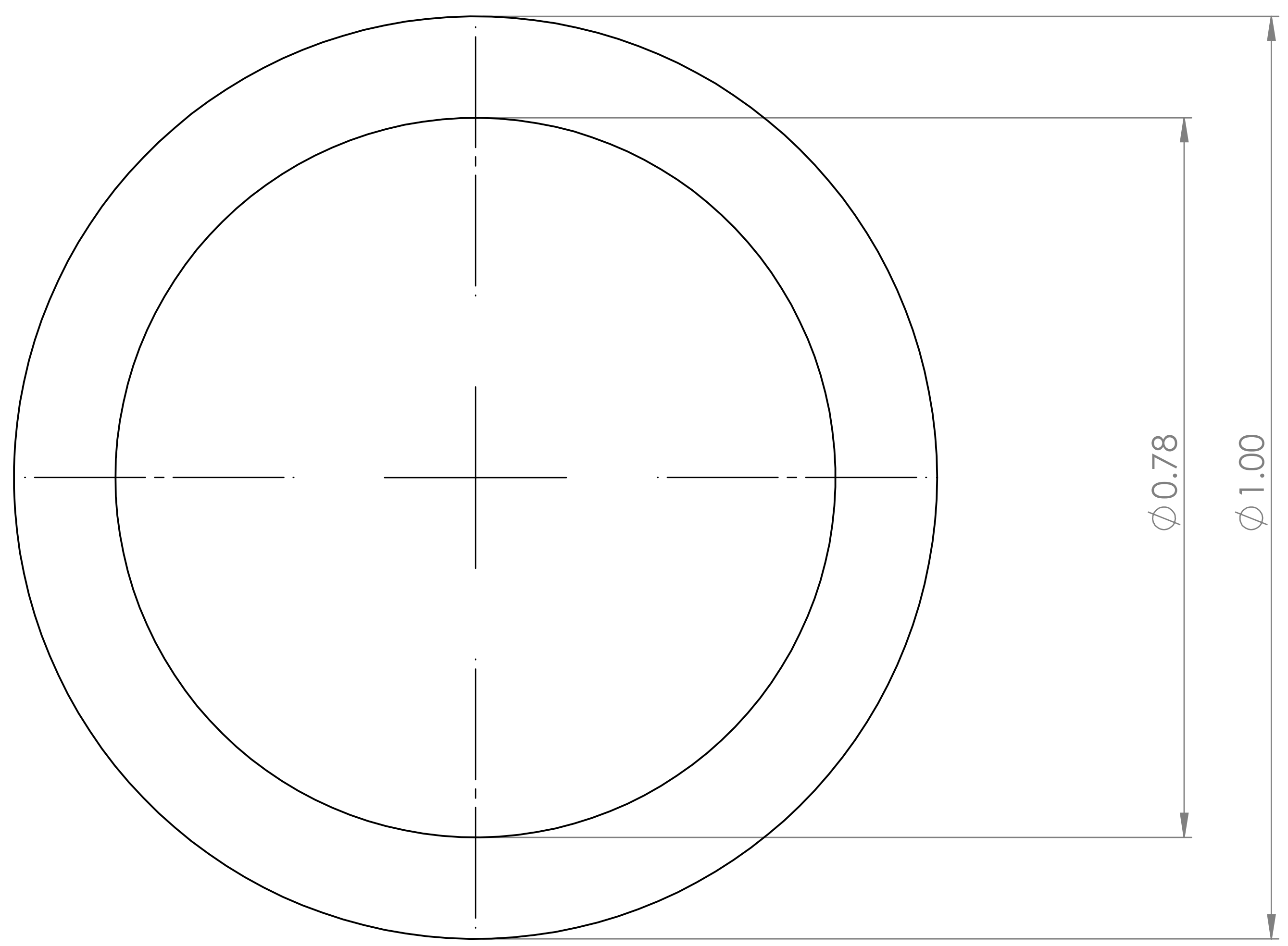

UNLESS OTHERWISE SPECIFIED: DIMENSIONS ARE IN MILLIMETERS SURFACE FINISH: TOLERANCES: LINEAR: ANGULAR:			FINISH:			DEBURR AND BREAK SHARP EDGES	DO NOT SCALE DRAWING	REVISION
	NAME	SIGNATURE	DATE				TITLE: Joint	
DRAWN	JB		04/08/22					
CHK'D	JP		4/27/22					
APPV'D								
MFG								
Q.A				MATERIAL: ABS			DWG NO. Arm Assem 04	A2
				WEIGHT:			SCALE:5:1	SHEET 1 OF 1

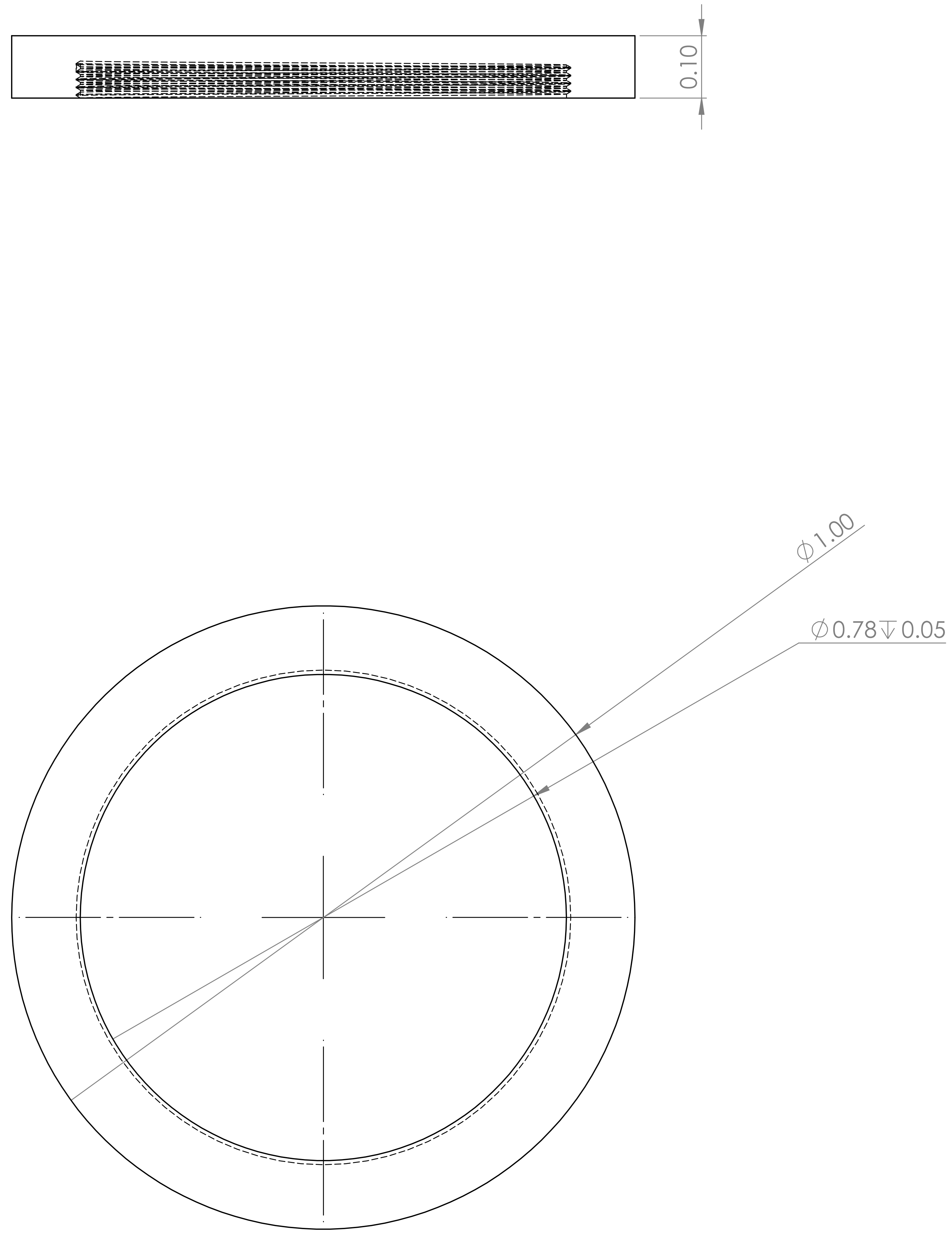

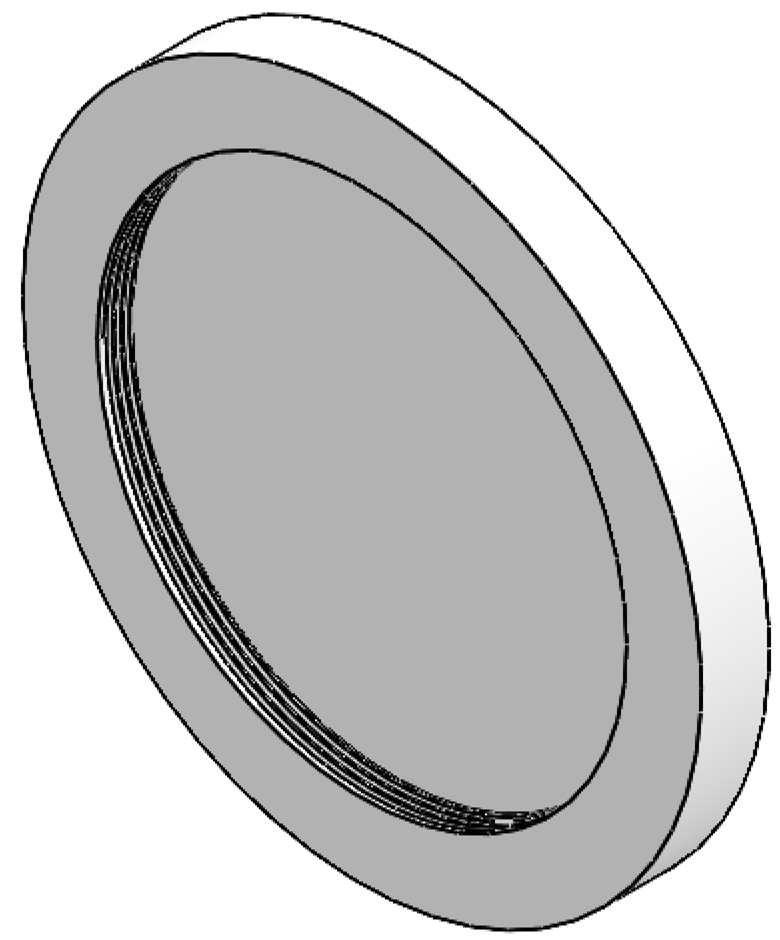

UNLESS OTHERWISE SPECIFIED: DIMENSIONS ARE IN MILLIMETERS SURFACE FINISH: TOLERANCES: LINEAR: ANGULAR:	FINISH:		DEBURR AND BREAK SHARP EDGES		DO NOT SCALE DRAWING	REVISION
	NAME	SIGNATURE	DATE		TITLE:	Joint Top
DRAWN	JB		04/08/22			
CHK'D	JP		4/27/22			
APPV'D						
MFG						
Q.A				MATERIAL: ABS	DWG NO. Arm Assem 05	A2
				WEIGHT:	SCALE:5:1	SHEET 1 OF 1

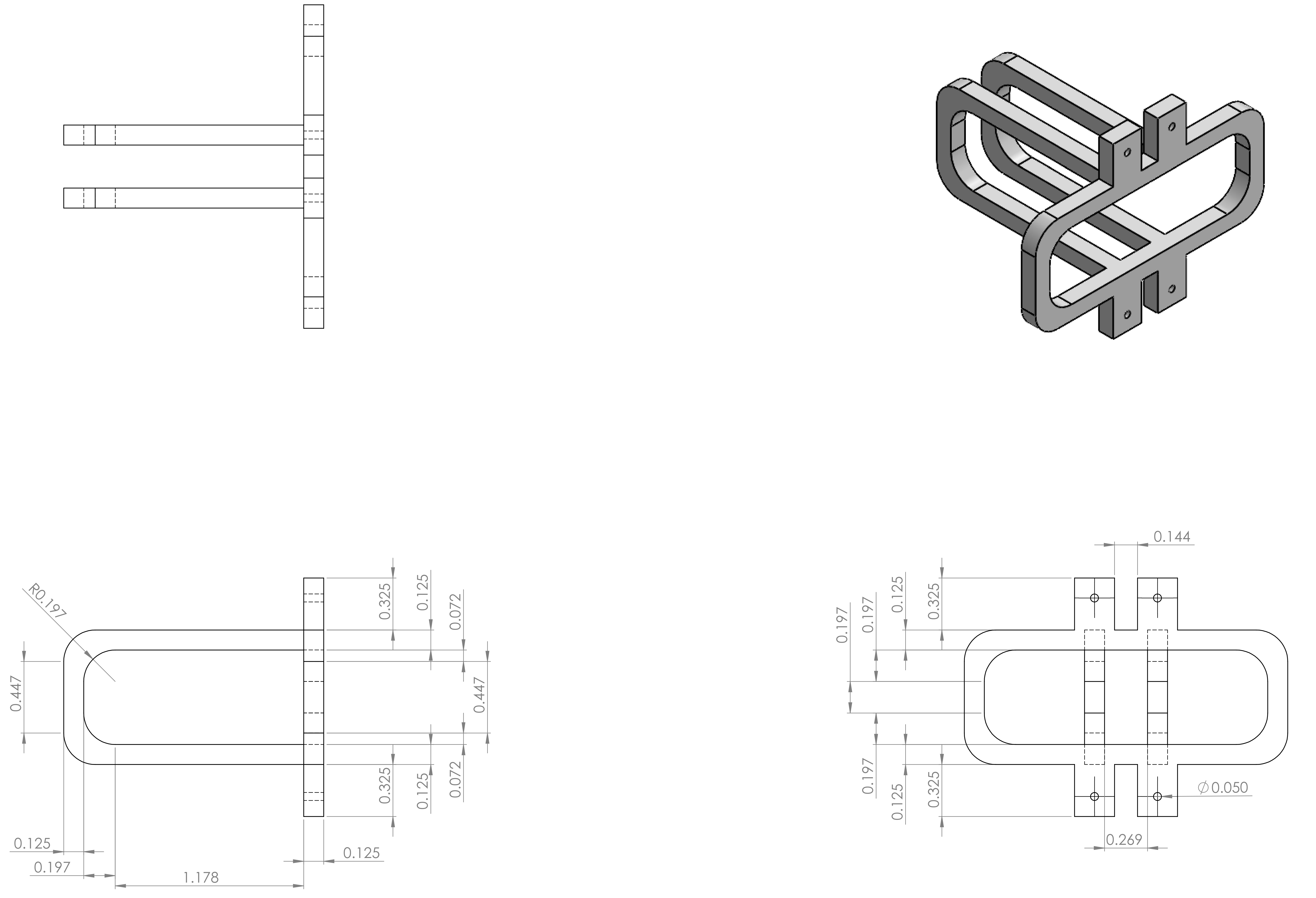

UNLESS OTHERWISE SPECIFIED: DIMENSIONS ARE IN MILLIMETERS SURFACE FINISH: TOLERANCES: LINEAR: ANGULAR:	FINISH:		DEBURR AND BREAK SHARP EDGES	DO NOT SCALE DRAWING	REVISION
	NAME	SIGNATURE	DATE	TITLE: NPK Probe Fixturing	
DRAWN	JB		04/18/22		
CHK'D	JP		4/27/22		
APPV'D					
MFG					
Q.A			MATERIAL: ABS	DWG NO. Arm Assem 06	A2
			WEIGHT:	SCALE:2:1	SHEET 1 OF 1

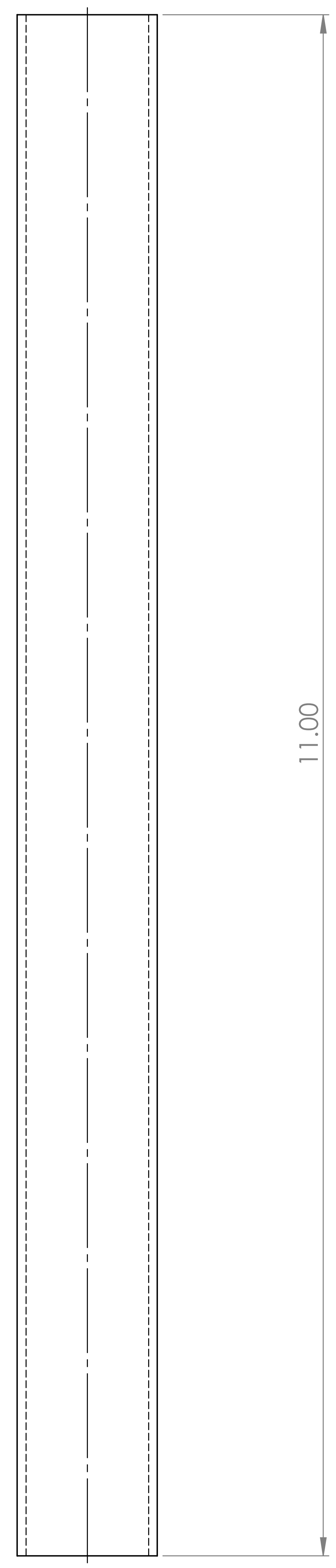

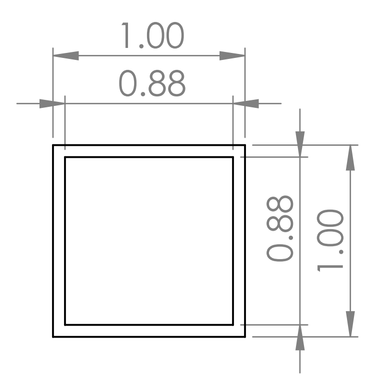

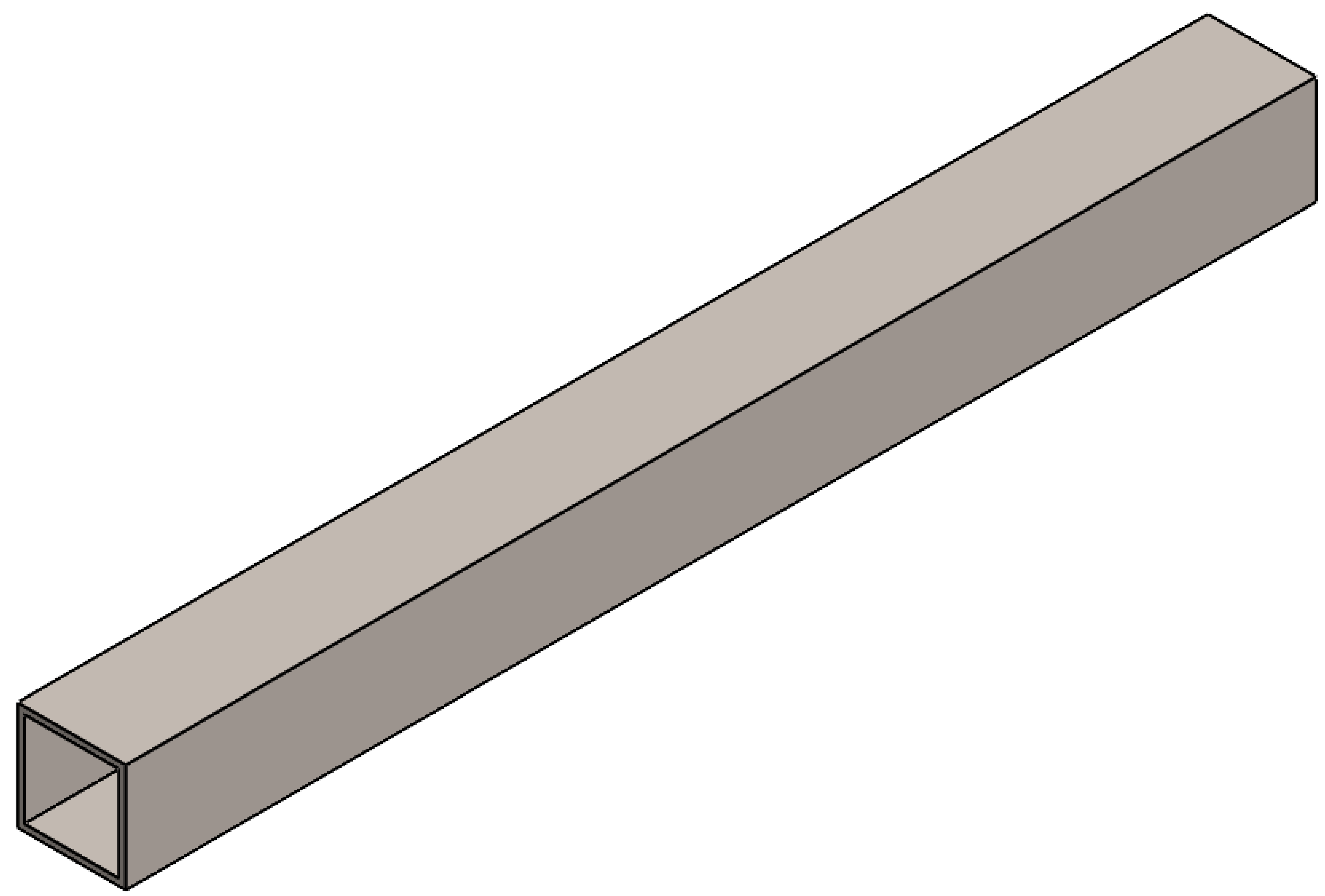

UNLESS OTHERWISE SPECIFIED: DIMENSIONS ARE IN MILLIMETERS SURFACE FINISH: TOLERANCES: LINEAR: ANGULAR:	FINISH:				DEBURR AND BREAK SHARP EDGES	DO NOT SCALE DRAWING	REVISION
	NAME	SIGNATURE	DATE			TITLE: 11 Inch	
DRAWN	JB		04/06/22				
CHK'D	JP		4/27/22				
APPV'D							
MFG							
Q.A				MATERIAL: Alloy Steel		DWG NO. Frame Assem 01	A2
				WEIGHT:		SCALE:1:2	SHEET 1 OF 1

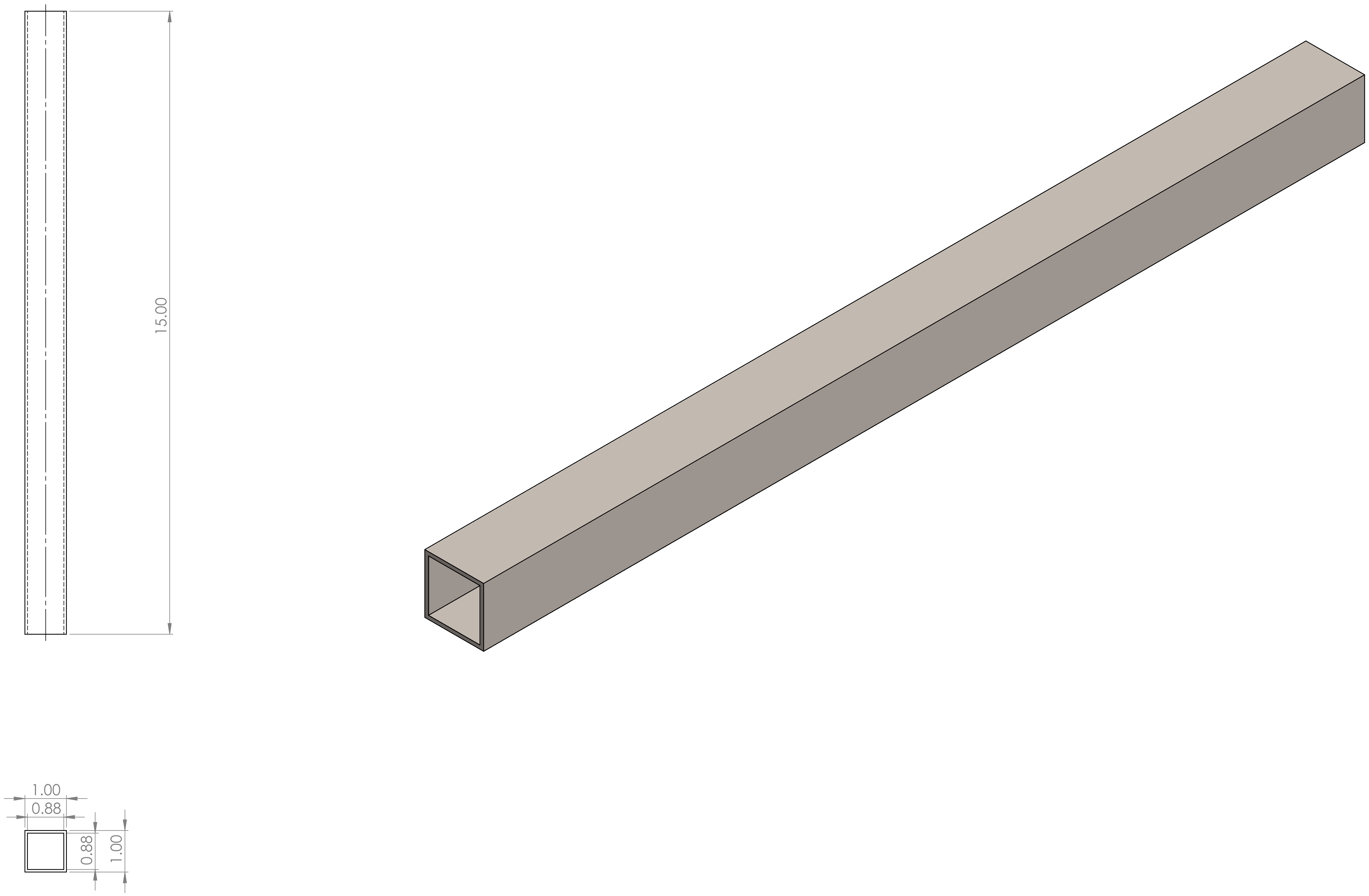

UNLESS OTHERWISE SPECIFIED: DIMENSIONS ARE IN MILLIMETERS SURFACE FINISH: TOLERANCES: LINEAR: ANGULAR:		FINISH:		DEBURR AND BREAK SHARP EDGES		DO NOT SCALE DRAWING	REVISION
	NAME	SIGNATURE	DATE			TITLE: 15 Inch	
DRAWN	JB		04/06/22				
CHK'D	JP		4/27/22				
APPV'D							
MFG							
Q.A				MATERIAL: Alloy Steel		DWG NO. Frame Assem 02	A2
				WEIGHT:		SCALE:1:2	SHEET 1 OF 1

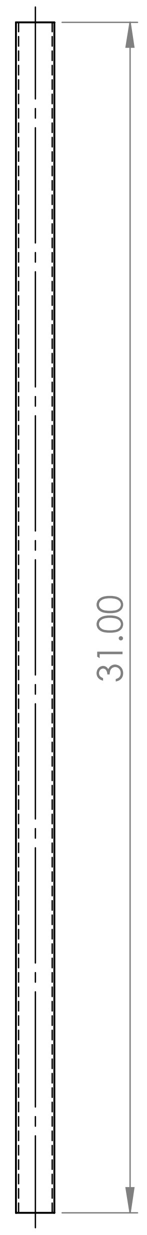

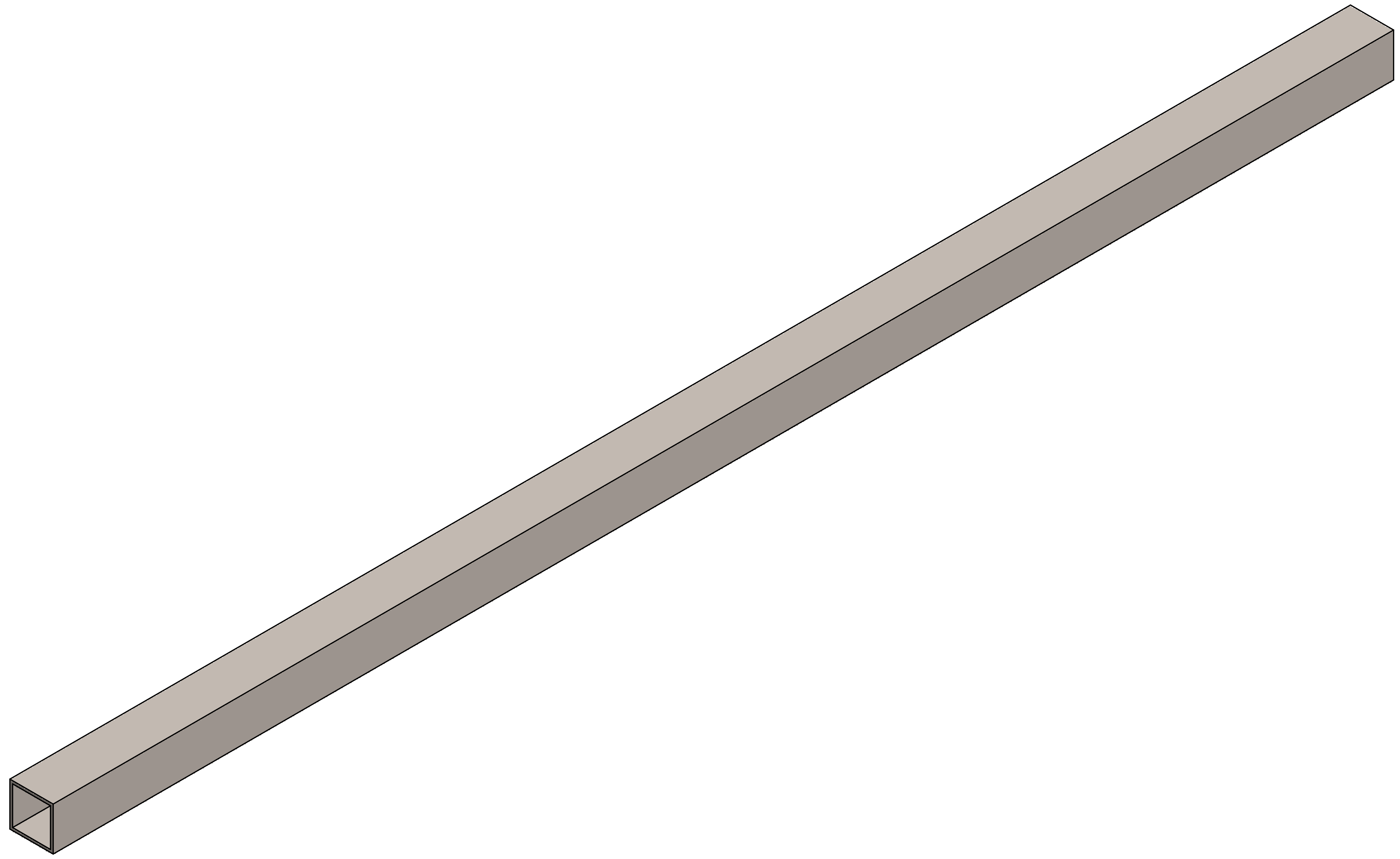

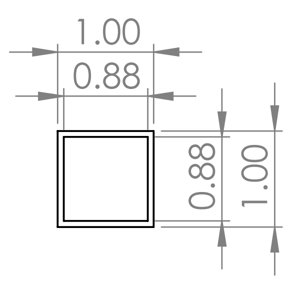

UNLESS OTHERWISE SPECIFIED: DIMENSIONS ARE IN MILLIMETERS SURFACE FINISH: TOLERANCES: LINEAR: ANGULAR:		FINISH:			DEBURR AND BREAK SHARP EDGES	DO NOT SCALE DRAWING	REVISION
	NAME	SIGNATURE	DATE			TITLE:	
DRAWN	JB		04/06/22			31 Inch	
CHK'D	JP		4/27/22				
APPV'D							
MFG							
Q.A				MATERIAL: Alloy Steel		DWG NO. Frame Assem 03	A2
				WEIGHT:		SCALE:1:5	SHEET 1 OF 1

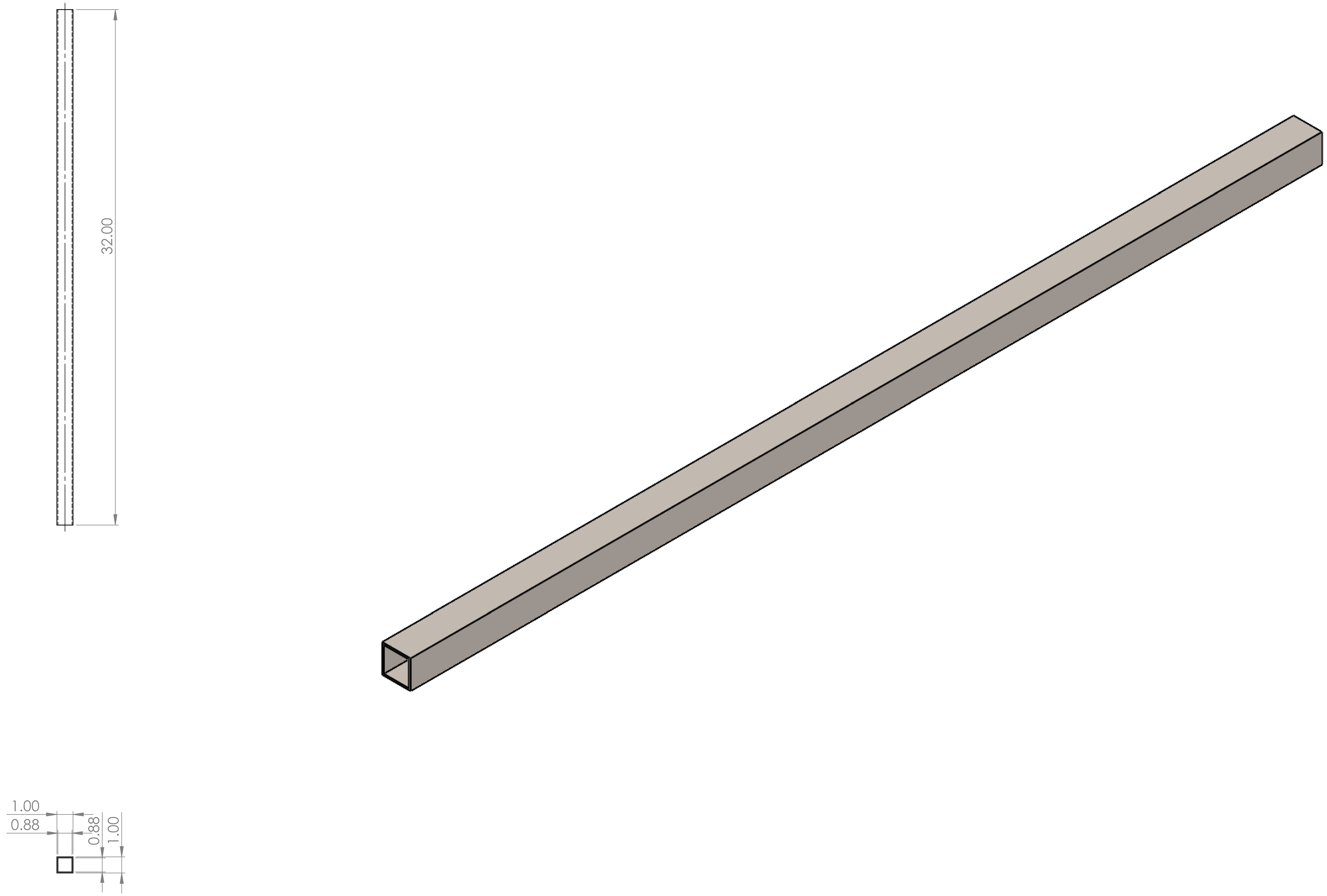

UNLESS OTHERWISE SPECIFIED: DIMENSIONS ARE IN MILLIMETERS SURFACE FINISH: TOLERANCES: LINEAR: ANGULAR:	FINISH:		DEBURR AND BREAK SHARP EDGES	DO NOT SCALE DRAWING / REVISION
	NAME	SIGNATURE	DATE	TITLE: 32 Inch
DRAWN	JB		04/06/22	
CHK'D	JP		4/27/22	
APPV'D				
MFG				
Q.A			MATERIAL: Alloy Steel	DWG NO. Frame Assem 04 A2
			WEIGHT:	SCALE:1:5 SHEET 1 OF 1

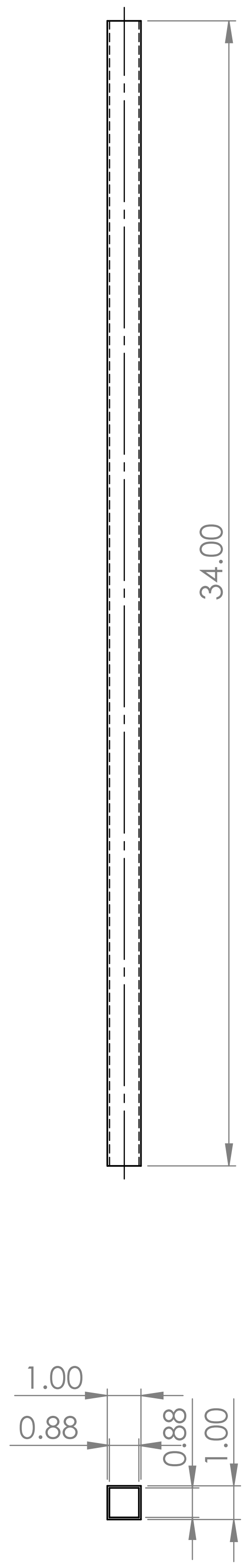

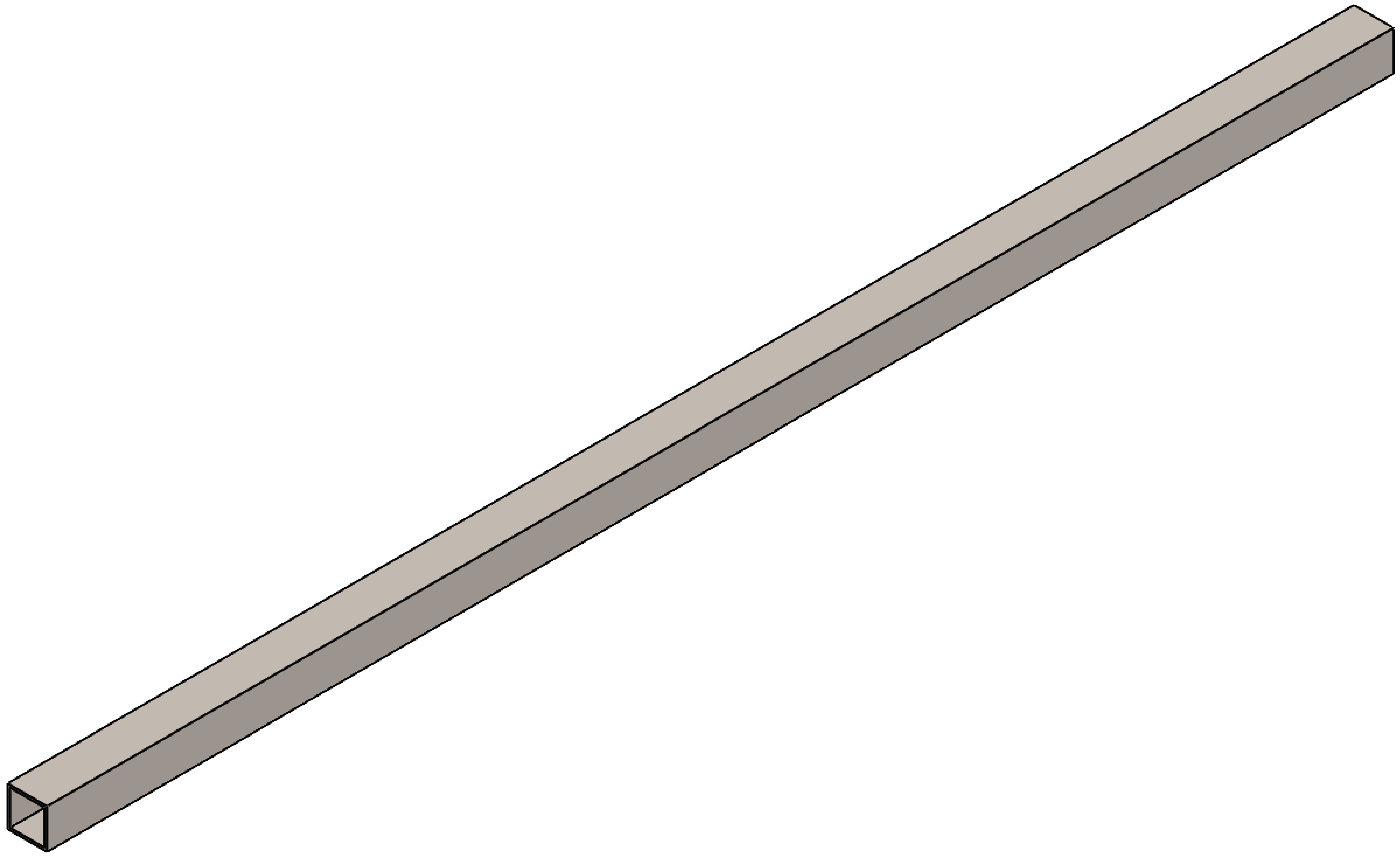

UNLESS OTHERWISE SPECIFIED: DIMENSIONS ARE IN MILLIMETERS SURFACE FINISH: TOLERANCES: LINEAR: ANGULAR:		FINISH:		DEBURR AND BREAK SHARP EDGES		DO NOT SCALE DRAWING	REVISION
	NAME	SIGNATURE	DATE			TITLE:	34 Inch
DRAWN	JB		04/06/22				
CHK'D	JP		4/27/22				
APPV'D							
MFG							
Q.A				MATERIAL: Alloy Steel		DWG NO. Frame Assem 05	A2
				WEIGHT:		SCALE:1:5	SHEET 1 OF 1

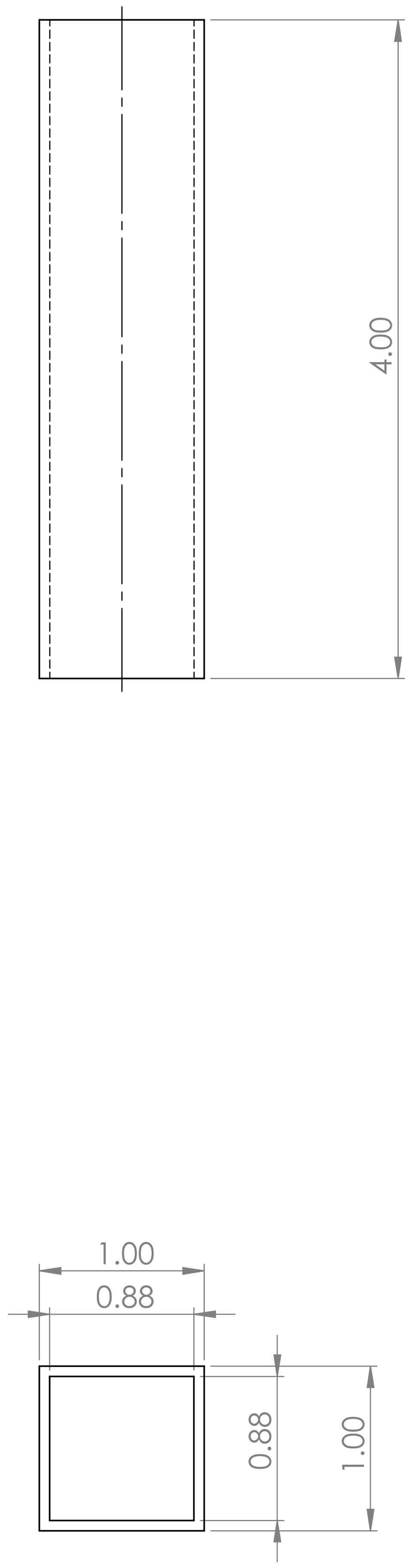

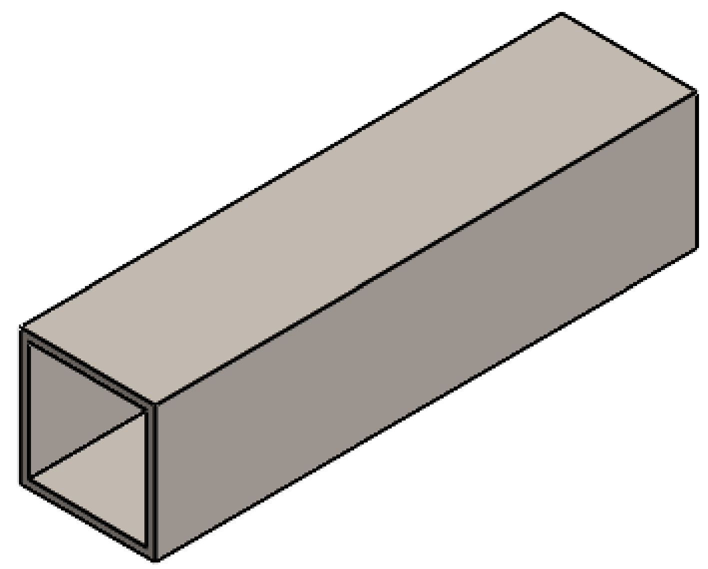

UNLESS OTHERWISE SPECIFIED: DIMENSIONS ARE IN MILLIMETERS SURFACE FINISH: TOLERANCES: LINEAR: ANGULAR:	FINISH:	DEBURR AND BREAK SHARP EDGES	DO NOT SCALE DRAWING	REVISION
	NAME	SIGNATURE	DATE	TITLE: 4 Inch
DRAWN	JB		04/06/22	
CHK'D	JP		4/27/22	
APPV'D				
MFG				
Q.A			MATERIAL: Alloy Steel	DWG NO. Frame Assem 06 — A2
			WEIGHT:	SCALE:1:1 — SHEET 1 OF 1

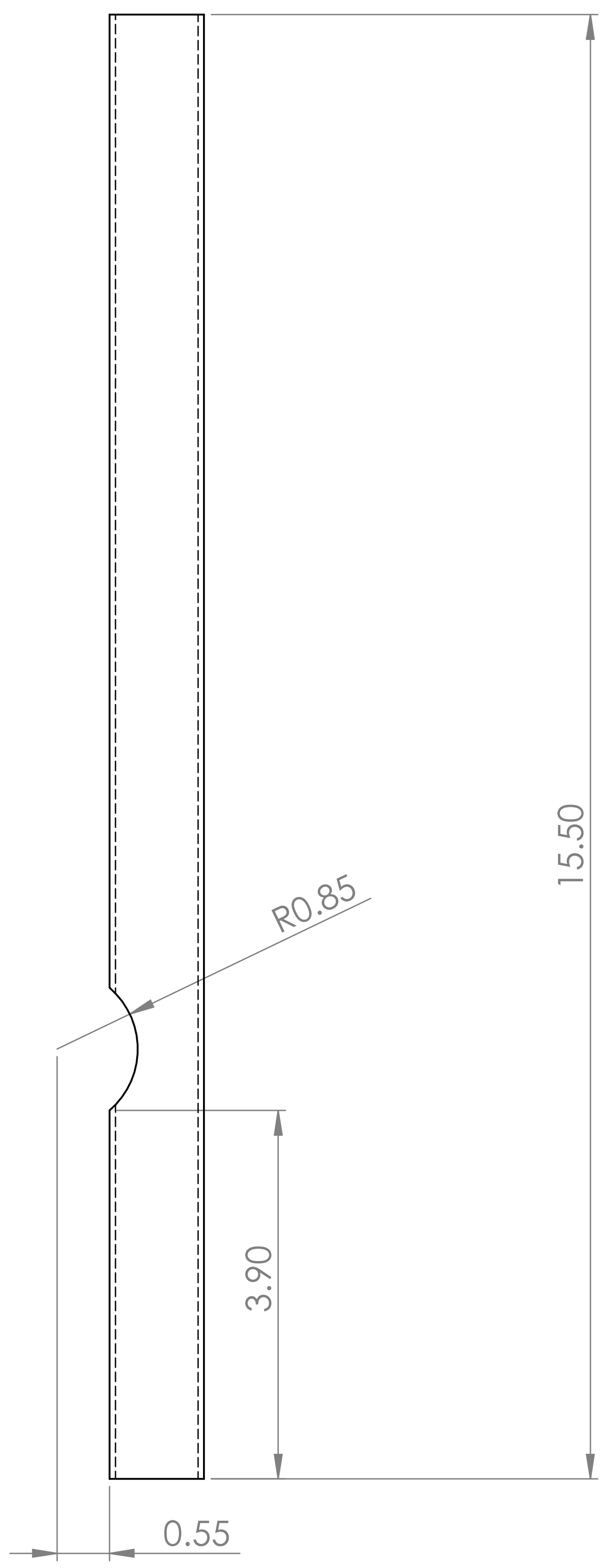

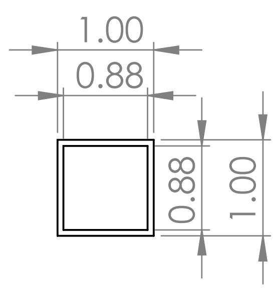

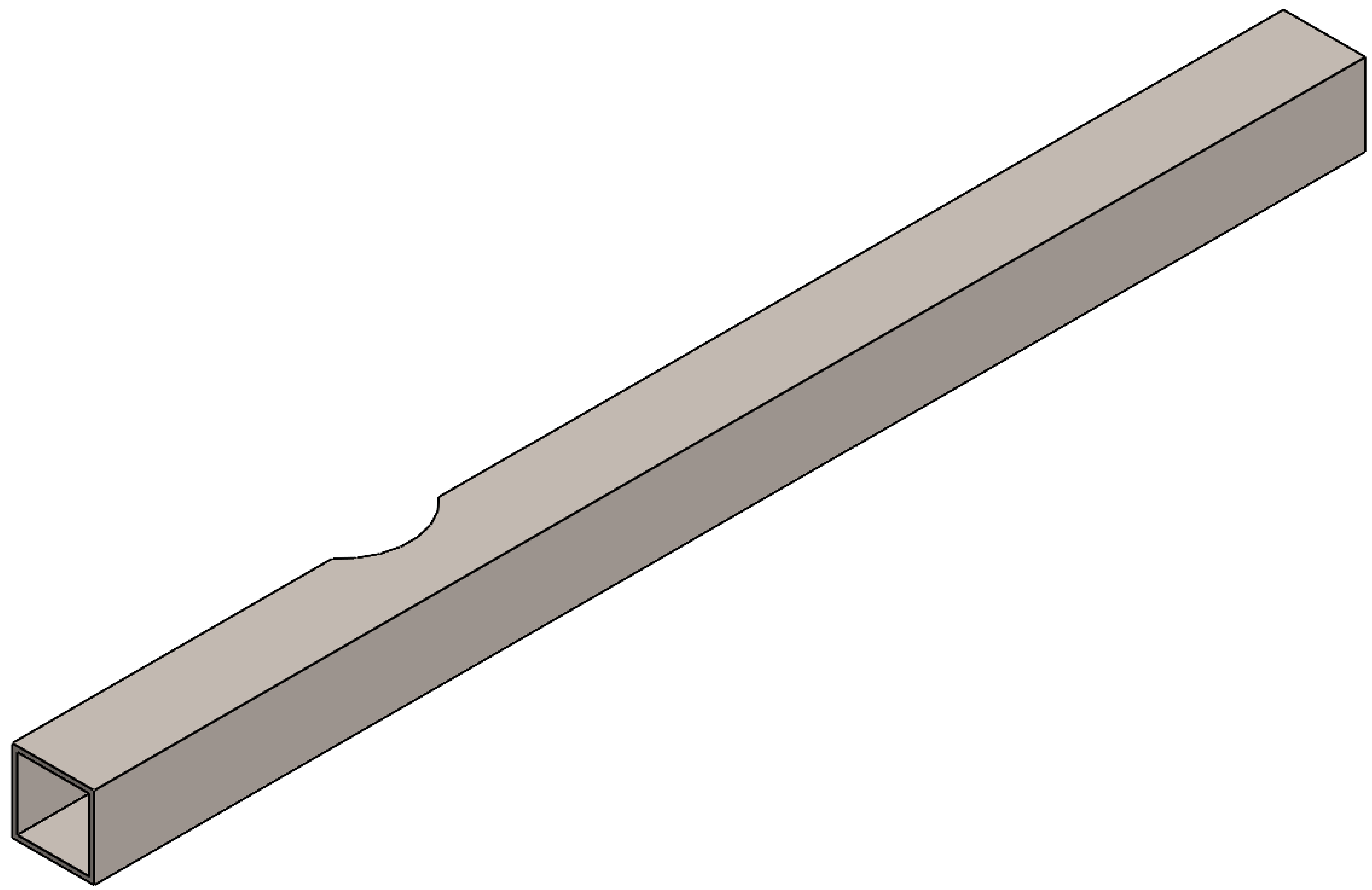

UNLESS OTHERWISE SPECIFIED: DIMENSIONS ARE IN MILLIMETERS SURFACE FINISH: TOLERANCES: LINEAR: ANGULAR:	FINISH:		DEBURR AND BREAK SHARP EDGES		DO NOT SCALE DRAWING	REVISION
	NAME	SIGNATURE	DATE		TITLE:	Motor Support
DRAWN	JB		04/06/22			
CHK'D	JP		4/27/22			
APPV'D						
MFG						
Q.A				MATERIAL: Alloy Steel	DWG NO. Frame Assem 07	A2
				WEIGHT:	SCALE:1:2	SHEET 1 OF 1

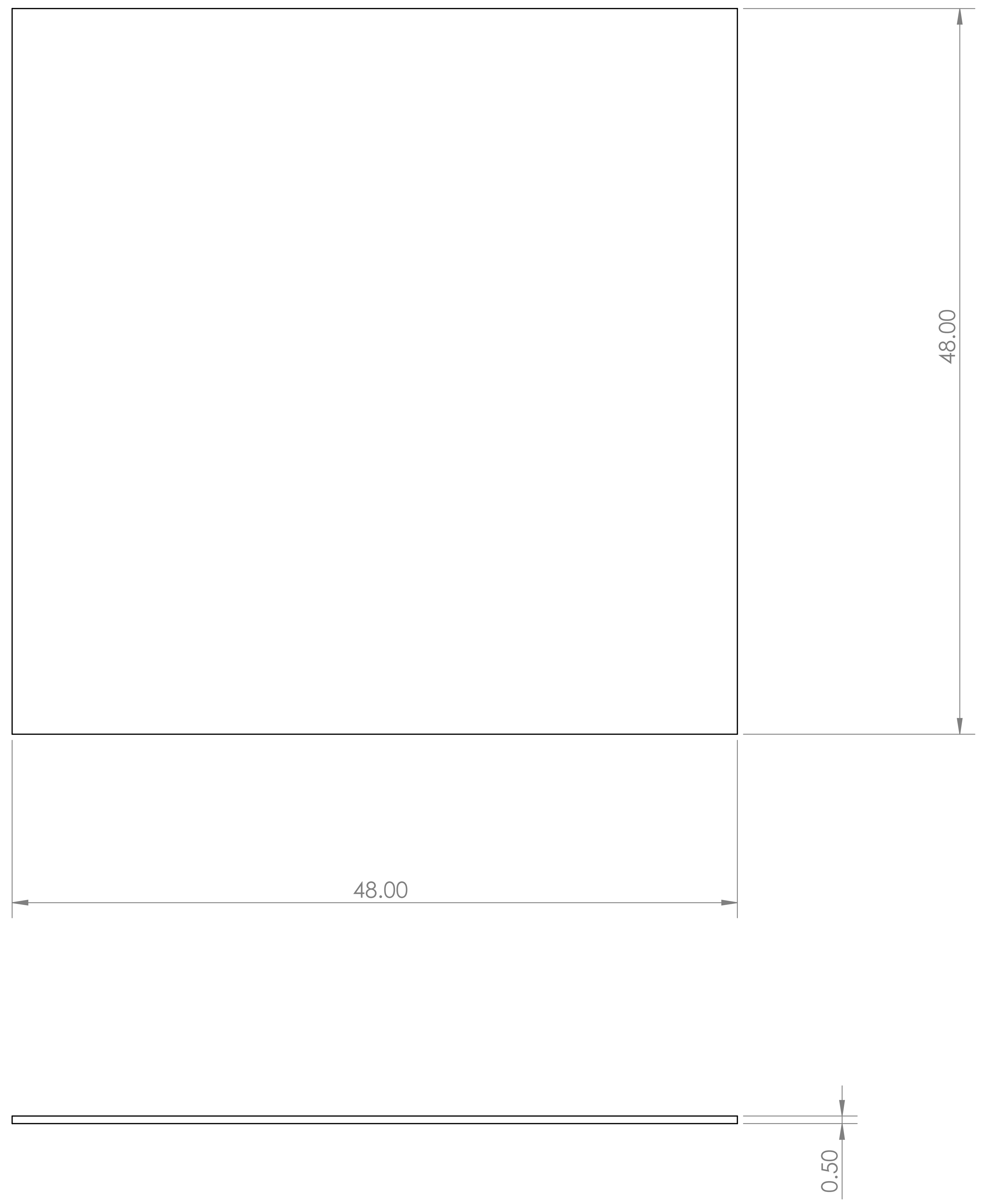

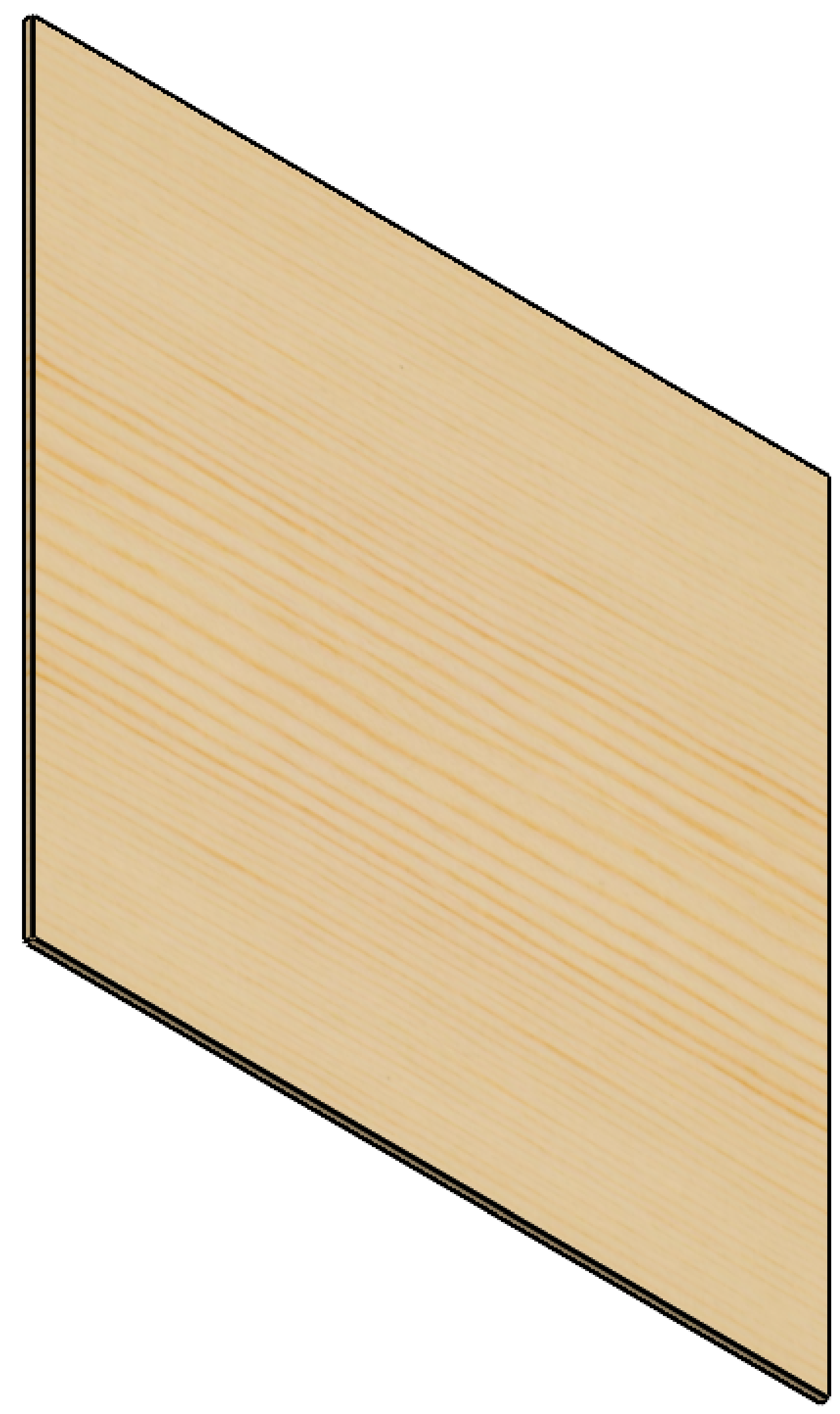

UNLESS OTHERWISE SPECIFIED: DIMENSIONS ARE IN MILLIMETERS SURFACE FINISH: TOLERANCES: LINEAR: ANGULAR:	FINISH:	DEBURR AND BREAK SHARP EDGES	DO NOT SCALE DRAWING	REVISION

	NAME	SIGNATURE	DATE
DRAWN	CT		04/06/22
CHK'D	JB		04/21/22
APPV'D			
MFG			
Q.A			

TITLE: **Base Plate**

MATERIAL: Wood

WEIGHT:

DWG NO. Hub Assem 01 | A2

SCALE:1:8 | SHEET 1 OF 1

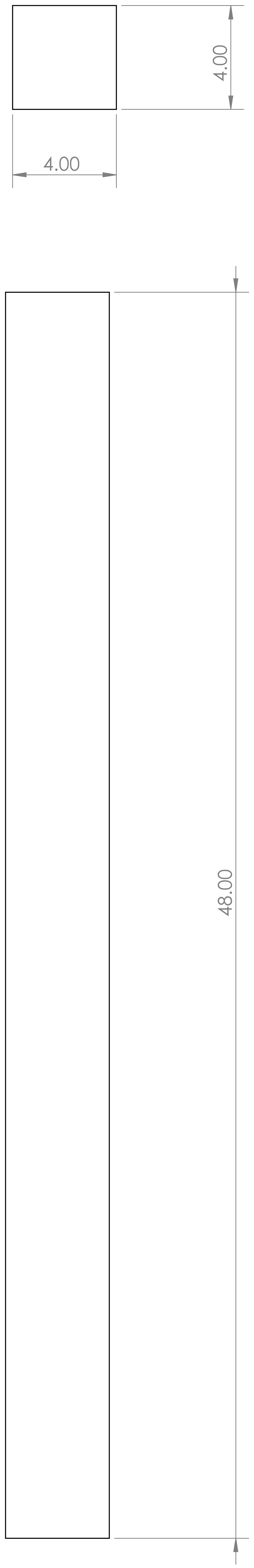

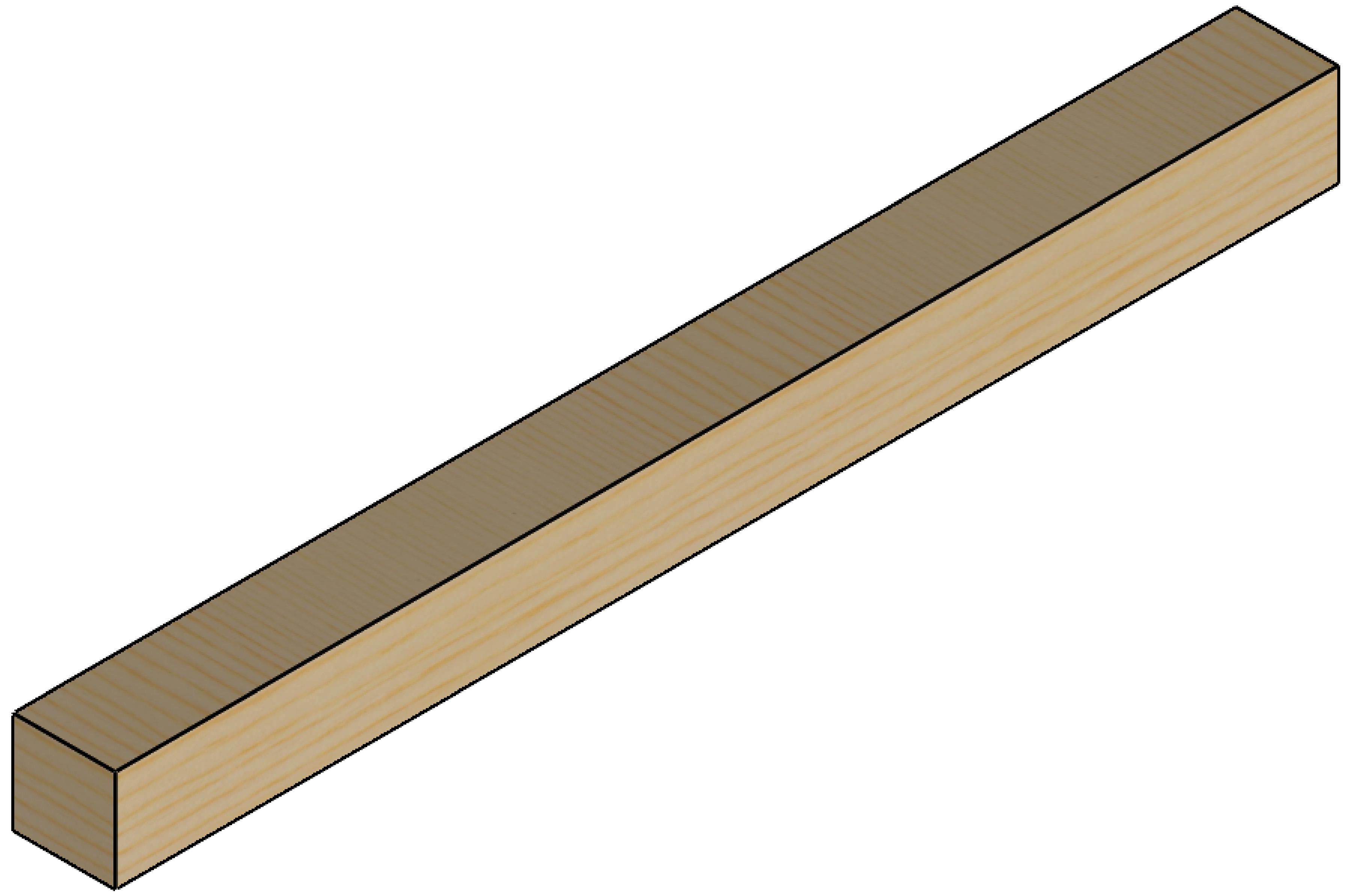

UNLESS OTHERWISE SPECIFIED: DIMENSIONS ARE IN MILLIMETERS SURFACE FINISH: TOLERANCES: LINEAR: ANGULAR:	FINISH:		DEBURR AND BREAK SHARP EDGES	DO NOT SCALE DRAWING	REVISION	
	NAME	SIGNATURE	DATE	TITLE:		
DRAWN	CT		04/18/2022	Support Post		
CHK'D	JB		4/27/22			
APPV'D						
MFG						
Q.A			MATERIAL: Wood	DWG NO. Hub Assem 02		A2
			WEIGHT:	SCALE:1:4	SHEET 1 OF 1	

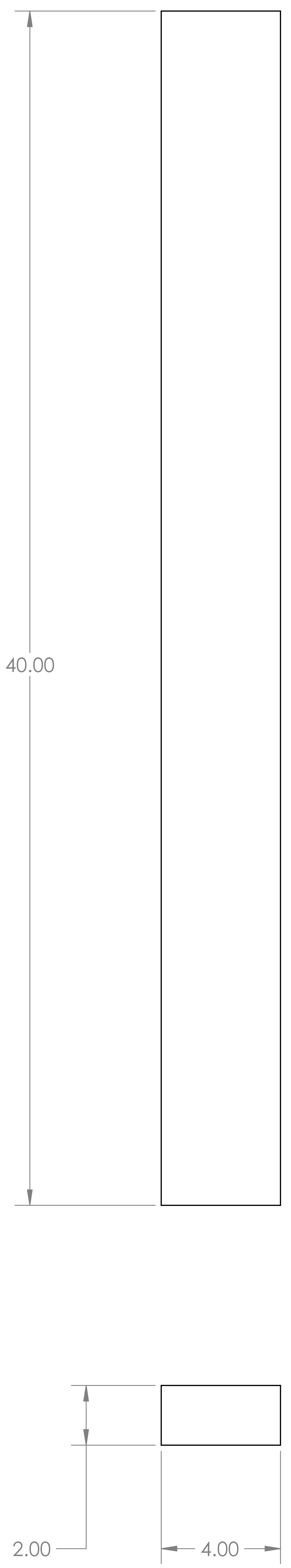

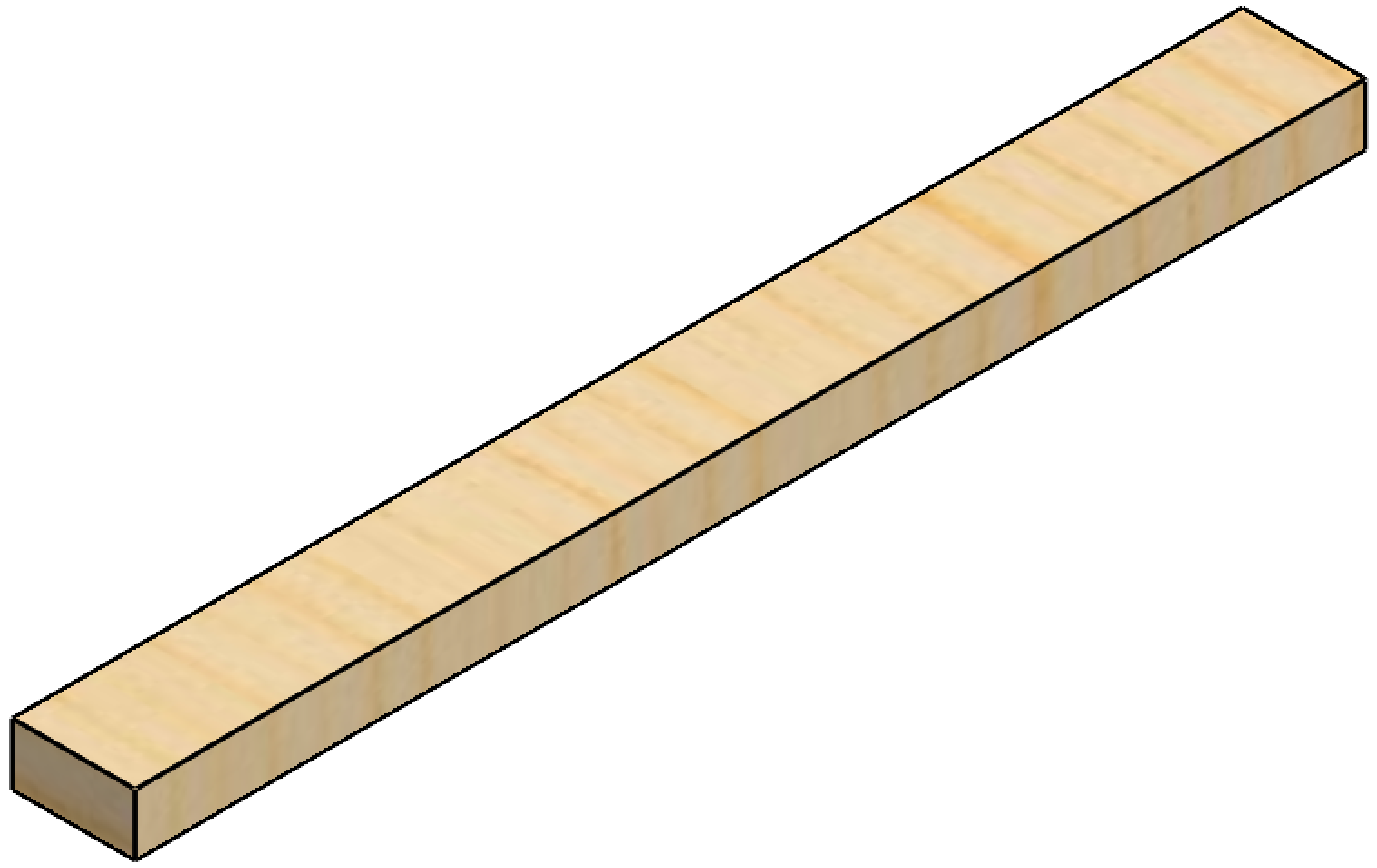

UNLESS OTHERWISE SPECIFIED:
DIMENSIONS ARE IN MILLIMETERS
SURFACE FINISH:
TOLERANCES:
LINEAR:
ANGULAR:

FINISH:

DEBURR AND BREAK SHARP EDGES

DO NOT SCALE DRAWING

REVISION

	NAME	SIGNATURE	DATE
DRAWN	JP		4/18/22
CHK'D	JB		04/21/22
APPV'D			
MFG			
Q.A			

TITLE:

Horizontal Post

MATERIAL: Wood

WEIGHT:

DWG NO. Hub Assem 03

A2

SCALE:1:4

SHEET 1 OF 1

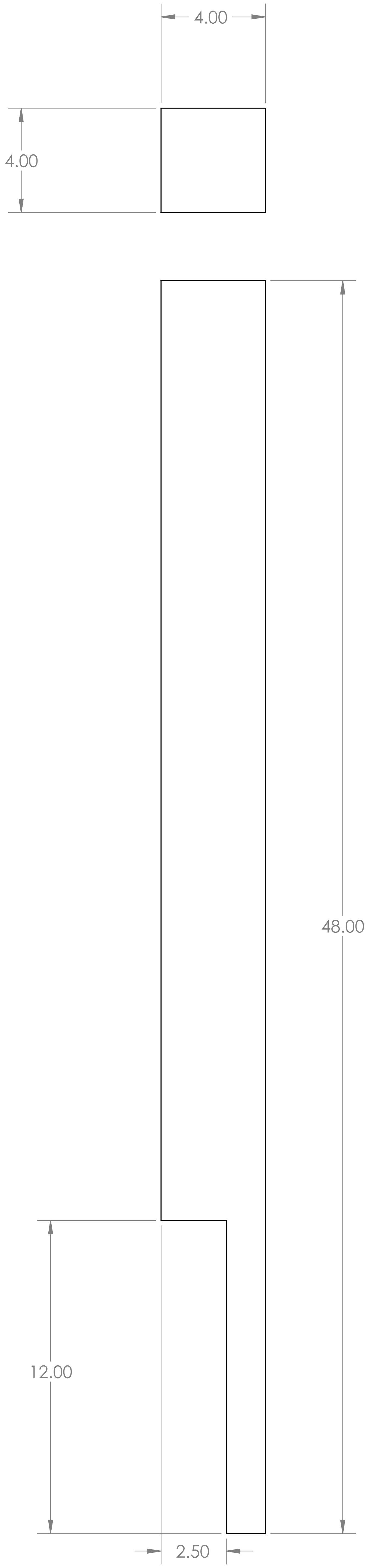

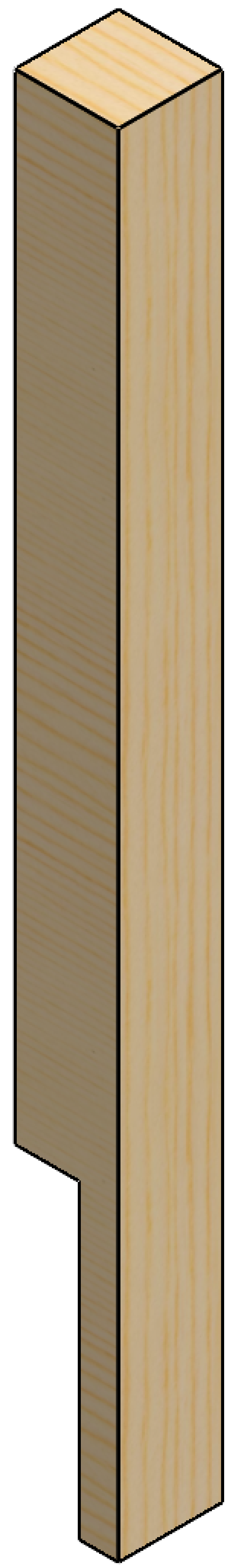

UNLESS OTHERWISE SPECIFIED: DIMENSIONS ARE IN MILLIMETERS SURFACE FINISH: TOLERANCES: LINEAR: ANGULAR:	FINISH:	DEBURR AND BREAK SHARP EDGES	DO NOT SCALE DRAWING	REVISION

	NAME	SIGNATURE	DATE
DRAWN	JP		4/27/22
CHK'D	JB		04/27/22
APPV'D			
MFG			
Q.A			

TITLE: Cut Post

MATERIAL: Pine

DWG NO. Hub Assem 04

A2

WEIGHT:

SCALE:1:4

SHEET 1 OF 1

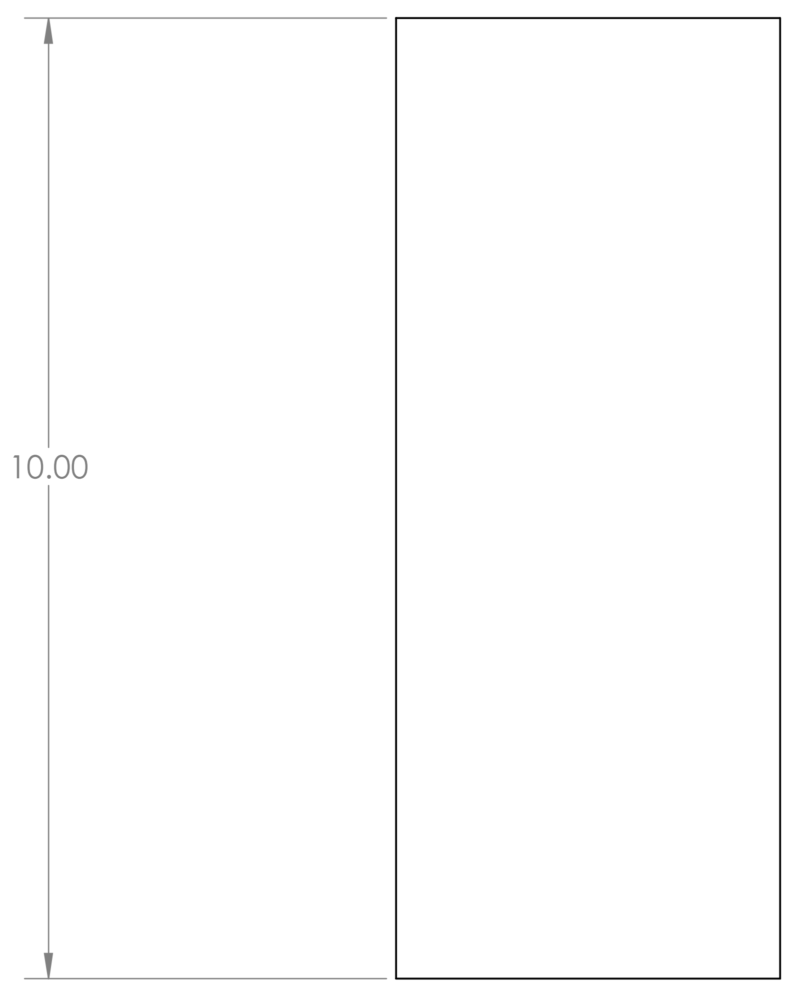

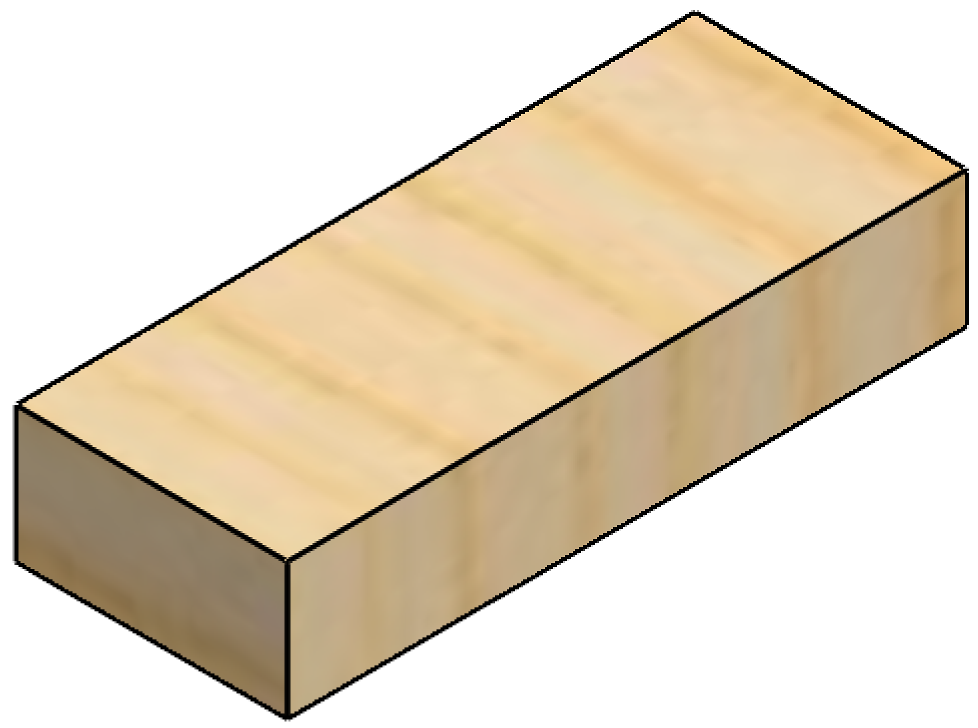

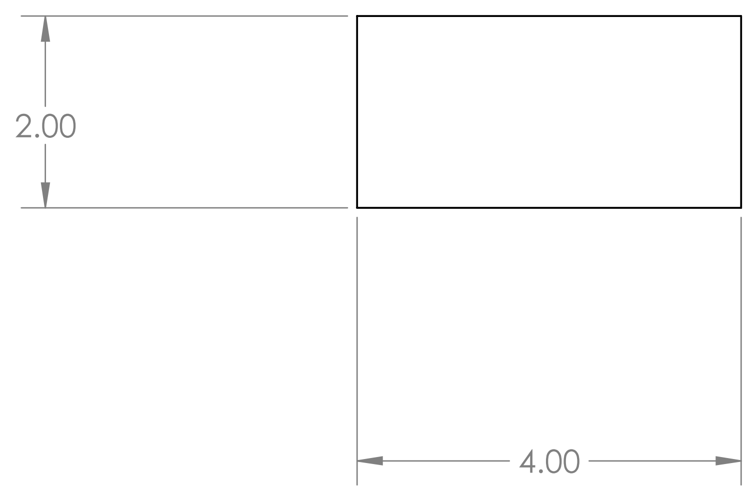

UNLESS OTHERWISE SPECIFIED: DIMENSIONS ARE IN MILLIMETERS SURFACE FINISH: TOLERANCES: LINEAR: ANGULAR:	FINISH:		DEBURR AND BREAK SHARP EDGES	DO NOT SCALE DRAWING	REVISION
	NAME	SIGNATURE	DATE		TITLE: Tank Reinforcement	
DRAWN	JP		04/18/22			
CHK'D	JB		04/21/22			
APPV'D						
MFG						
Q.A				MATERIAL: Pine	DWG NO. Hub Assem 05 - Tank Reinforcement	A2
				WEIGHT:	SCALE:1:2	SHEET 1 OF 1

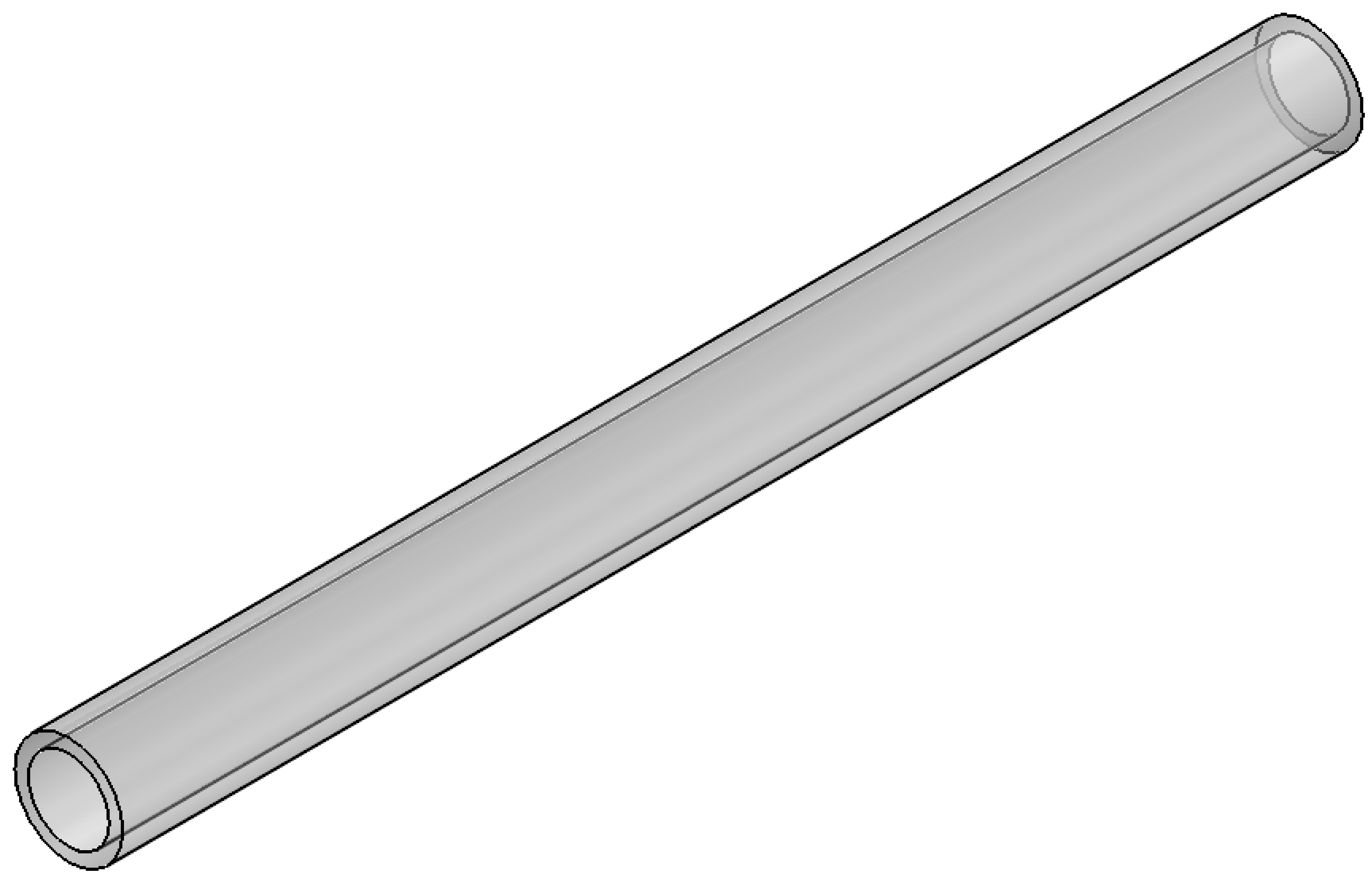

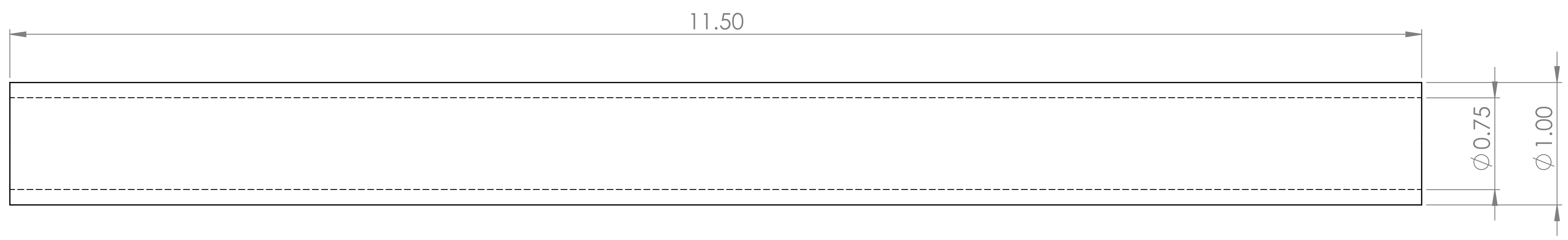

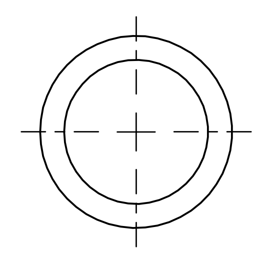

UNLESS OTHERWISE SPECIFIED:
DIMENSIONS ARE IN MILLIMETERS
SURFACE FINISH:
TOLERANCES:
LINEAR:
ANGULAR:

FINISH:

DEBURR AND BREAK SHARP EDGES

DO NOT SCALE DRAWING

REVISION

	NAME	SIGNATURE	DATE
DRAWN	NM		04/07/22
CHK'D	JB		04/27/22
APPV'D			
MFG			
Q.A			

TITLE:

Hub Tubing - Lower

MATERIAL: PPS

WEIGHT:

DWG NO. Hub Assem 06

A2

SCALE:1:2

SHEET 1 OF 1

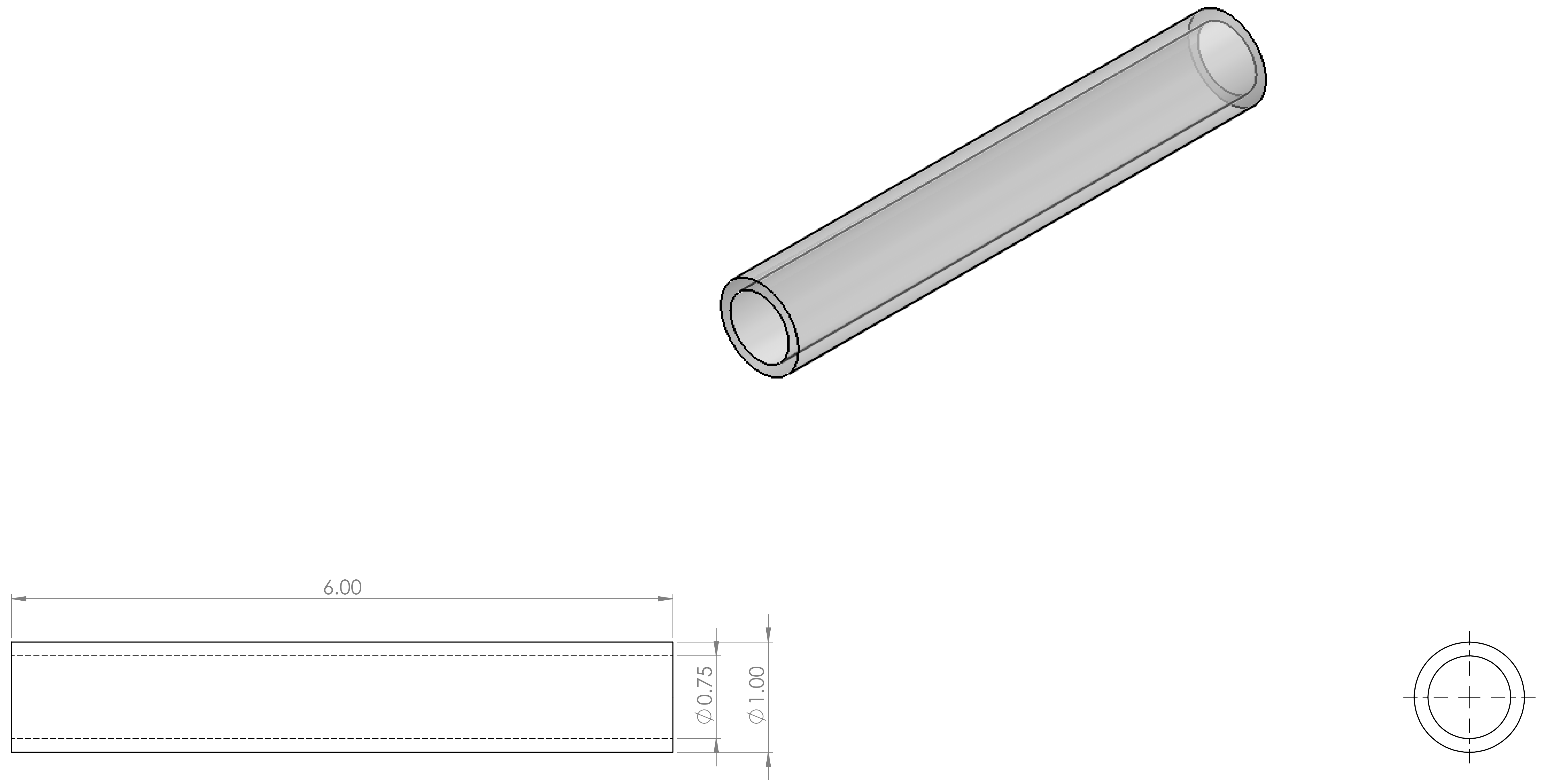

UNLESS OTHERWISE SPECIFIED:
DIMENSIONS ARE IN MILLIMETERS
SURFACE FINISH:
TOLERANCES:
LINEAR:
ANGULAR:

FINISH:

DEBURR AND BREAK SHARP EDGES

DO NOT SCALE DRAWING

REVISION

	NAME	SIGNATURE	DATE
DRAWN	NM		04/07/22
CHK'D	JB		04/27/22
APPV'D			
MFG			
Q.A			

TITLE: Hub Tubing - Upper

MATERIAL: PPS

WEIGHT:

DWG NO. Hub Assem 07

A2

SCALE:1:1

SHEET 1 OF 1

ITEM NO.	PART NUMBER	DESCRIPTION	QTY.
1	Rover Assem 02	Frame Assembly	1
2	Rover Assem 07	Acrylic Siding	2
3	Rover Assem 08	Acrylic Siding	4
4	Rover Assem 09	Acrylic Siding	1
5	Rover Assem 10	Acrylic Siding	2
6	Rover Assem 11	Acrylic Siding	2
7	Rover Assem 12	Motor	4
8	Rover Assem 03	Rover Top	1
9	Rover Assem 13	Washer	8
10	Transmission Assem 02	Wheel and Axle Assembly	4
11	Rover Assem 05	Fluild Tank Enclosure	1
12	Rover Assem 14	Fluid Refill Lid Guide	2
13	Rover Assem 15	Fluid Refill Lid Guide	2
14	Rover Assem 04	Spraybar Assembly	1
15	Rover Assem 16	Fluid Tank	1
16	Rover Assem 17	Fluid Refill Tube	1
17	Rover Assem 18	Axle Mounting	8
18	Rover Assem 01	Transmission Assembly	4
19	Rover Assem 19	Rack and Pinnion Assembly	1
20	Rover Assem 20	12v Submersible Pump	1
21	Rover Assem 21	Fluid System Refill Cover	1
22	Rover Assem 06	Sensor Arm Assembly	1
23	Spray Assem 03	Mounting Bracket	1
24	Rover Assem 22	Vex 17.5" Linear Slide Rail	1
25	Rover Assem 23	Vex Internal Linear Slide	1
26	Rover Assem 24	Screw	2
27	Rover Assem 25	12v Lithium Ion Battery	1

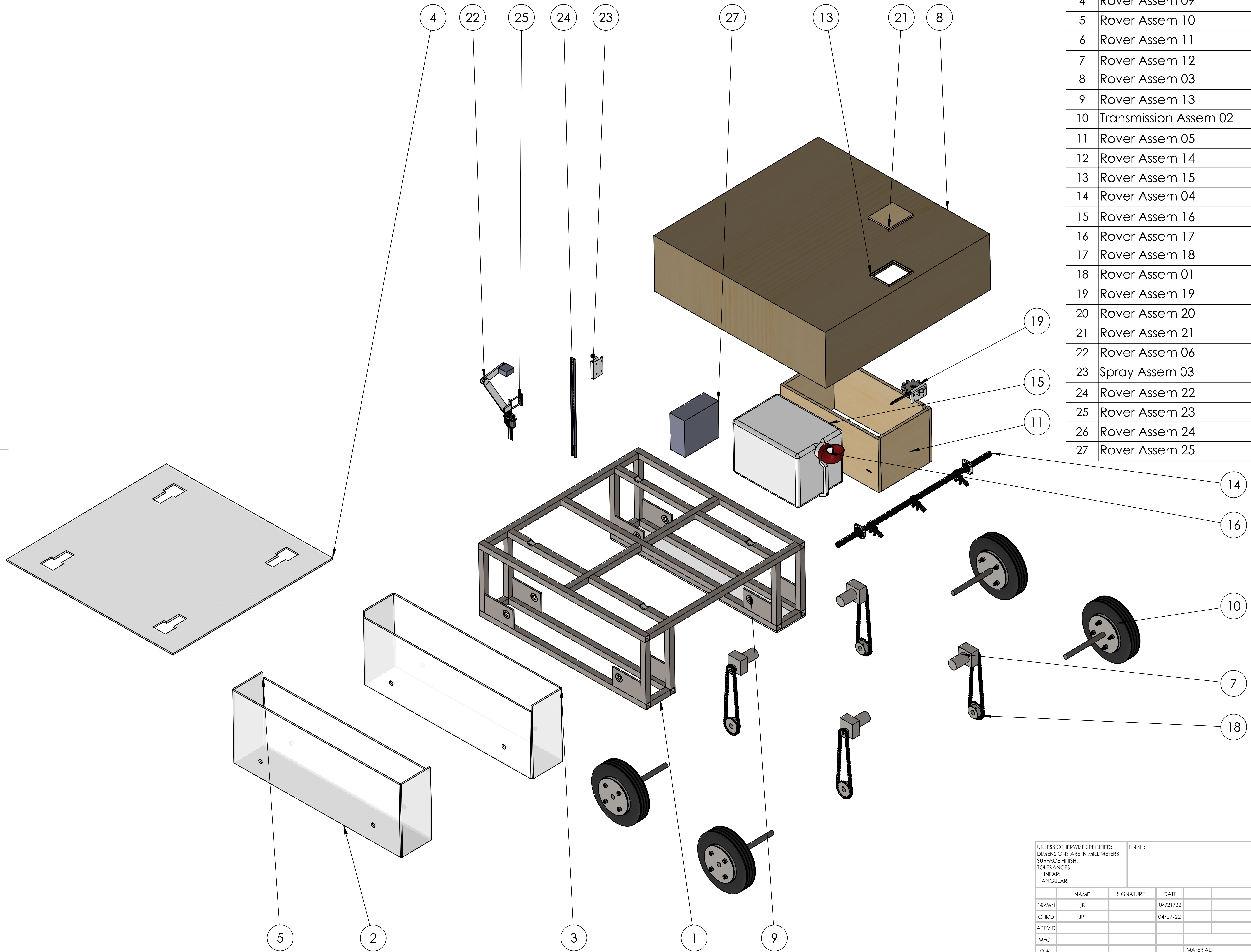

UNLESS OTHERWISE SPECIFIED:
DIMENSIONS ARE IN MILLIMETERS
SURFACE FINISH:
TOLERANCES:
LINEAR:
ANGULAR:

FINISH:

DEBURR AND BREAK SHARP EDGES

DO NOT SCALE DRAWING

REVISION

	NAME	SIGNATURE	DATE
DRAWN	JB		04/21/22
CHK'D	JP		04/27/22
APPV'D			
MFG			
Q.A			

MATERIAL:

WEIGHT:

TITLE:

Rover Assembly

DWG NO.

Rover Assem 00

A2

SCALE:1:10

SHEET 1 OF 1

ITEM NO.	PART NUMBER	DESCRIPTION	QTY.
1	Frame Assem 05	34 Inch square steel tubing	6
2	Frame Assem 03	31 Inch square steel tubing	2
3	Frame Assem 04	32 Inch square steel tubing	1
4	Frame Assem 02	15 Inch square steel tubing	2
5	Frame Assem 01	11 Inch square steel tubing	8
6	Frame Assem 06	4 Inch square steel tubing	4
7	Frame Assem 07	15.5 Inch square steel tubing with cut out for motor mounting	4

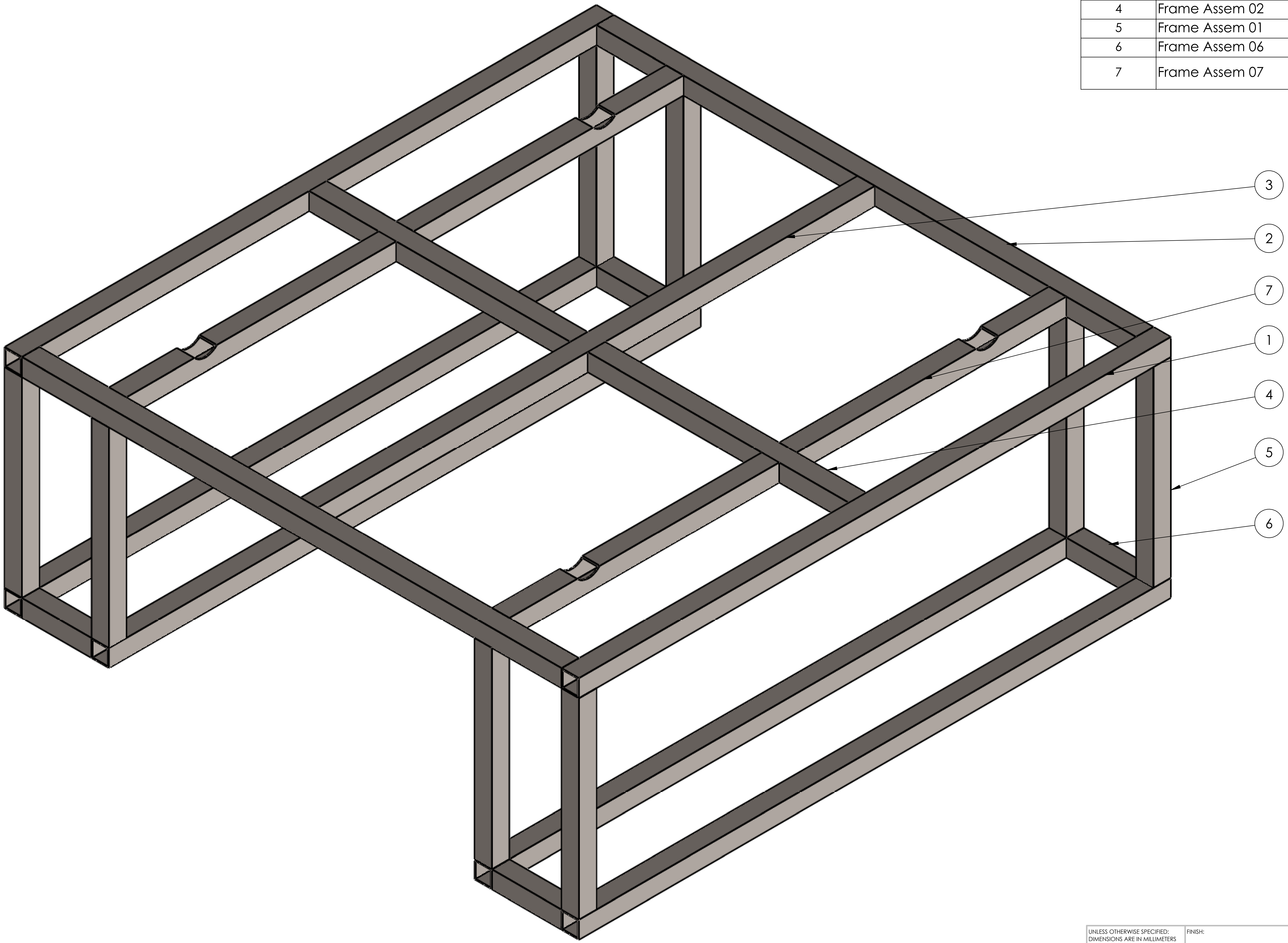

UNLESS OTHERWISE SPECIFIED:
DIMENSIONS ARE IN MILLIMETERS
SURFACE FINISH:
TOLERANCES:
LINEAR:
ANGULAR:

FINISH:

DEBURR AND BREAK SHARP EDGES

DO NOT SCALE DRAWING

REVISION

	NAME	SIGNATURE	DATE
DRAWN	JB		04/06/22
CHK'D	JP		4/27/22
APPV'D			
MFG			
Q.A			

MATERIAL:

WEIGHT:

TITLE: Frame Assem

DWG NO. Rover Assem 02

A2

SCALE:1:3

SHEET 1 OF 1

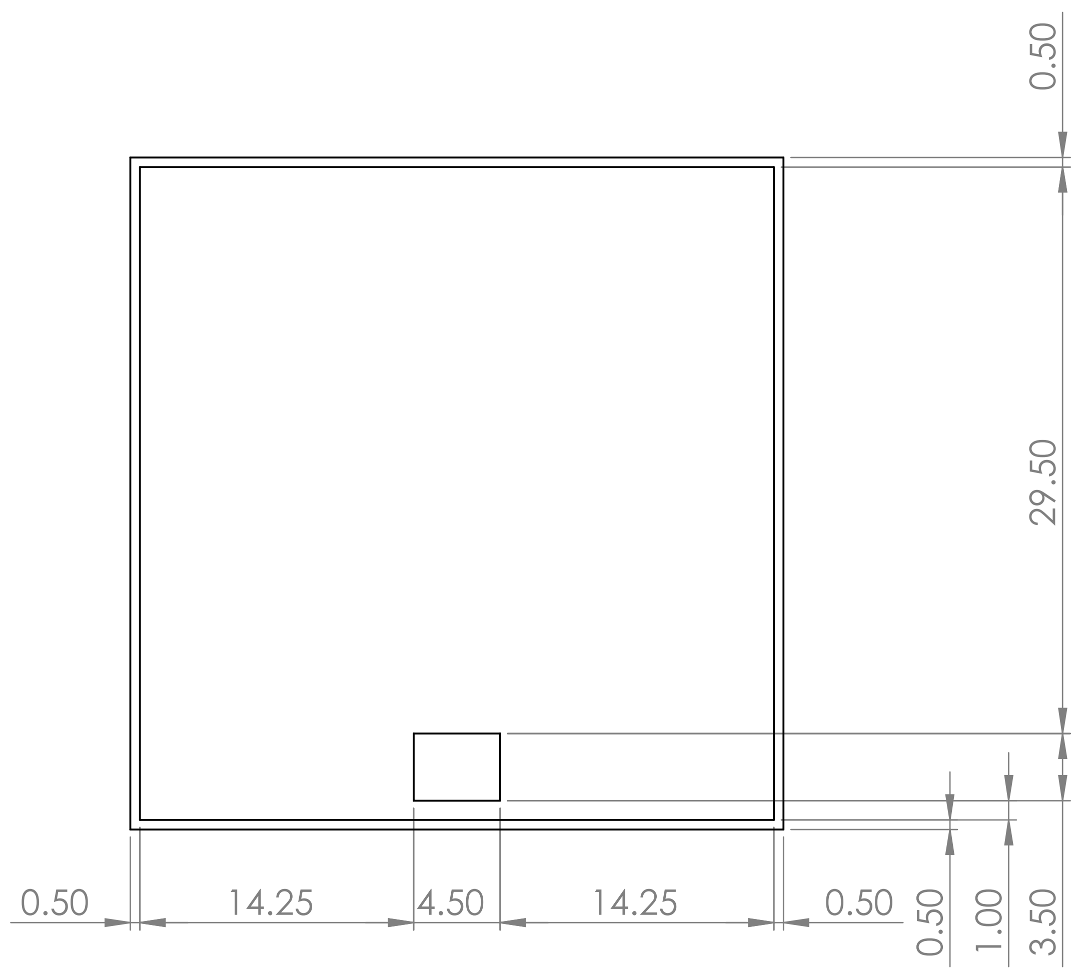

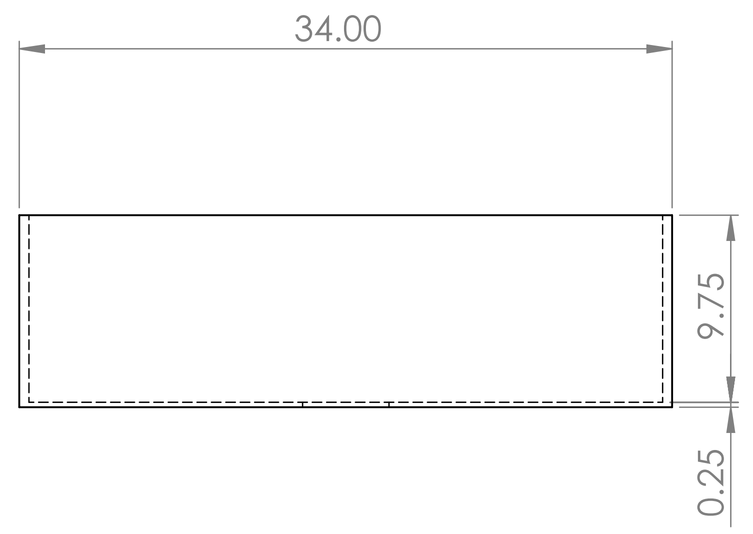

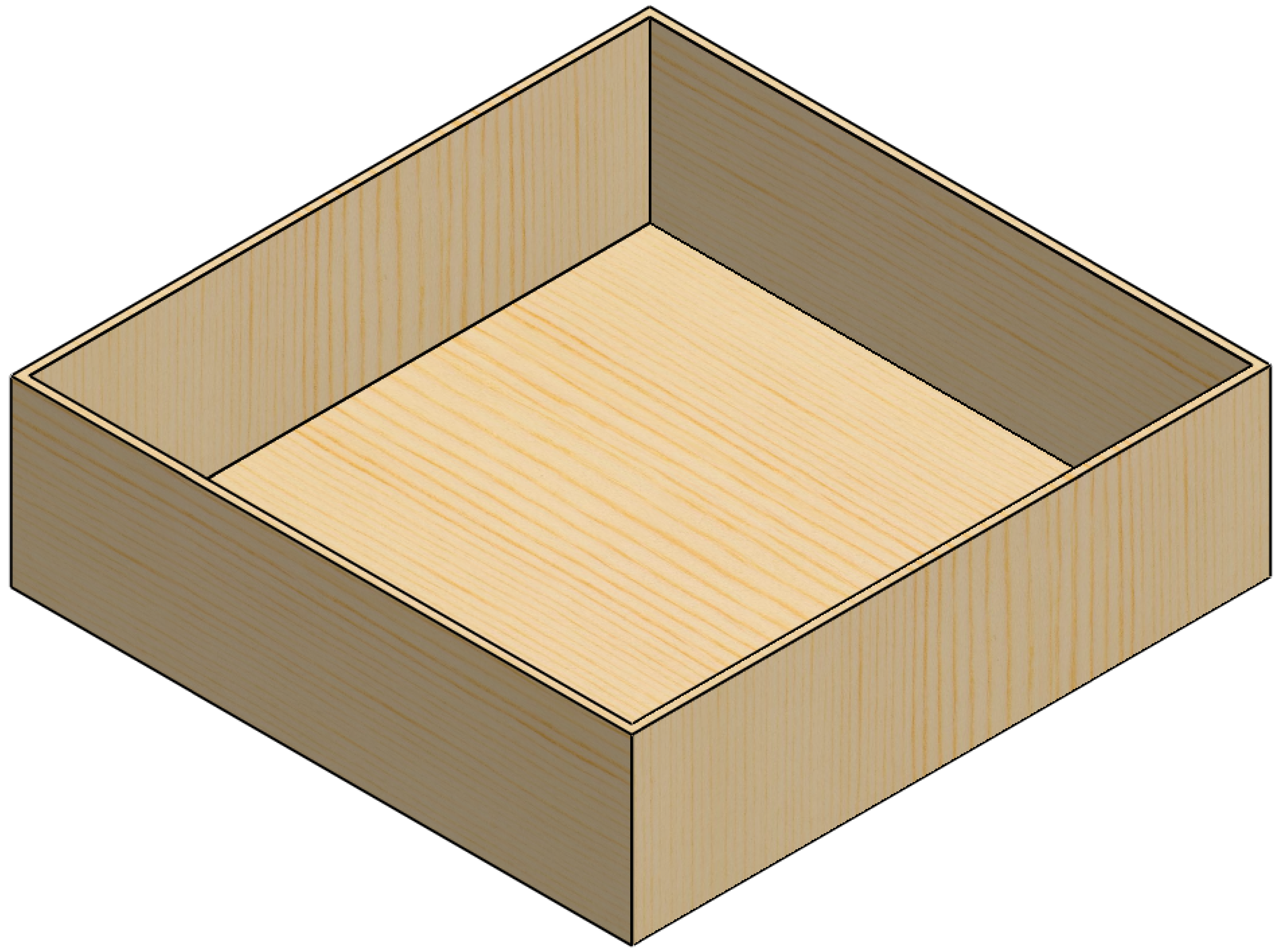

UNLESS OTHERWISE SPECIFIED:
DIMENSIONS ARE IN MILLIMETERS
SURFACE FINISH:
TOLERANCES:
LINEAR:
ANGULAR:

FINISH:

DEBURR AND BREAK SHARP EDGES

DO NOT SCALE DRAWING

REVISION

	NAME	SIGNATURE	DATE
DRAWN	JB		04/07/22
CHK'D	JP		4/27/22
APPV'D			
MFG			
Q.A			

MATERIAL: Pine

WEIGHT:

TITLE: Rover Top

DWG NO. Rover Assem 03

A2

SCALE:1:10

SHEET 1 OF 1

ITEM NO.	PART NUMBER	DESCRIPTION	QTY.
1	Spray_Nozzle_Fan_1	Green Plastic Fan Nozzle Tip	3
2	Spray_Nozzle_Body	Black Plastic Fan Nozzle Body	3
3	Spraybar_Bar	800mm Carbon Fiber bar	1
4	Spraybar_Mounting_Bracket	White 3D-printed bracket	2
5	Flange	Black 3D-printed flange	2

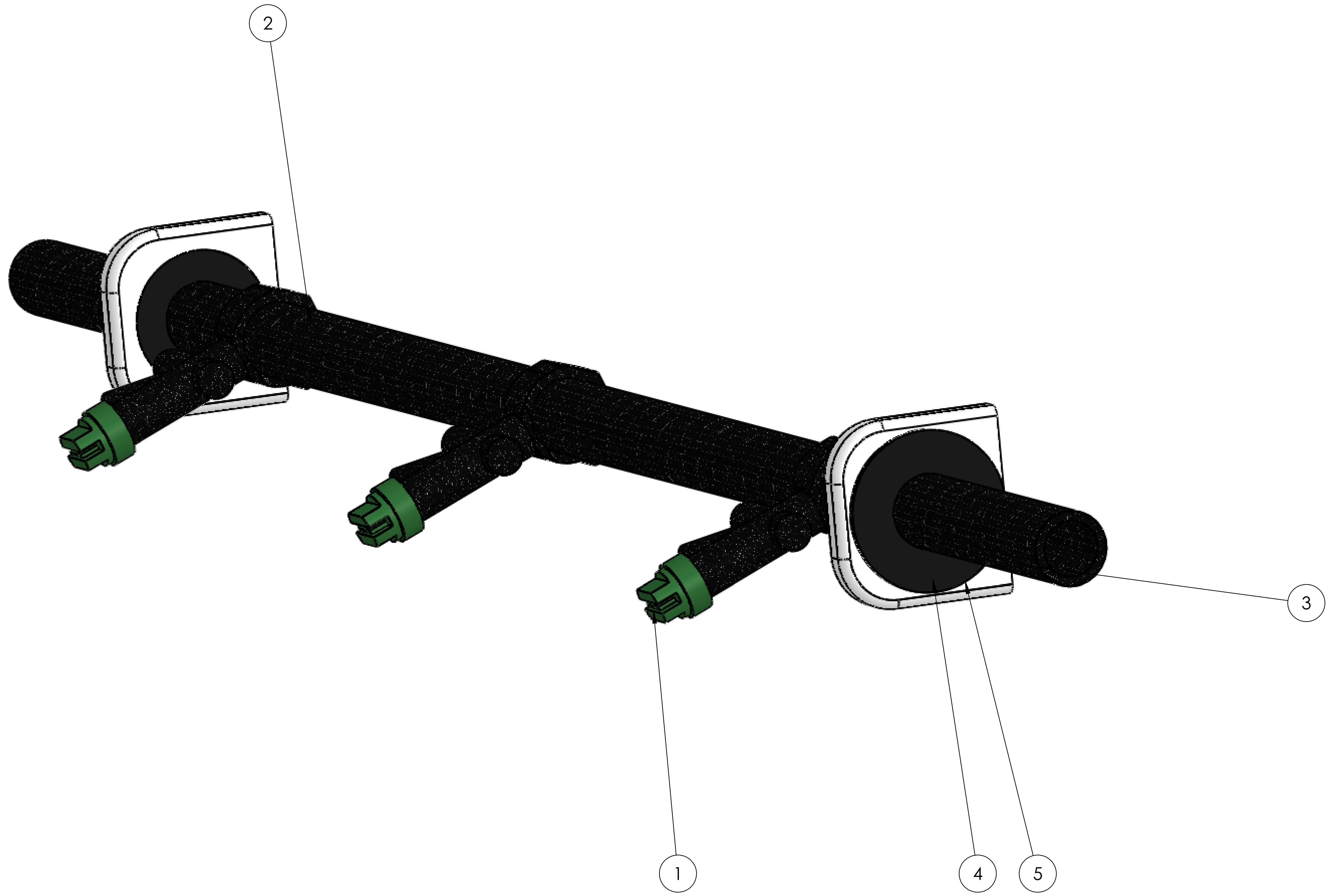

UNLESS OTHERWISE SPECIFIED: DIMENSIONS ARE IN MILLIMETERS SURFACE FINISH: TOLERANCES: LINEAR: ANGULAR:	FINISH:	DEBURR AND BREAK SHARP EDGES	DO NOT SCALE DRAWING	REVISION
	NAME	SIGNATURE	DATE	TITLE: Spraybar Assembly
DRAWN	JB		04/06/22	
CHK'D	JP		4/27/22	
APPV'D				
MFG				
Q.A			MATERIAL:	DWG NO. Rover Assem 04 — A2
			WEIGHT:	SCALE:1:5 — SHEET 1 OF 1

ITEM NO.	PART NUMBER	DESCRIPTION	QTY.
1	Short size wood	10" x 9.5" Plywood sheet	2
2	long side wood	20" x 9.5" Plywood sheet	2

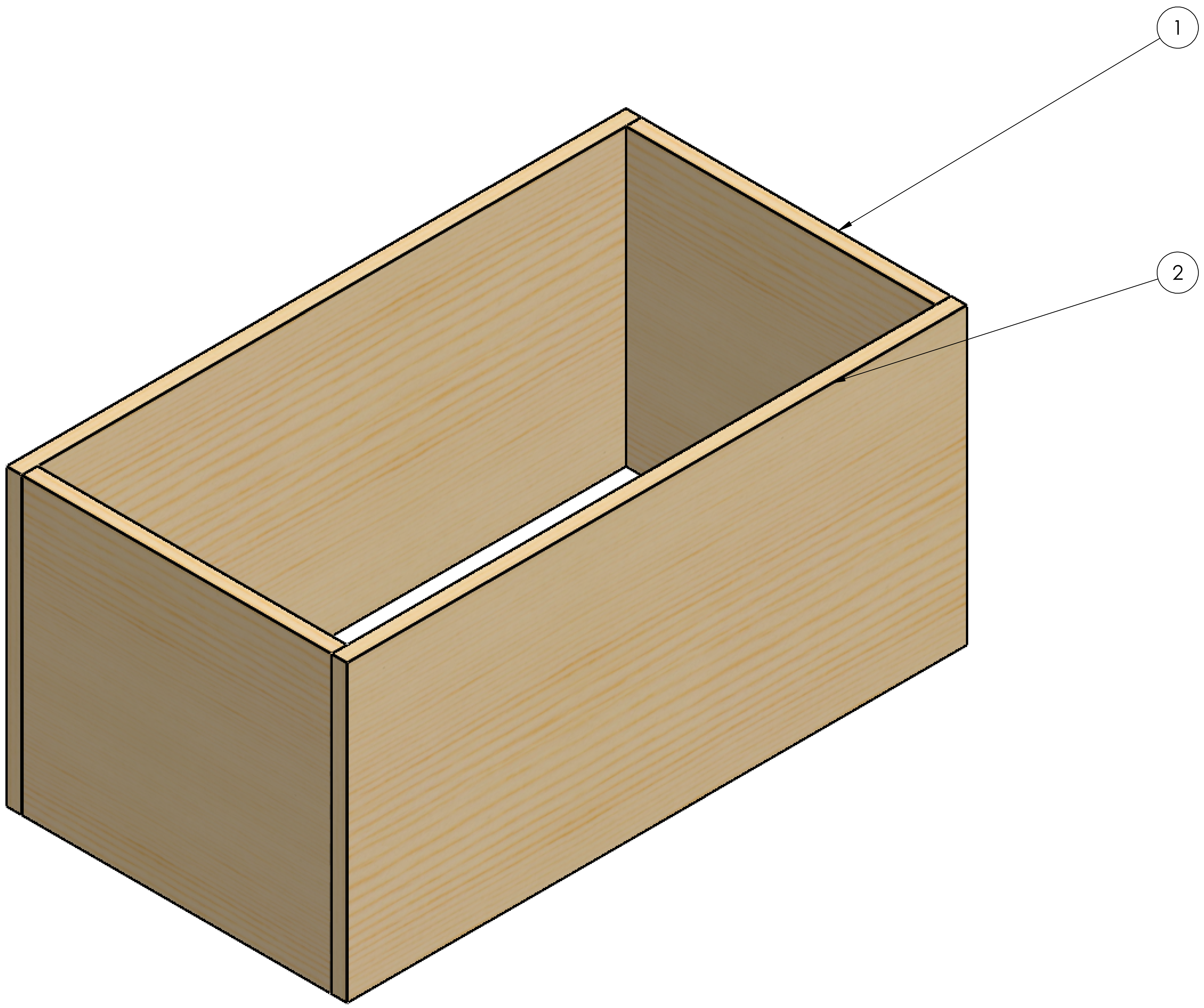

UNLESS OTHERWISE SPECIFIED: DIMENSIONS ARE IN MILLIMETERS SURFACE FINISH: TOLERANCES: LINEAR: ANGULAR:	FINISH:	DEBURR AND BREAK SHARP EDGES	DO NOT SCALE DRAWING / REVISION

	NAME	SIGNATURE	DATE
DRAWN	NM		04/09/22
CHK'D	JB		04/27/22
APPV'D			
MFG			
Q.A			

TITLE: Enclosure

MATERIAL: Plywood Sheet

WEIGHT:

DWG NO. Rover Assem 05

A2

SCALE:1:5

SHEET 1 OF 1

ITEM NO.	PART NUMBER	DESCRIPTION	QTY.
1	Arm Assem 02	Crank	1
2	Arm Assem 01	Link	1
3	Arm Assem 04	Joint	1
4	Arm Assem 05	Joint Top	2
5	Arm Assem 03	Slider	1
6	Arm Assem 06	NPK Probe Fixtureing	1
7	Arm Assem 07	Servo Motor	1

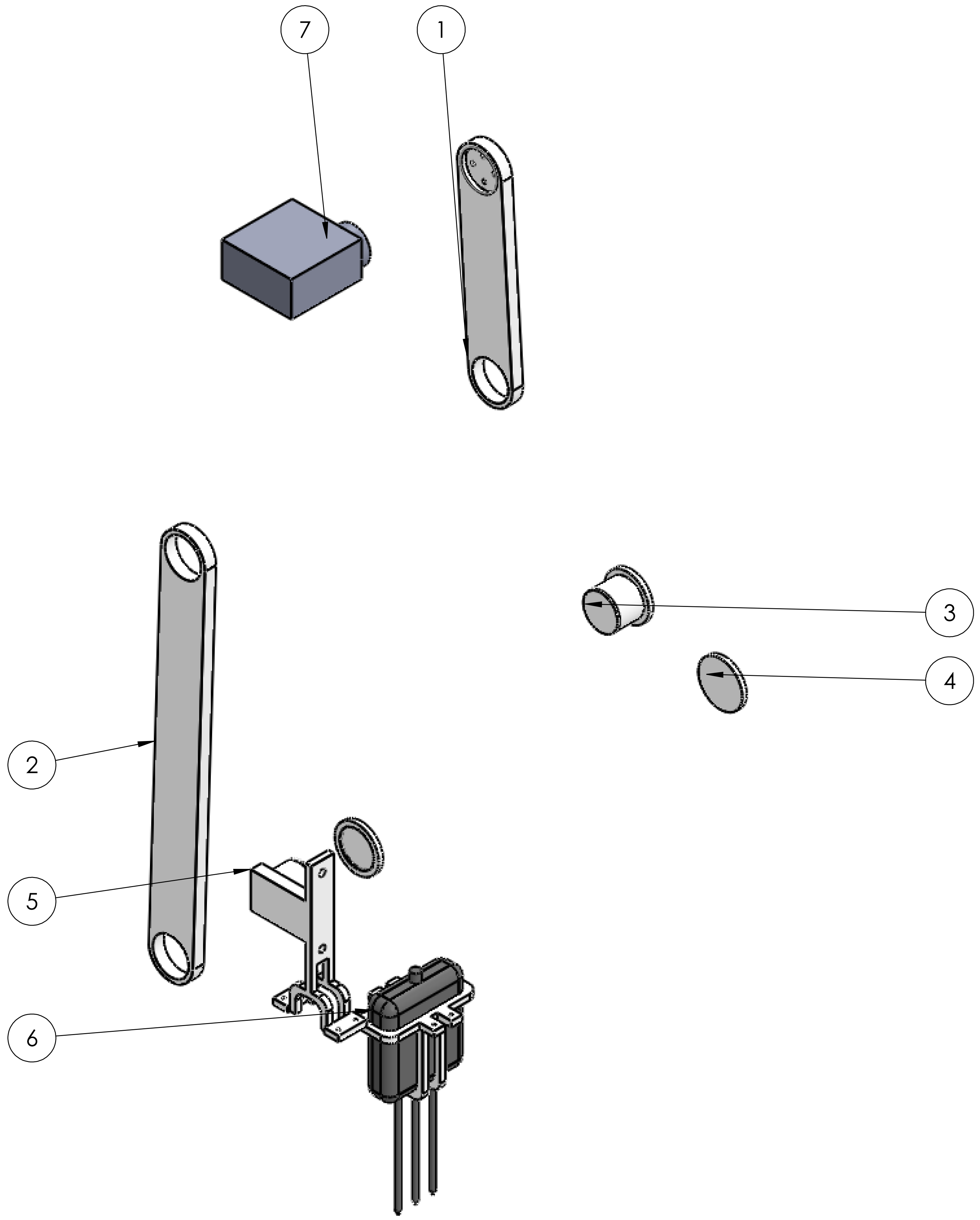

UNLESS OTHERWISE SPECIFIED:
DIMENSIONS ARE IN MILLIMETERS
SURFACE FINISH:
TOLERANCES:
LINEAR:
ANGULAR:

FINISH:

DEBURR AND BREAK SHARP EDGES

DO NOT SCALE DRAWING

REVISION

	NAME	SIGNATURE	DATE
DRAWN	JB		04/18/22
CHK'D	JP		4/27/22
APPV'D			
MFG			
Q.A			

MATERIAL:

WEIGHT:

TITLE:
Sensor Arm Assembly

DWG NO.
Rover Assem 06

A2

SCALE:1:2

SHEET 1 OF 1

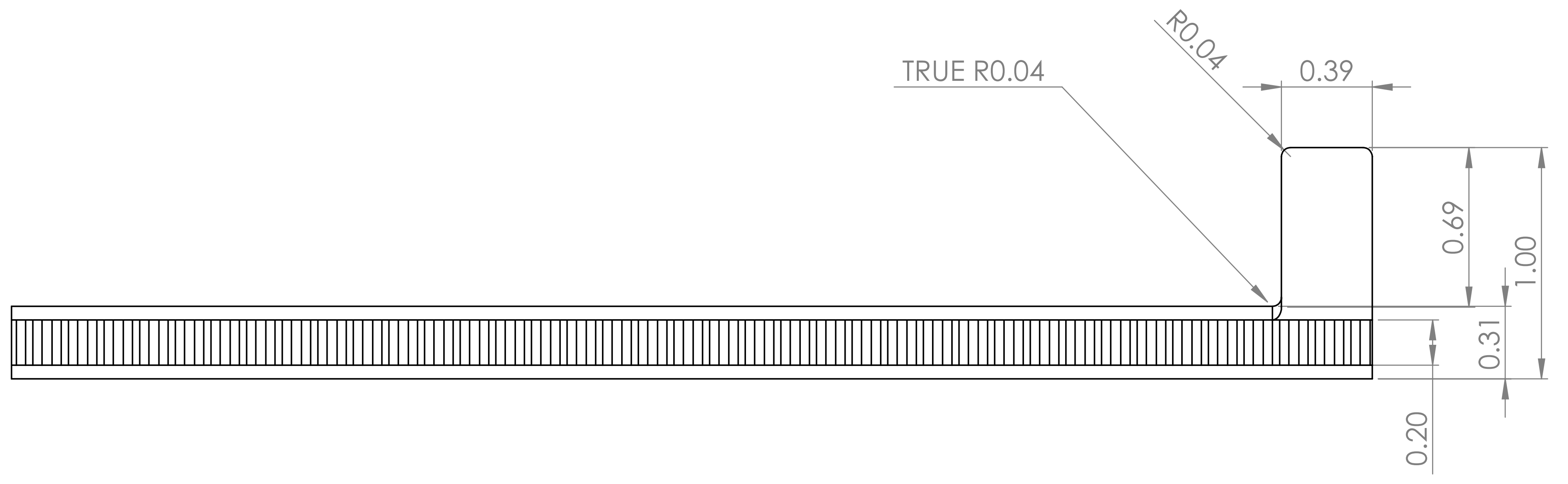

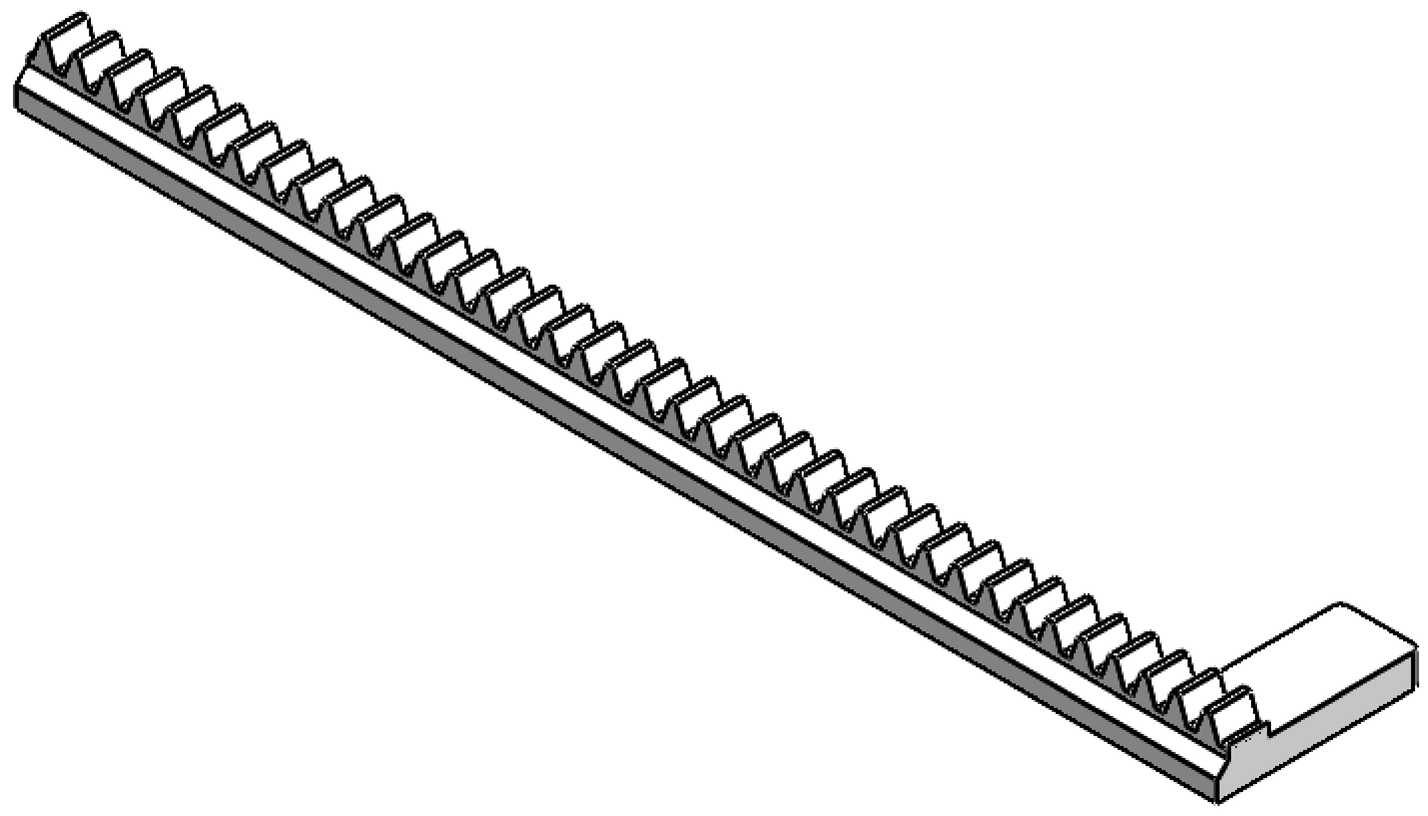

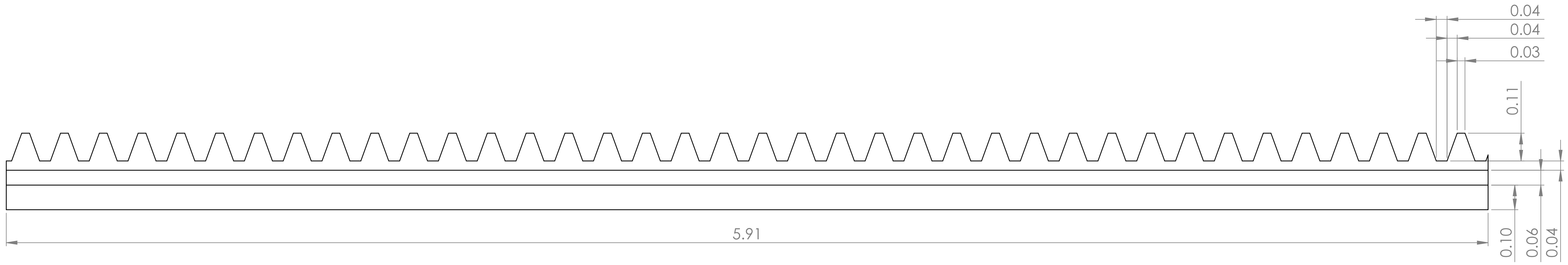

UNLESS OTHERWISE SPECIFIED: DIMENSIONS ARE IN MILLIMETERS SURFACE FINISH: TOLERANCES: LINEAR: ANGULAR:	FINISH:		DEBURR AND BREAK SHARP EDGES	DO NOT SCALE DRAWING	REVISION
	NAME	SIGNATURE	DATE	TITLE:	
DRAWN	NM		04/06/22	Rack Arm	
CHK'D	JB		04/27/22		
APPV'D					
MFG					
Q.A			MATERIAL: ABS	DWG NO. Spray Assem 01	A2
			WEIGHT:	SCALE:1:1	SHEET 1 OF 1

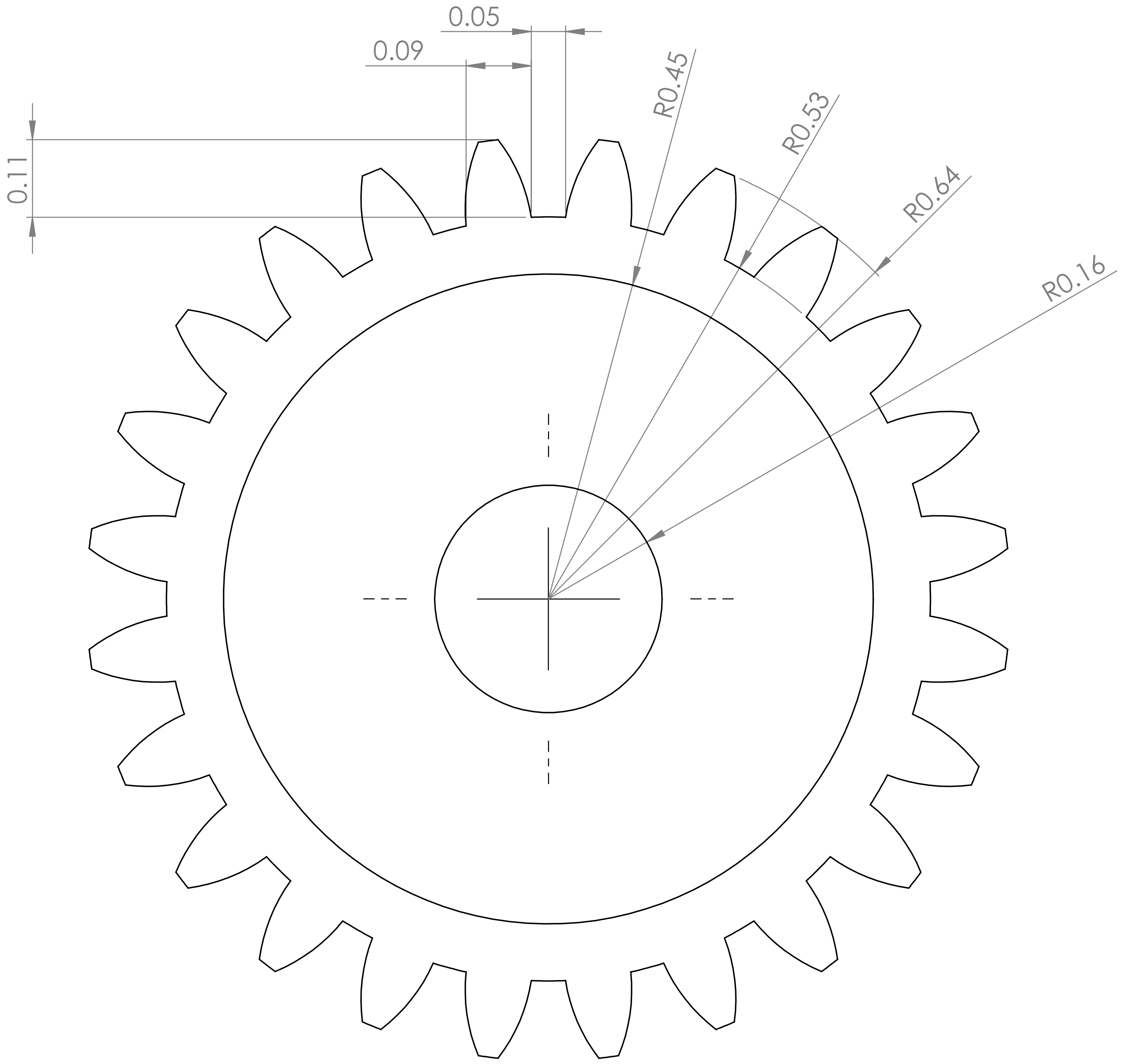

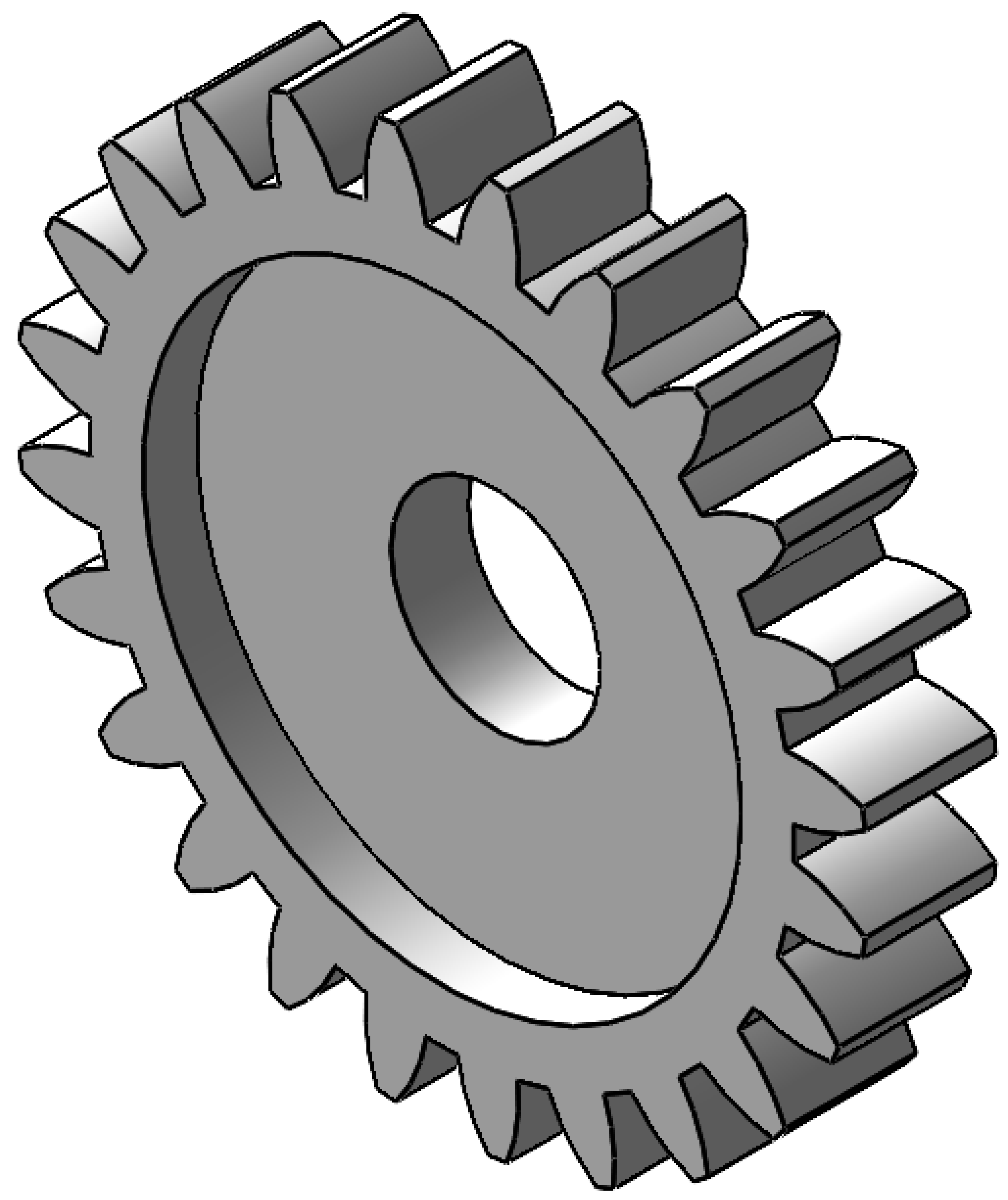

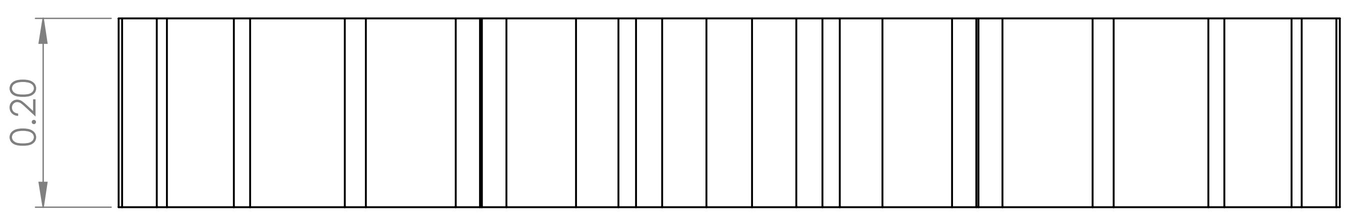

UNLESS OTHERWISE SPECIFIED: DIMENSIONS ARE IN MILLIMETERS SURFACE FINISH: TOLERANCES: LINEAR: ANGULAR:	FINISH:		DEBURR AND BREAK SHARP EDGES	DO NOT SCALE DRAWING	REVISION
	NAME	SIGNATURE	DATE	TITLE:	
DRAWN	NM		04/06/22	Spur Gear	
CHK'D	JB		04/27/22		
APPV'D					
MFG					
Q.A			MATERIAL: ABS	DWG NO. Spray Assem 02	A2
			WEIGHT:	SCALE:5:1	SHEET 1 OF 1

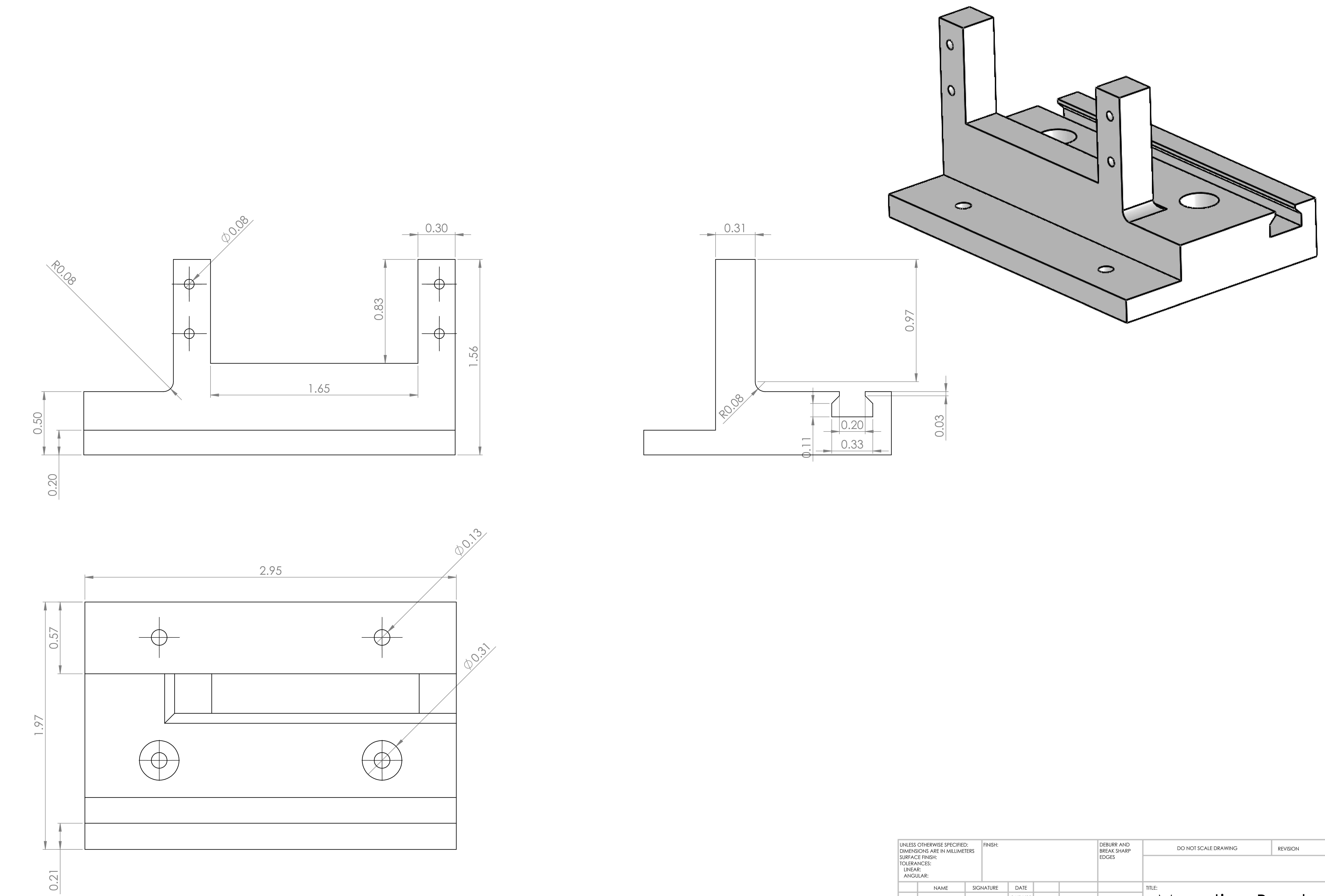

UNLESS OTHERWISE SPECIFIED: DIMENSIONS ARE IN MILLIMETERS SURFACE FINISH: TOLERANCES: LINEAR: ANGULAR:	FINISH:		DEBURR AND BREAK SHARP EDGES	DO NOT SCALE DRAWING	REVISION
	NAME	SIGNATURE	DATE	TITLE: Mounting Bracket	
DRAWN	NM		04/06/22		
CHK'D	JB		04/27/22		
APPV'D					
MFG					
Q.A			MATERIAL: ABS	DWG NO. Spray Assem 03	A2
			WEIGHT:	SCALE:2:1	SHEET 1 OF 1

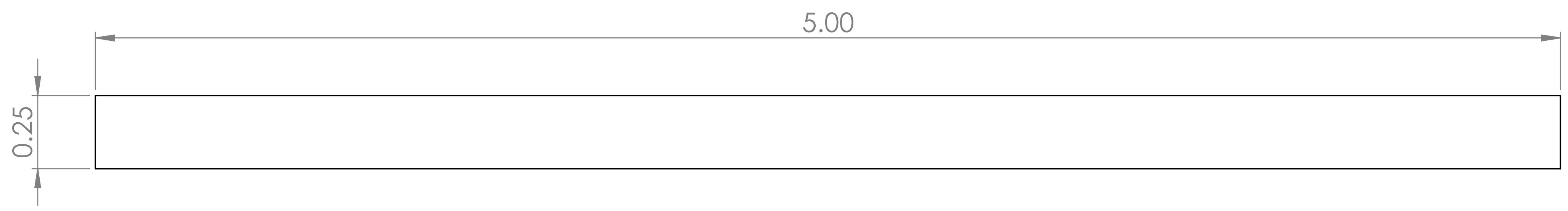

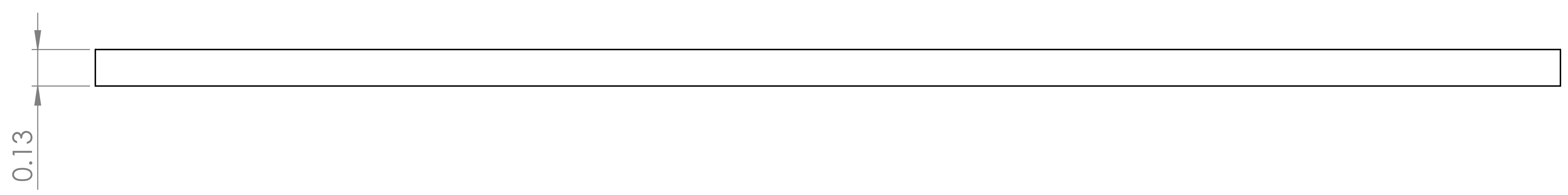

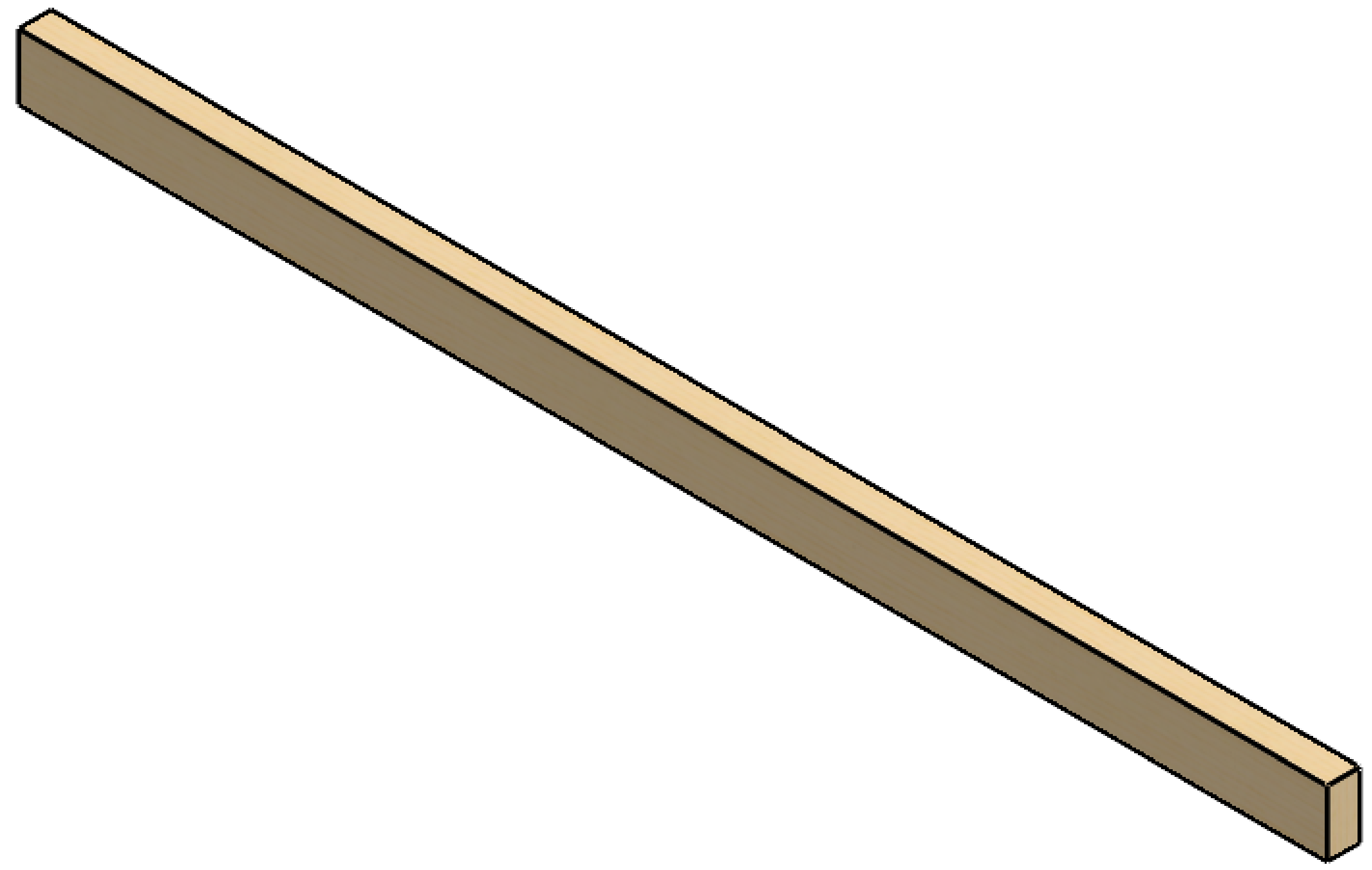

UNLESS OTHERWISE SPECIFIED: DIMENSIONS ARE IN MILLIMETERS SURFACE FINISH: TOLERANCES: LINEAR: ANGULAR:	FINISH:		DEBURR AND BREAK SHARP EDGES	DO NOT SCALE DRAWING	REVISION
	NAME	SIGNATURE	DATE	TITLE:	
DRAWN	NM		04/06/22	Rail	
CHK'D	JB		04/27/22		
APPV'D					
MFG					
Q.A			MATERIAL: Pine	DWG NO. Spray Asssem 04	A2
			WEIGHT:	SCALE:2:1	SHEET 1 OF 1

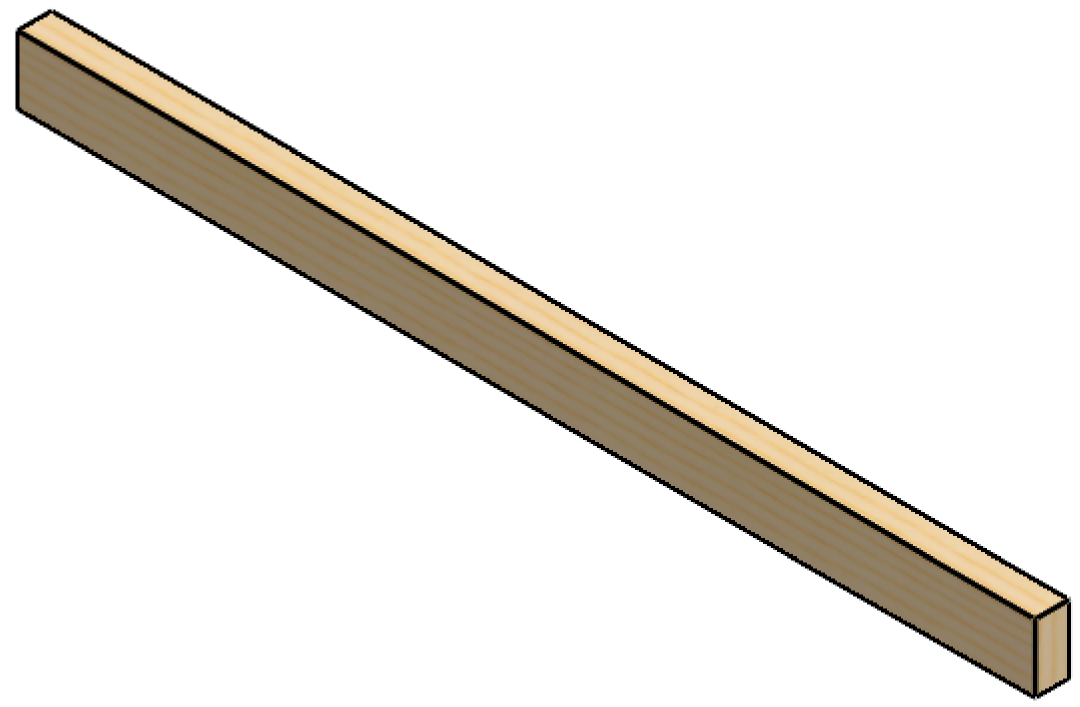

UNLESS OTHERWISE SPECIFIED:
DIMENSIONS ARE IN MILLIMETERS
SURFACE FINISH:
TOLERANCES:
LINEAR:
ANGULAR:

FINISH:

DEBURR AND BREAK SHARP EDGES

DO NOT SCALE DRAWING

REVISION

	NAME	SIGNATURE	DATE
DRAWN	NM		04/06/22
CHK'D	JB		04/27/22
APPV'D			
MFG			
Q.A			

MATERIAL: Pine

WEIGHT:

TITLE: Rail 2

DWG NO. Spray Assem 05

A2

SCALE:2:1

SHEET 1 OF 1

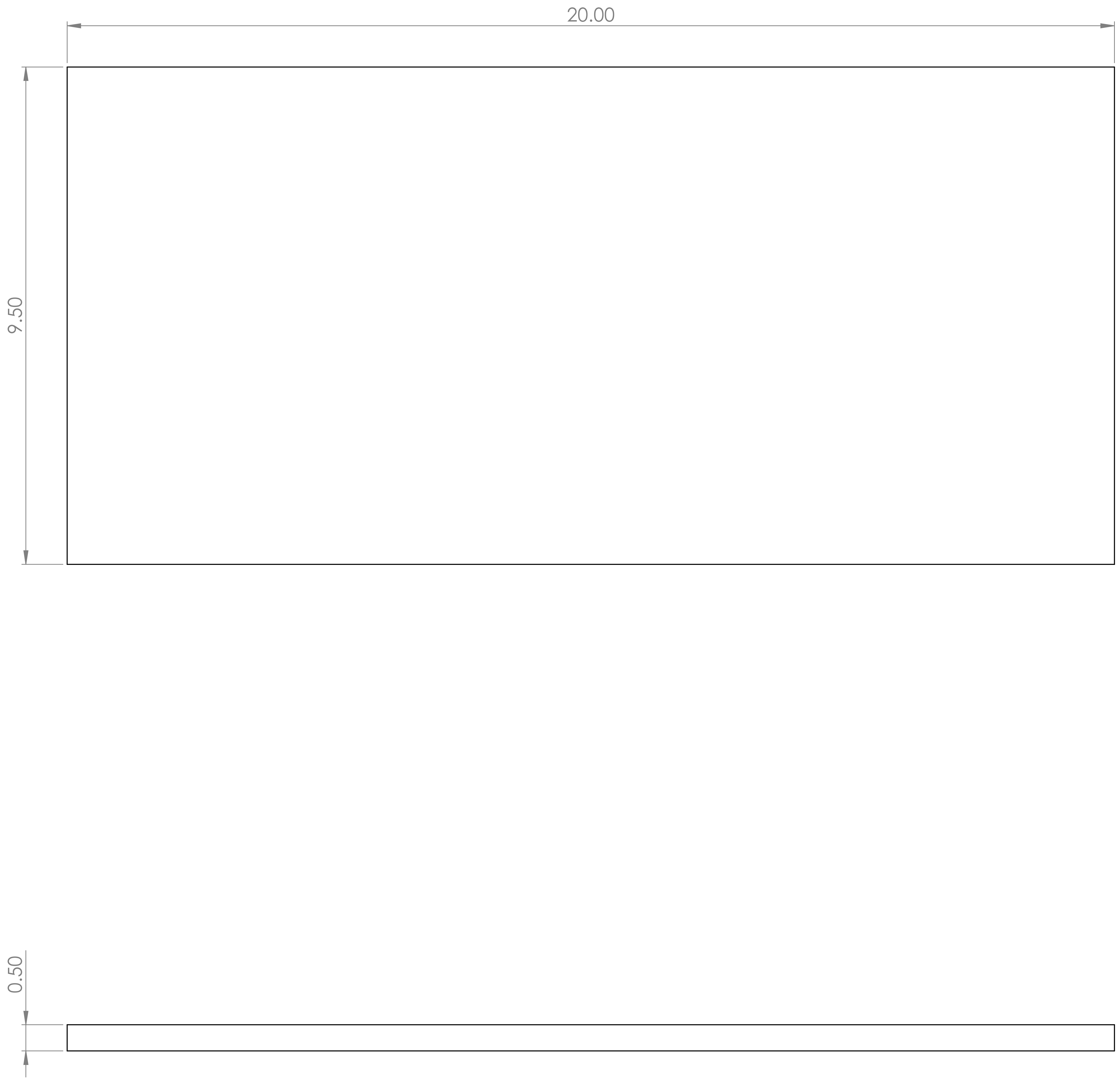

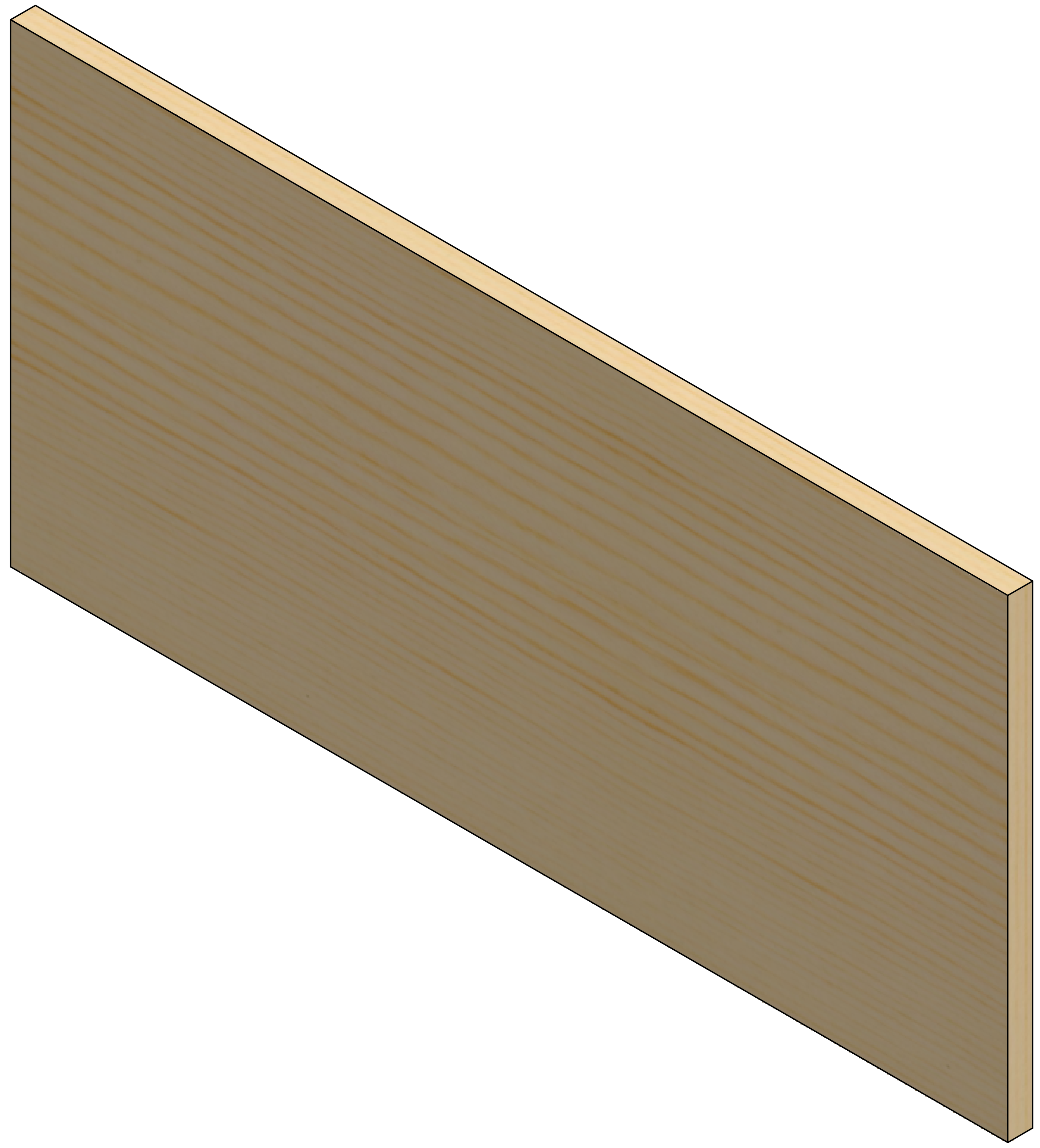

UNLESS OTHERWISE SPECIFIED: DIMENSIONS ARE IN MILLIMETERS SURFACE FINISH: TOLERANCES: LINEAR: ANGULAR:	FINISH:		DEBURR AND BREAK SHARP EDGES		DO NOT SCALE DRAWING	REVISION
	NAME	SIGNATURE	DATE		TITLE:	
DRAWN	NM		04/06/22		Long Side Enclosure	
CHK'D	JB		04/27/22			
APPV'D						
MFG						
Q.A				MATERIAL: Pine	DWG NO. Spray Assem 06	A2
				WEIGHT:	SCALE:1:2	SHEET 1 OF 1

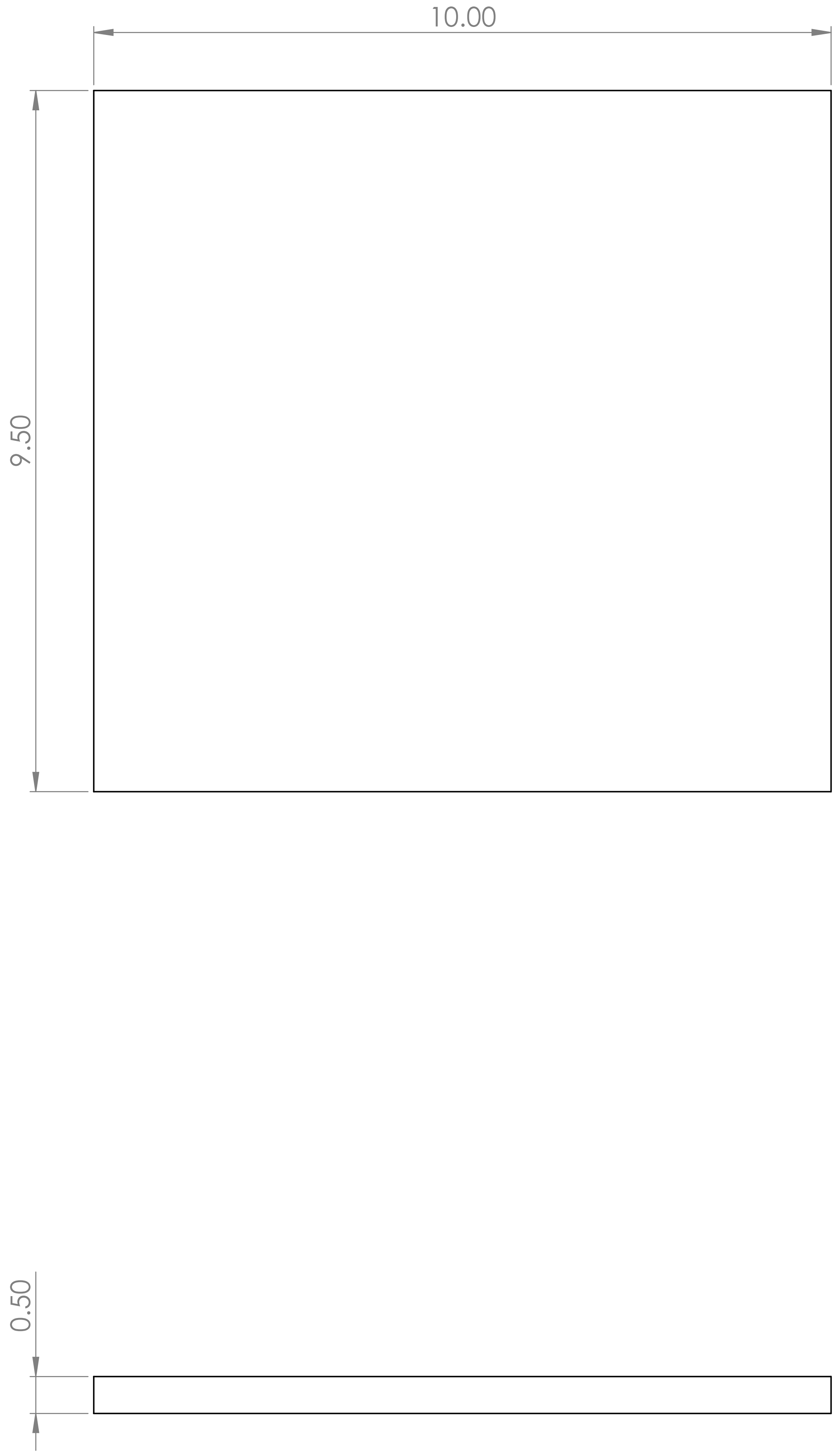

UNLESS OTHERWISE SPECIFIED: DIMENSIONS ARE IN MILLIMETERS SURFACE FINISH: TOLERANCES: LINEAR: ANGULAR:	FINISH:		DEBURR AND BREAK SHARP EDGES	DO NOT SCALE DRAWING	REVISION
	NAME	SIGNATURE	DATE	TITLE:	
DRAWN	NM		04/06/22	Short Wood Enclosure	
CHK'D	JB		04/27/22		
APPV'D					
MFG					
Q.A			MATERIAL: Pine	DWG NO. Spray Assem 07	A2
			WEIGHT:	SCALE:1:2	SHEET 1 OF 1

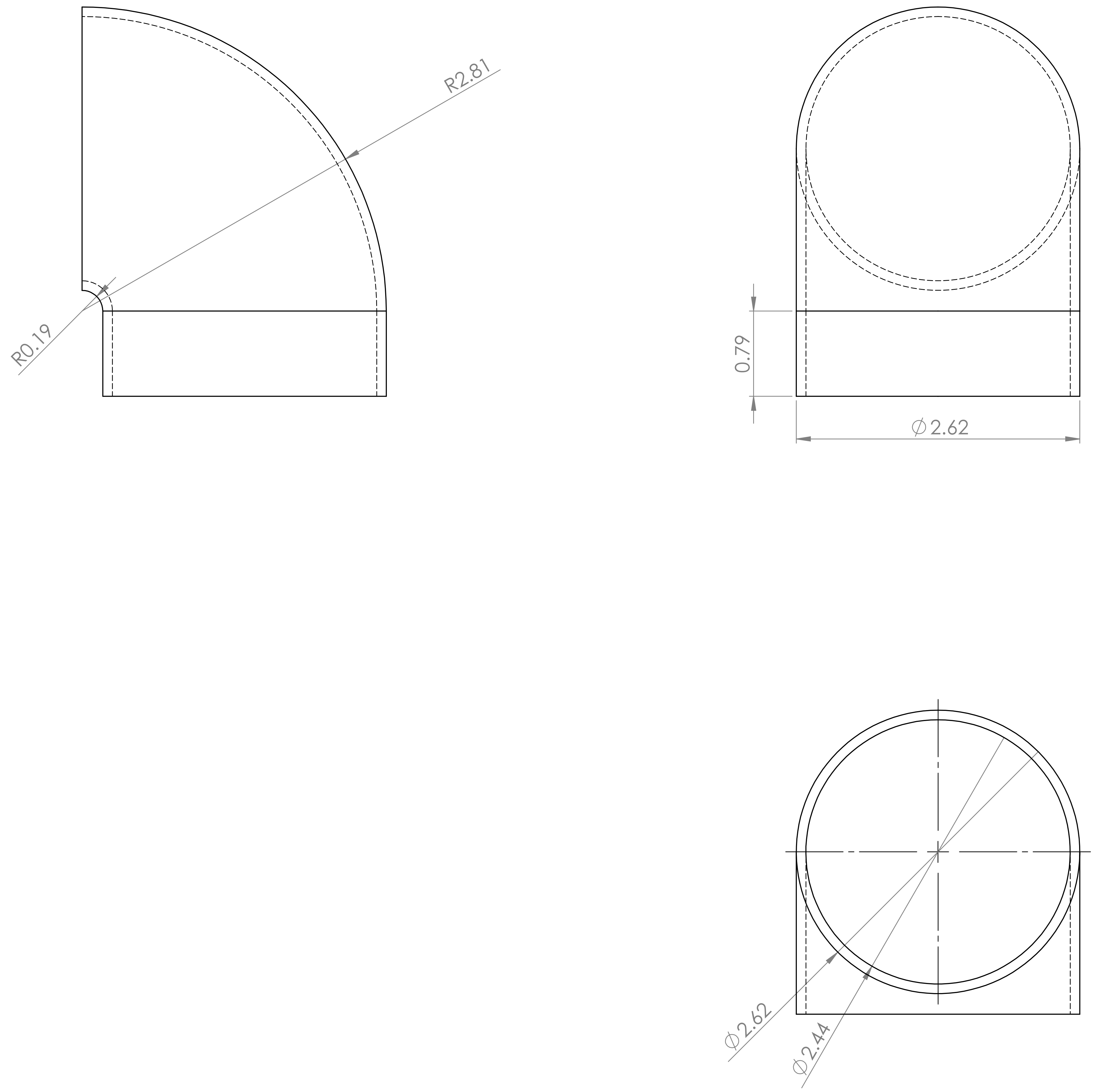

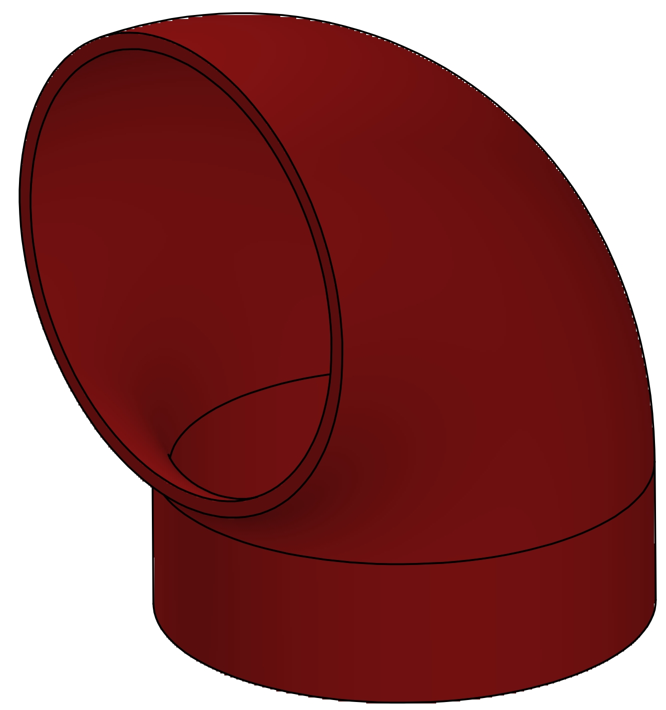

UNLESS OTHERWISE SPECIFIED: DIMENSIONS ARE IN MILLIMETERS SURFACE FINISH: TOLERANCES: LINEAR: ANGULAR:		FINISH:	DEBURR AND BREAK SHARP EDGES	DO NOT SCALE DRAWING	REVISION	
	NAME	SIGNATURE	DATE	TITLE: Tank Elbow		
DRAWN	NM		04/06/22			
CHK'D	JB		04/27/22			
APPV'D						
MFG						
Q.A				MATERIAL: ABS	DWG NO. Spray Assem 08	A2
				WEIGHT:	SCALE:1:1	SHEET 1 OF 1

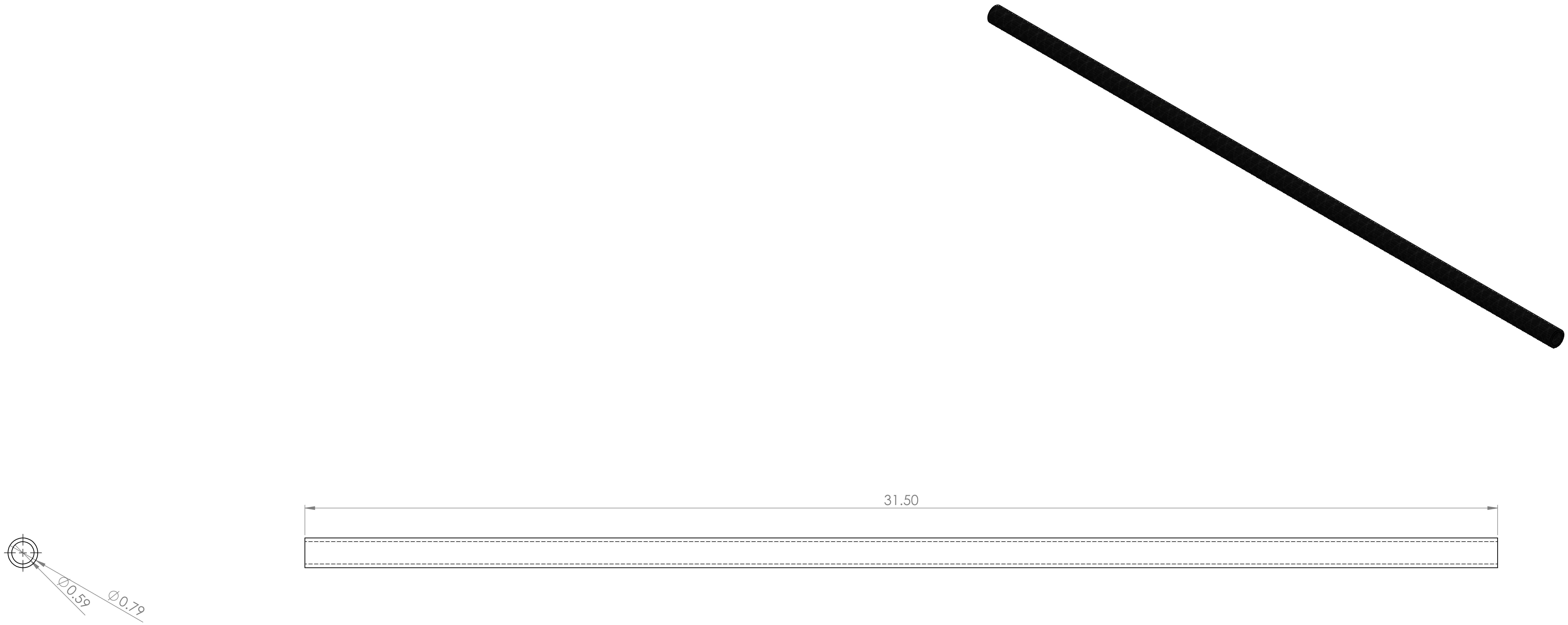

UNLESS OTHERWISE SPECIFIED: DIMENSIONS ARE IN MILLIMETERS SURFACE FINISH: TOLERANCES: LINEAR: ANGULAR:	FINISH:	DEBURR AND BREAK SHARP EDGES	DO NOT SCALE DRAWING	REVISION	
	NAME	SIGNATURE	DATE	TITLE:	Spraybar Bar
DRAWN	NM		04/06/22		
CHK'D	JB		04/27/22		
APPV'D					
MFG					
Q.A				MATERIAL: Hexcel AS4C (3000 Filaments)	DWG NO. Spray Assem 09 — A2
				WEIGHT:	SCALE:1:5 — SHEET 1 OF 1

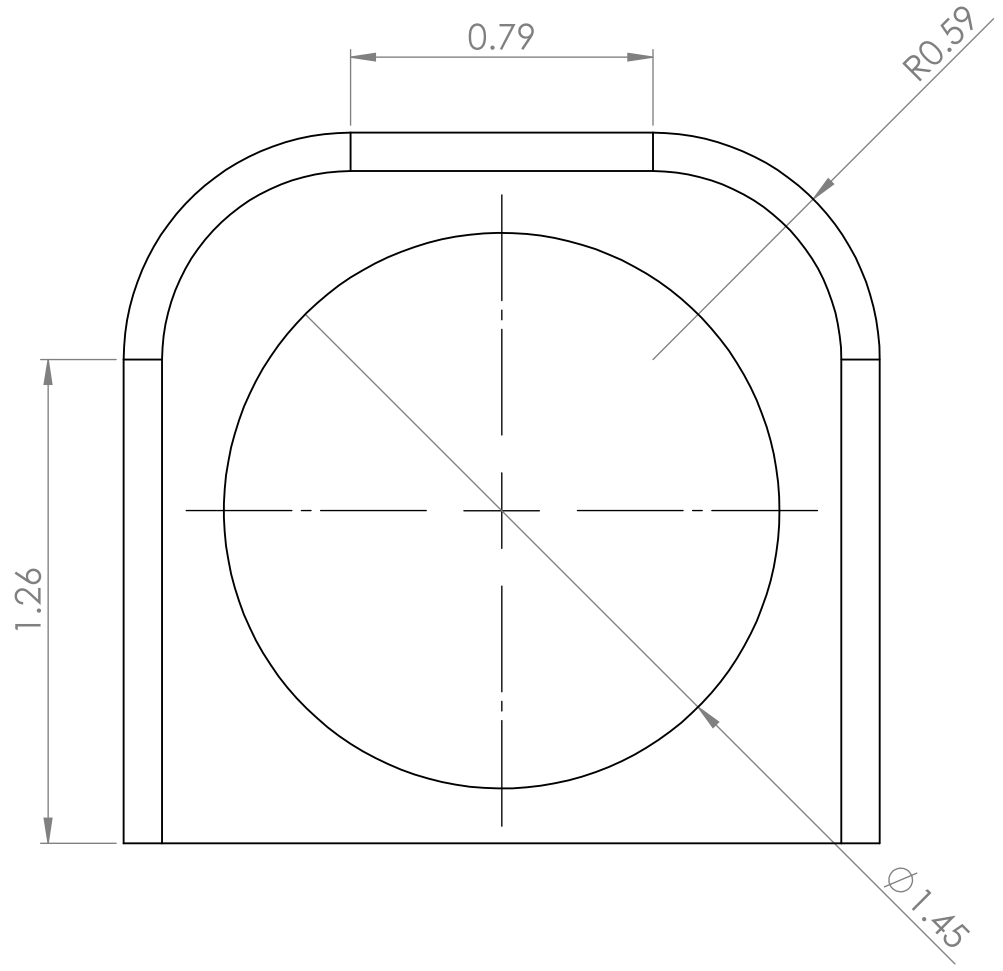

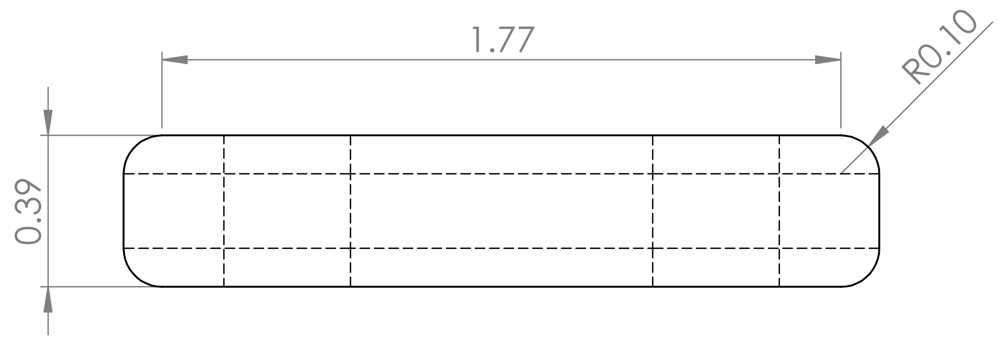

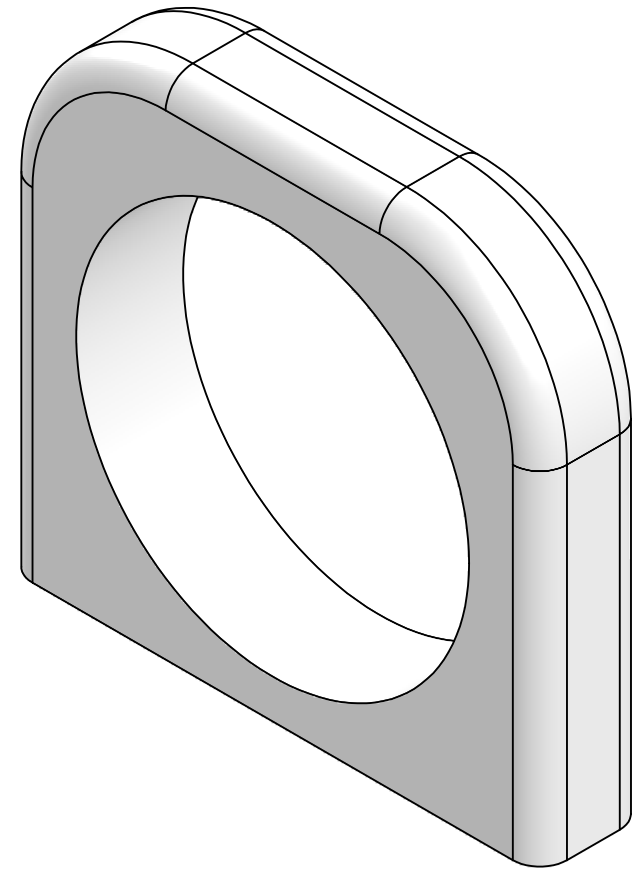

UNLESS OTHERWISE SPECIFIED: DIMENSIONS ARE IN MILLIMETERS SURFACE FINISH: TOLERANCES: LINEAR: ANGULAR:	FINISH:		DEBURR AND BREAK SHARP EDGES	DO NOT SCALE DRAWING	REVISION	
	NAME	SIGNATURE	DATE	TITLE: Spraybar Mounting Bracket		
DRAWN	NM		04/06/22			
CHK'D	JB		04/27/22			
APPV'D						
MFG						
Q.A			MATERIAL: ABS	DWG NO. Spray Assem 10	A2	
			WEIGHT:	SCALE:2:1	SHEET 1 OF 1	

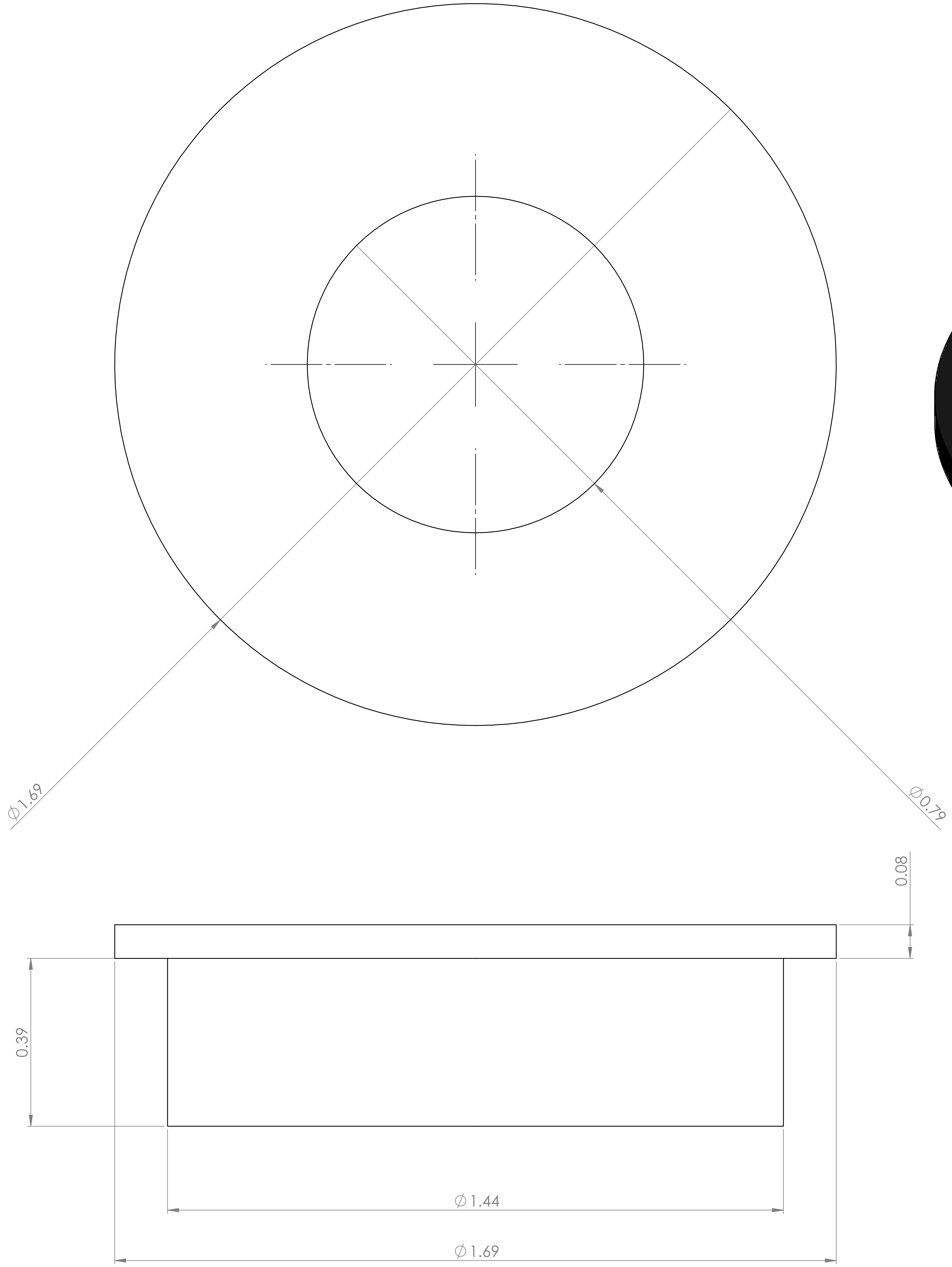

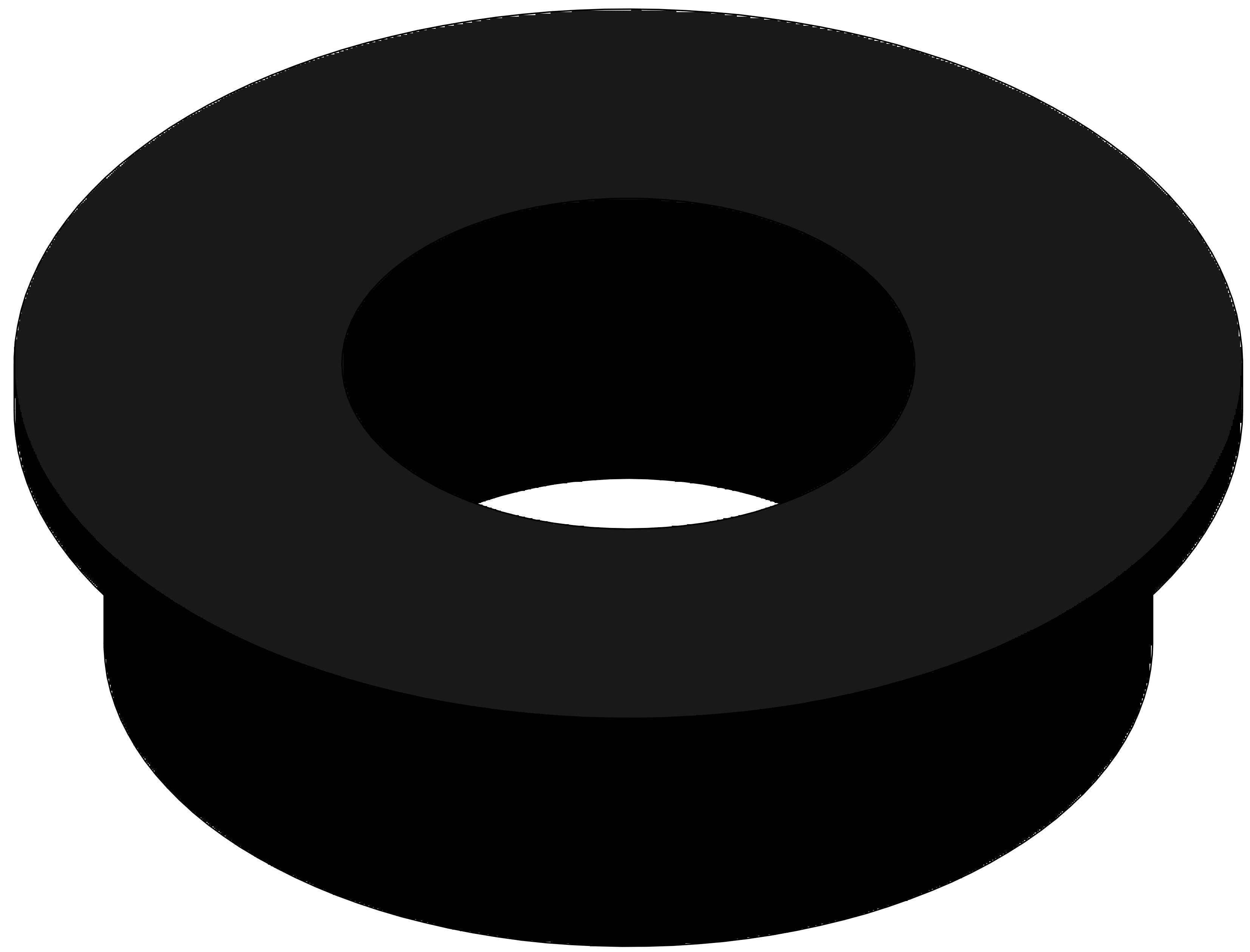

UNLESS OTHERWISE SPECIFIED: DIMENSIONS ARE IN MILLIMETERS SURFACE FINISH: TOLERANCES: LINEAR: ANGULAR:	FINISH:			DEBURR AND BREAK SHARP EDGES	DO NOT SCALE DRAWING	REVISION
	NAME	SIGNATURE	DATE		TITLE: Flange	
DRAWN	NM		04/06/22			
CHK'D	JB		04/27/22			
APPV'D						
MFG						
Q.A				MATERIAL: ABS	DWG NO. Spray Assem 11	A2
				WEIGHT:	SCALE:5:1	SHEET 1 OF 1

ITEM NO.	PART NUMBER	DESCRIPTION	QTY.
1	Chain Profile 020822	Chain Dimension Sketch	1
2	6261K241	Adding Link for ANSI Number 35 Single Strand Roller Chain	35
3	6261K191	Connecting Link for ANSI Number 35 Single Strand Roller Chain	35

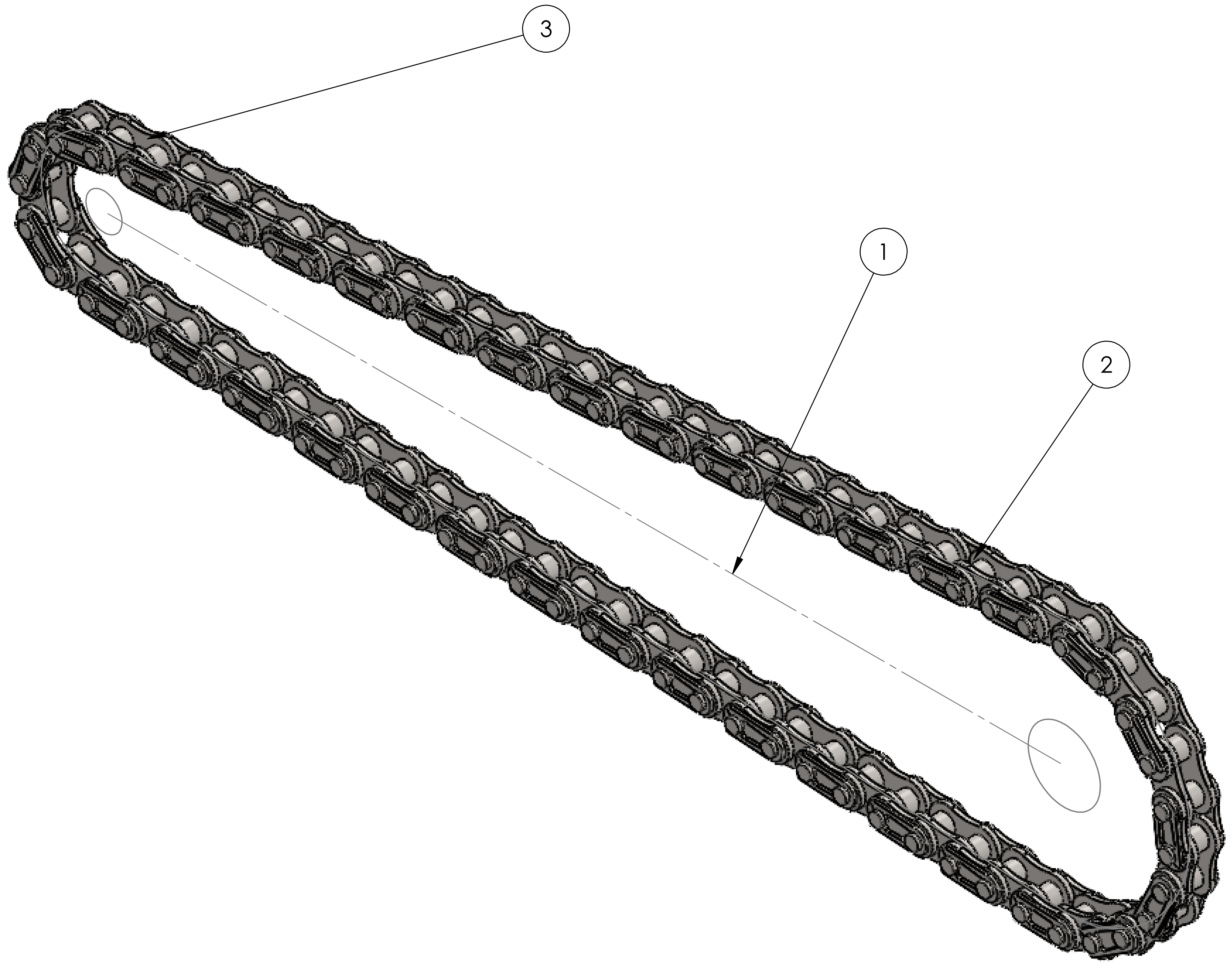

UNLESS OTHERWISE SPECIFIED:
DIMENSIONS ARE IN MILLIMETERS
SURFACE FINISH:
TOLERANCES:
LINEAR:
ANGULAR:

FINISH:

DEBURR AND BREAK SHARP EDGES

DO NOT SCALE DRAWING

REVISION

	NAME	SIGNATURE	DATE
DRAWN	SRK		4/21/22
CHK'D	JP		4/27/22
APPV'D			
MFG			
Q.A			

MATERIAL:

WEIGHT:

TITLE:

Chain Assembly

DWG NO.
Transimission Assem 01 - Chain Assembly

A2

SCALE:1:2

SHEET 1 OF 1

ITEM NO.	PART NUMBER	DESCRIPTION	QTY.
1	Trasmission Assem 03	Axles	1
2	Wheel Assem 01	Wheel	1
3	Wheel Assem 02	Wheel Hub	2
4	95462A031	Medium-Strength Steel Hex Nut	8
5	95475A642	Low-Strength Threaded Rods	4
6	tire rubber		1
7	Wheel Assem 03	Shaft Collar	1

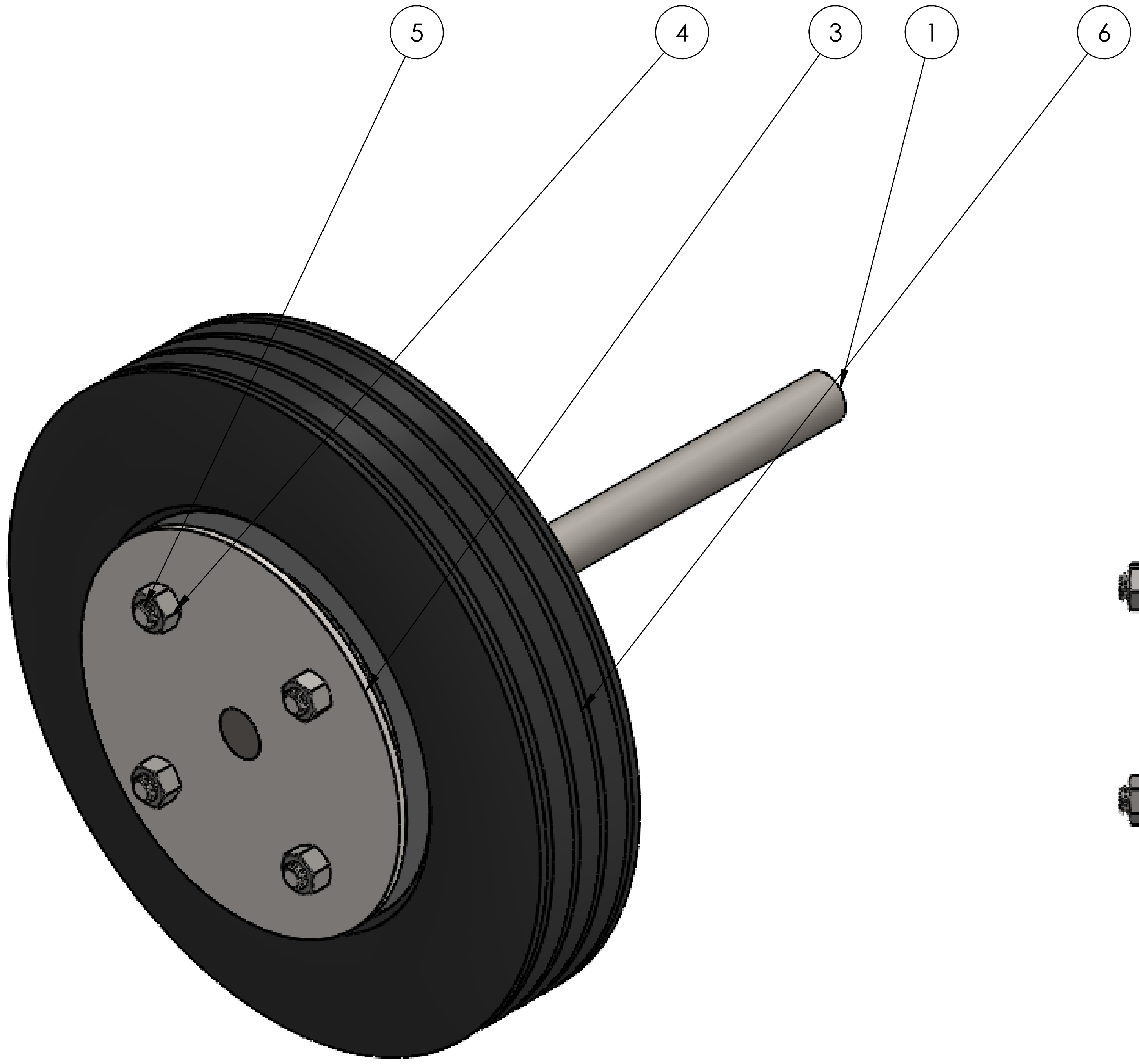

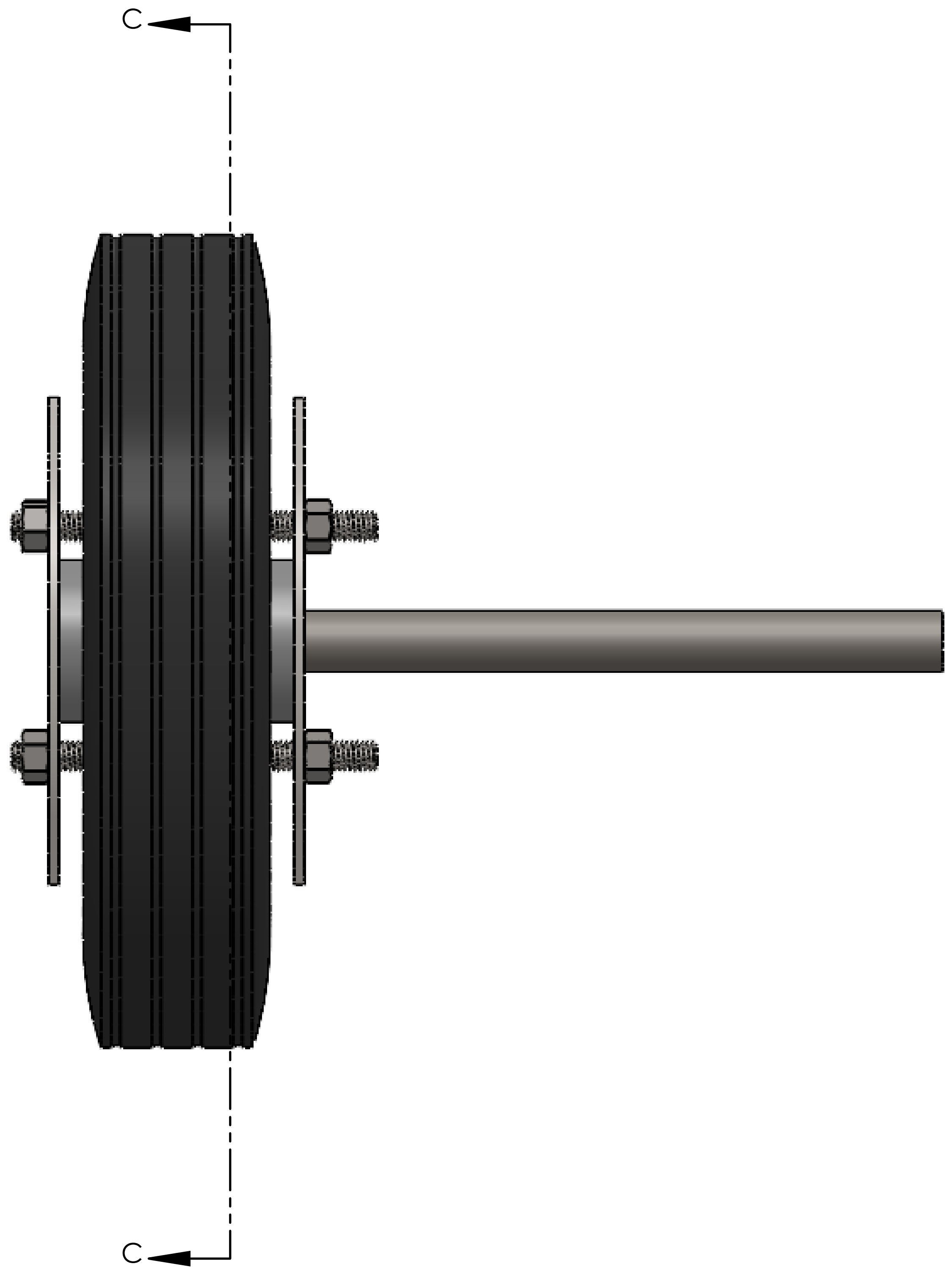

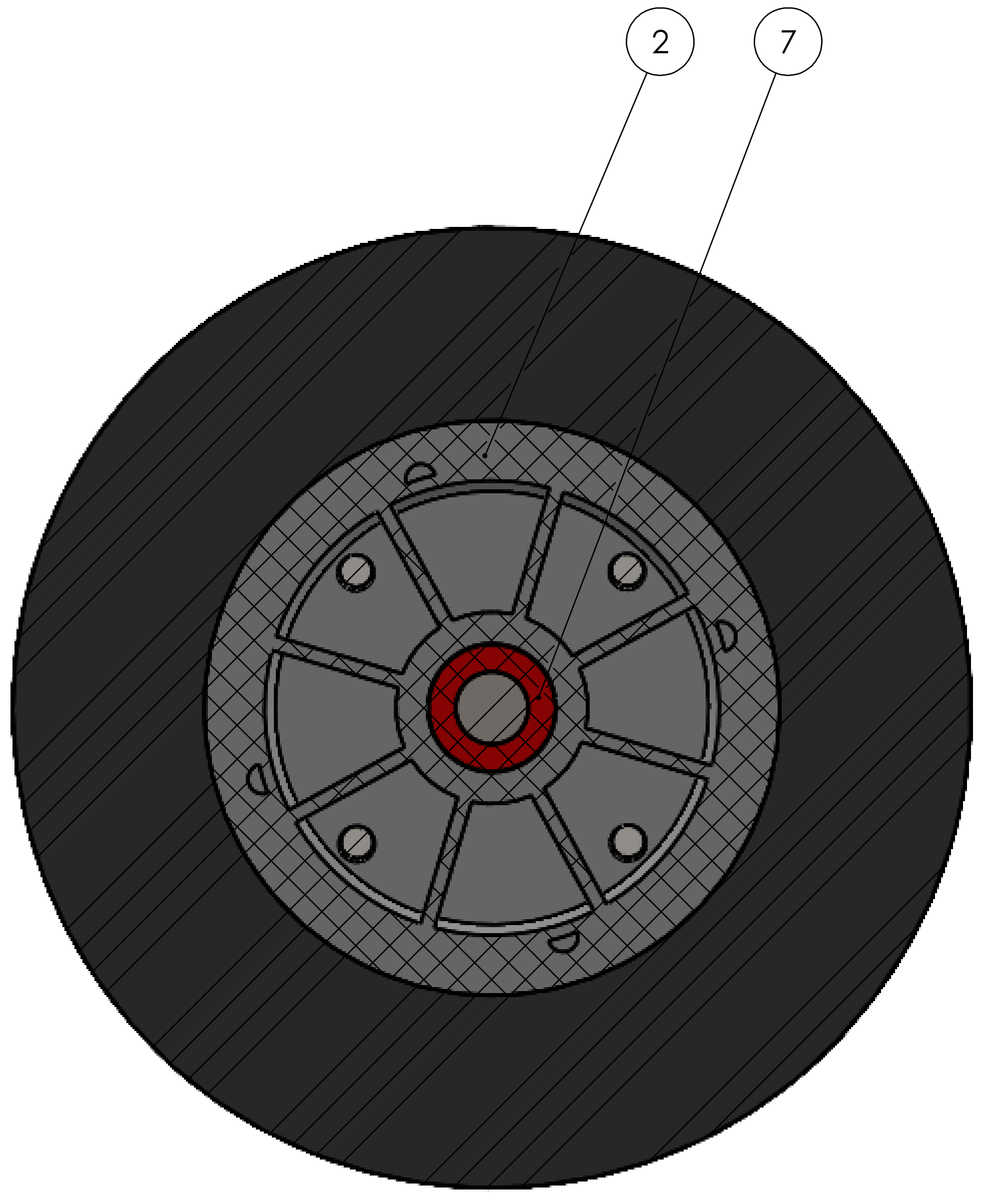

SECTION C-C
SCALE 1 : 2

UNLESS OTHERWISE SPECIFIED: DIMENSIONS ARE IN MILLIMETERS SURFACE FINISH: TOLERANCES: LINEAR: ANGULAR:	FINISH:		DEBURR AND BREAK SHARP EDGES	DO NOT SCALE DRAWING	REVISION	
	NAME	SIGNATURE	DATE	TITLE: Wheel Assem		
DRAWN	SRK		4/12/22			
CHK'D	JP		4/27/22			
APPV'D						
MFG						
Q.A			MATERIAL:	DWG NO. Trasnmission Assem 02 - Wheel Assem	A2	
			WEIGHT:	SCALE:1:4	SHEET 1 OF 1	

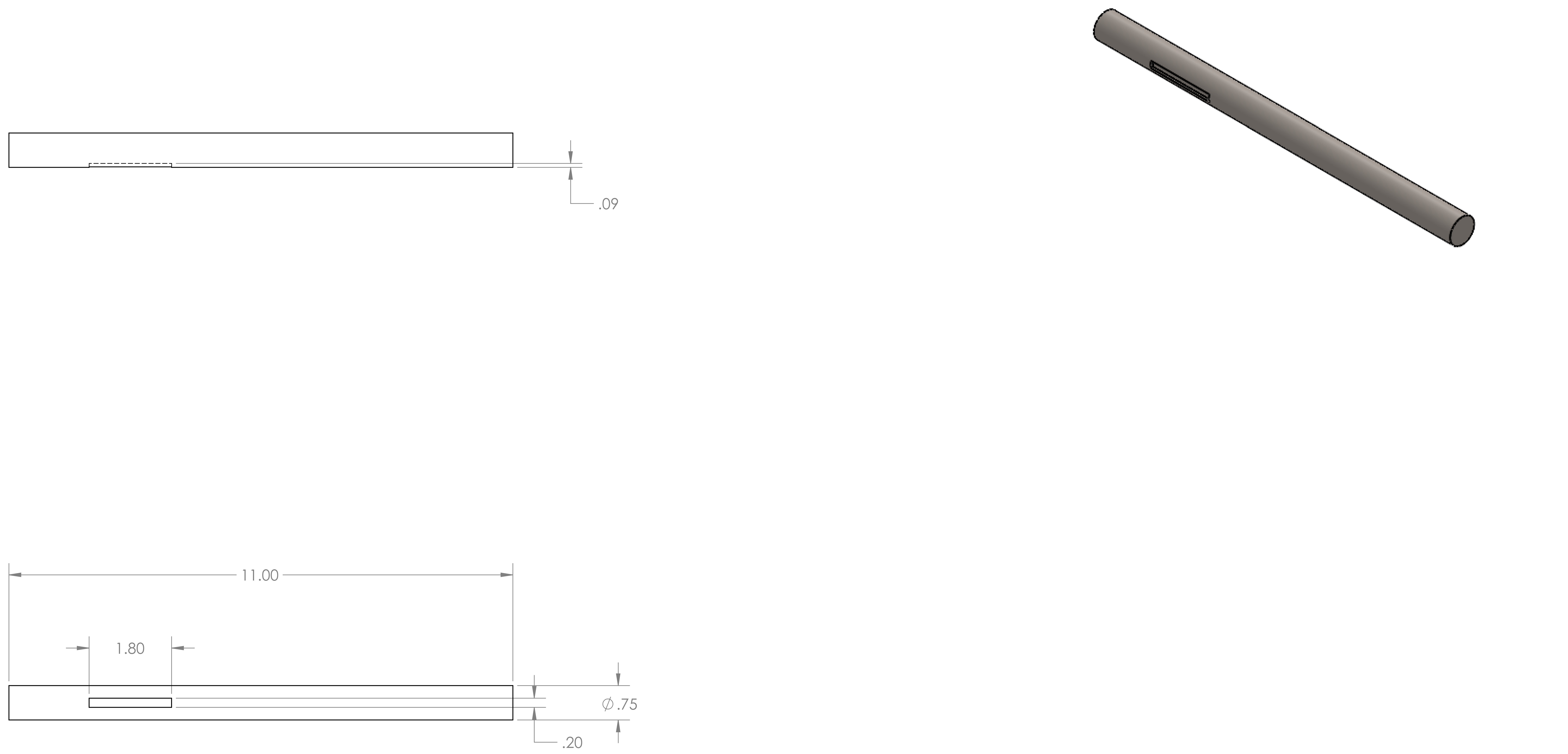

UNLESS OTHERWISE SPECIFIED:
DIMENSIONS ARE IN MILLIMETERS
SURFACE FINISH:
TOLERANCES:
LINEAR:
ANGULAR:

FINISH:

DEBURR AND BREAK SHARP EDGES

DO NOT SCALE DRAWING

REVISION

	NAME	SIGNATURE	DATE
DRAWN	SRK		4/21/22
CHK'D	JP		4/27/22
APPV'D			
MFG			
Q.A			

TITLE: Axle

MATERIAL: Alloy Steel

DWG NO. Transmission Assem 03 - Axle

A2

WEIGHT:

SCALE:1:2

SHEET 1 OF 1

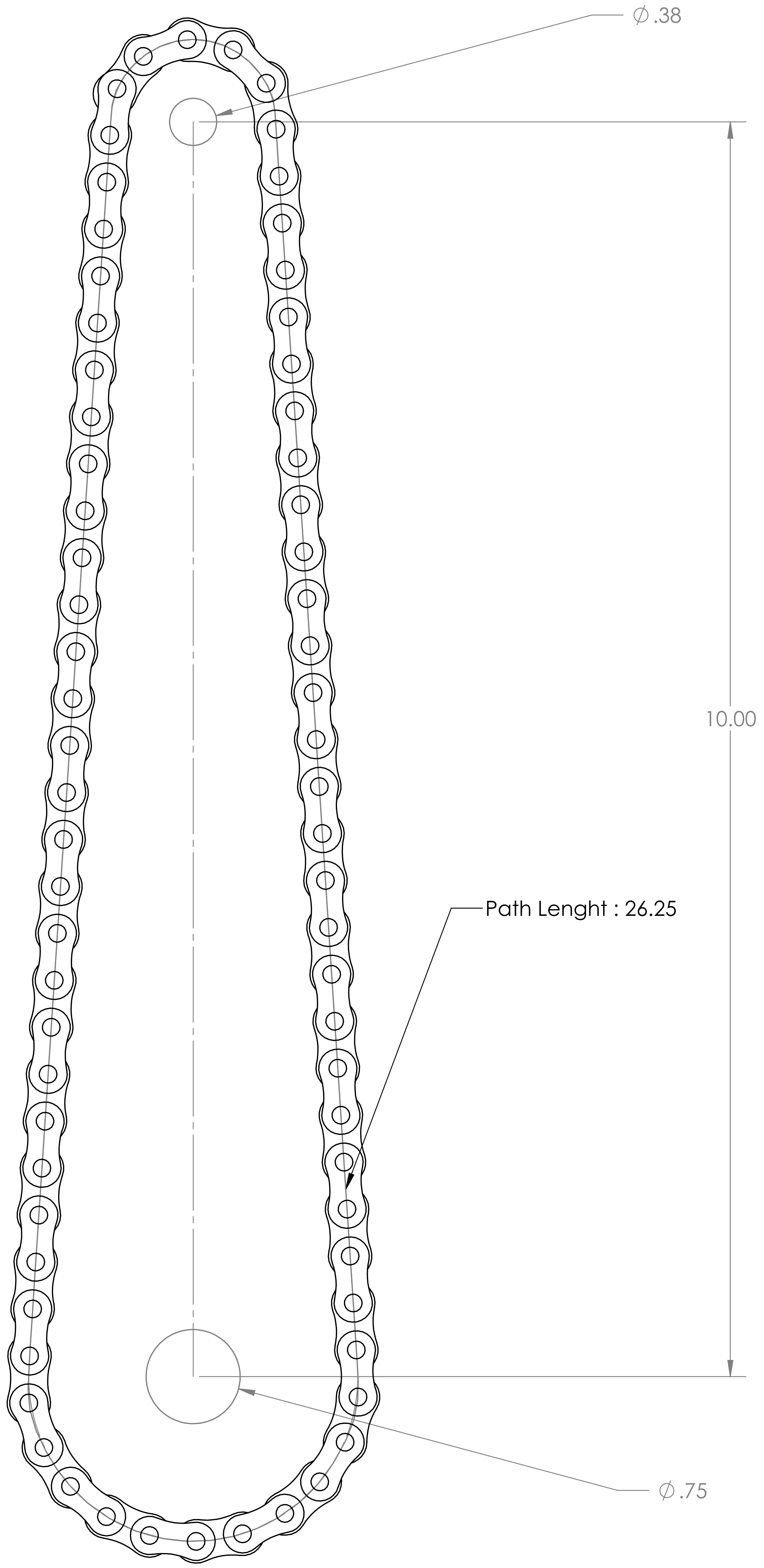

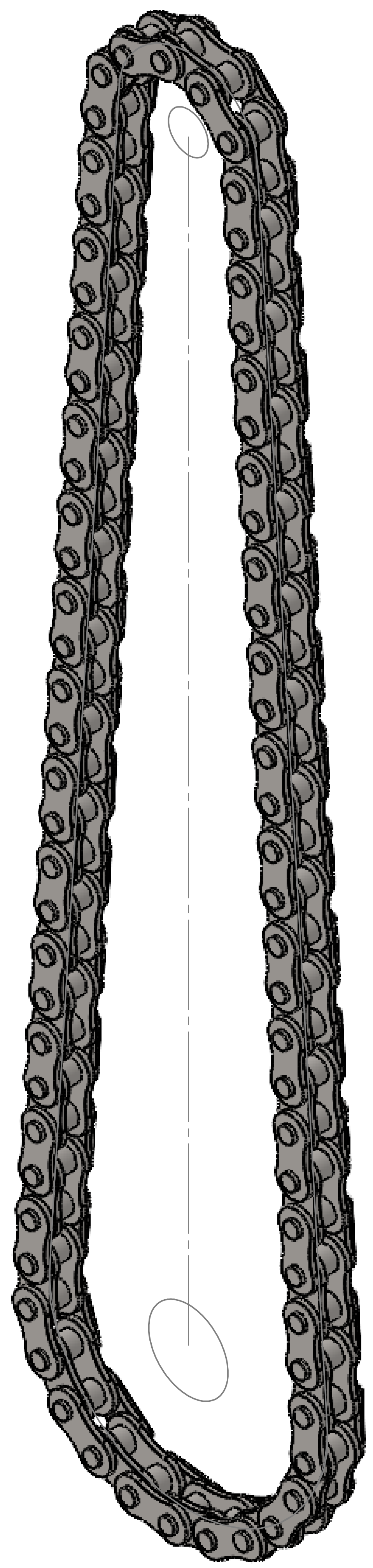

UNLESS OTHERWISE SPECIFIED: DIMENSIONS ARE IN MILLIMETERS SURFACE FINISH: TOLERANCES: LINEAR: ANGULAR:	FINISH:			DEBURR AND BREAK SHARP EDGES	DO NOT SCALE DRAWING	REVISION
	NAME	SIGNATURE	DATE		TITLE: Chain Dimension	
DRAWN	SRK		4/21/22			
CHK'D	JP		4/27/22			
APPV'D						
MFG						
Q.A				MATERIAL:	DWG NO. Transmission Assem 04 - Chain Dimension	A2
				WEIGHT:	SCALE:1:2	SHEET 1 OF 1

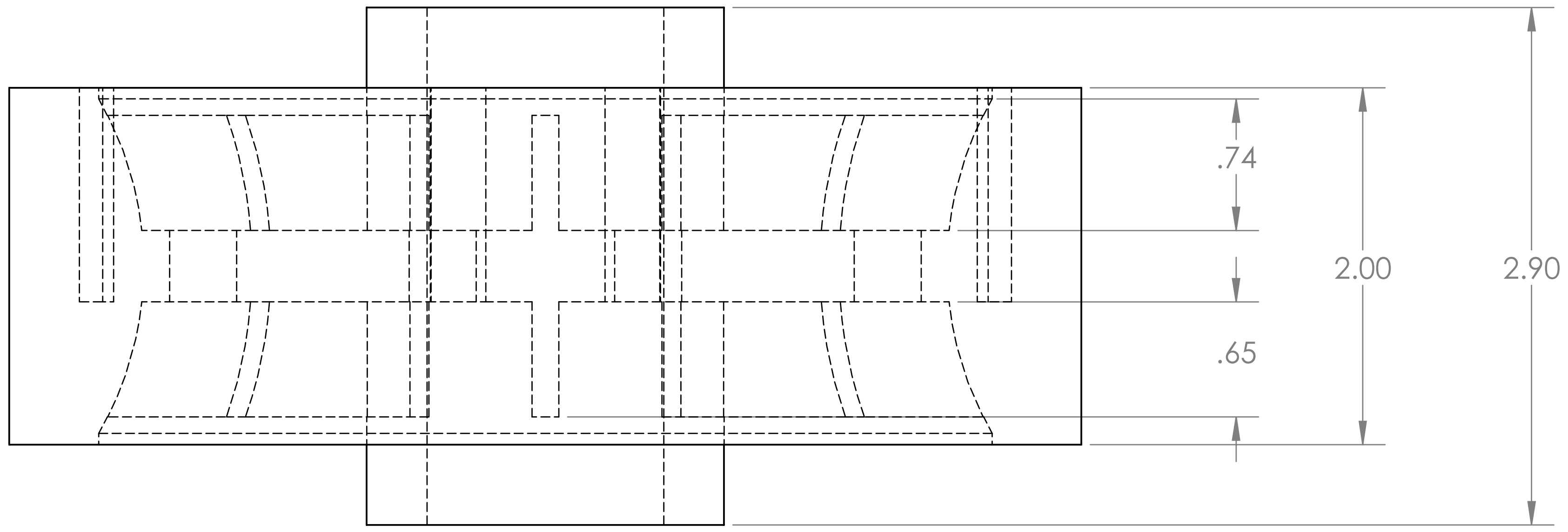

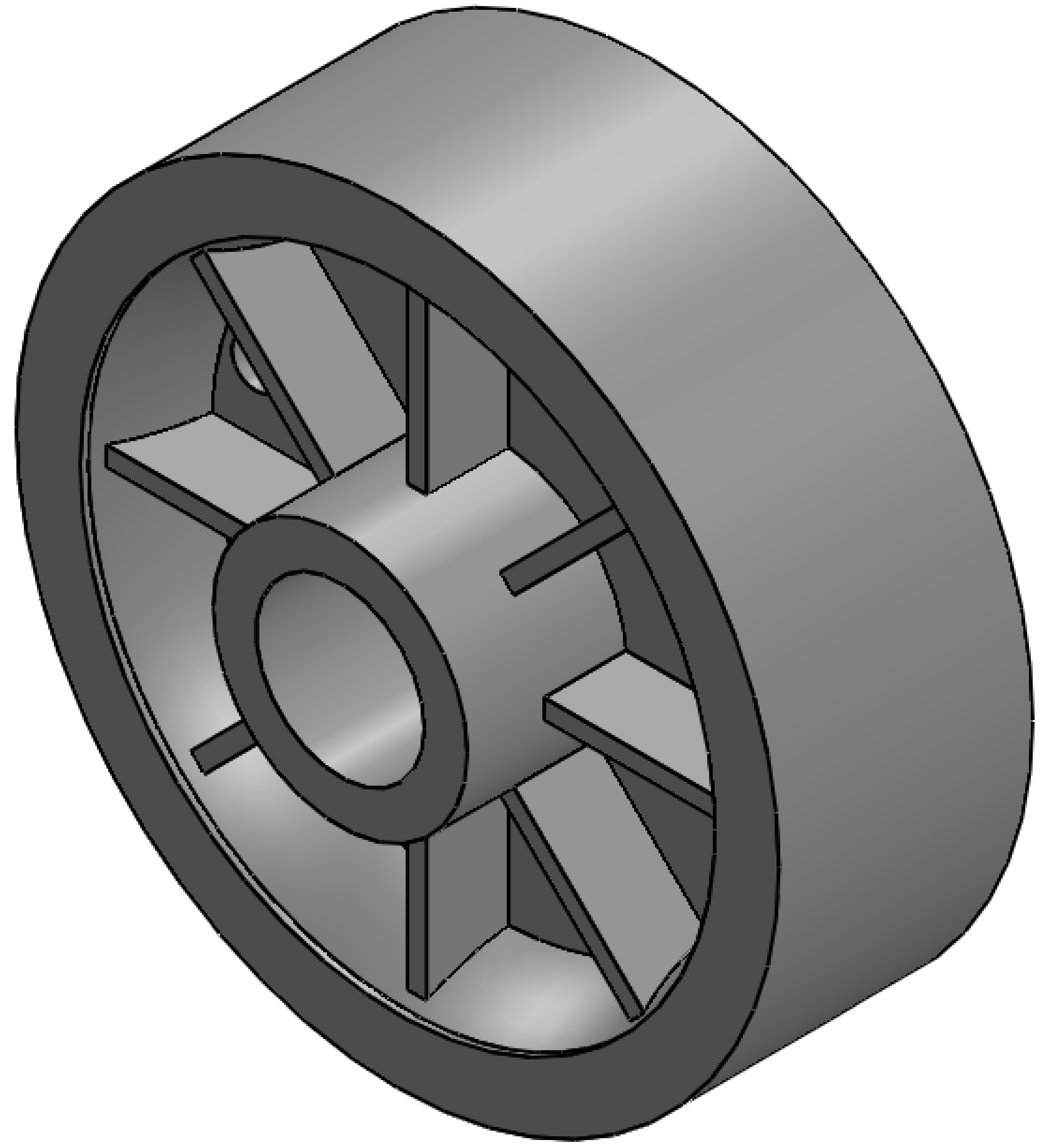

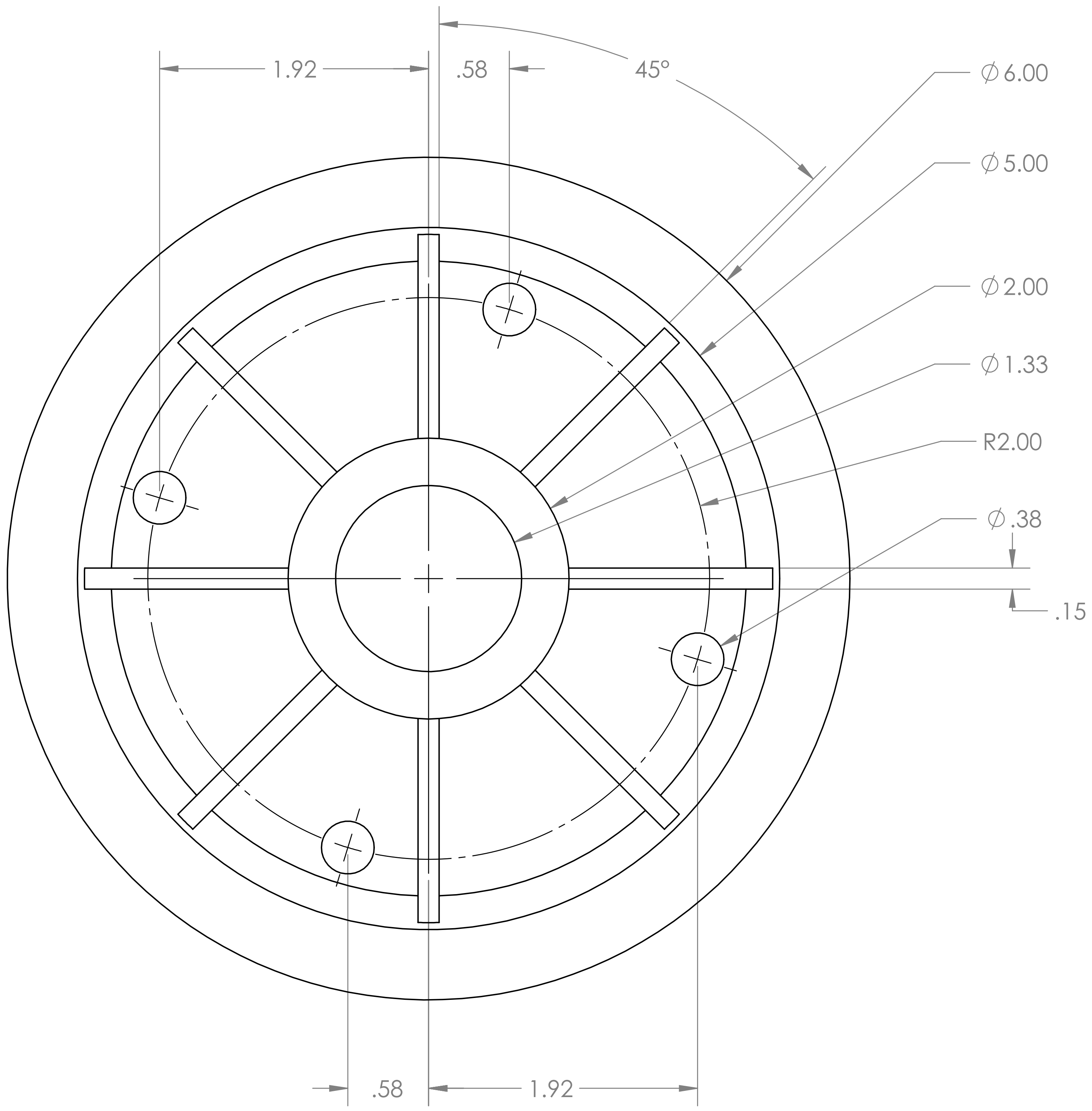

UNLESS OTHERWISE SPECIFIED: DIMENSIONS ARE IN MILLIMETERS SURFACE FINISH: TOLERANCES: LINEAR: ANGULAR:	FINISH:			DEBURR AND BREAK SHARP EDGES	DO NOT SCALE DRAWING	REVISION
	NAME	SIGNATURE	DATE		TITLE:	Wheel
DRAWN	SRK		04/12/22			
CHK'D	JB		04/21/22			
APPV'D						
MFG						
Q.A				MATERIAL: ABS	DWG NO. Wheel Assem 01- Wheel	A2
				WEIGHT:	SCALE:1:1	SHEET 1 OF 1

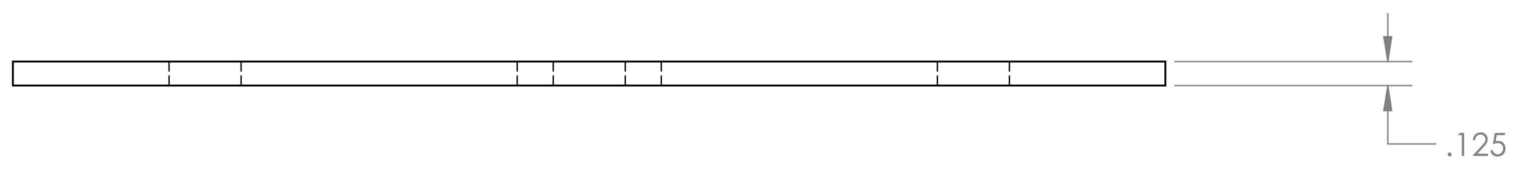

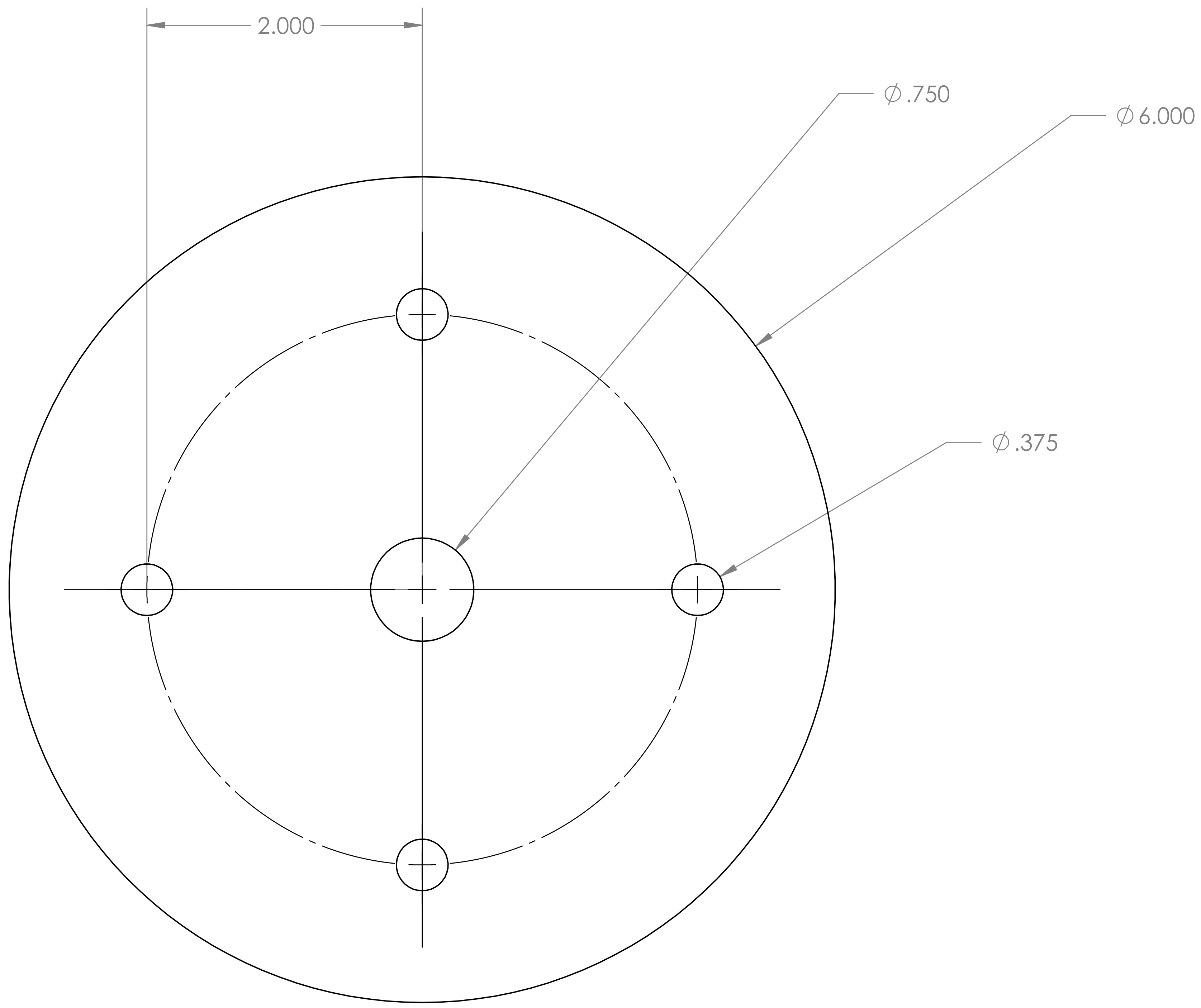

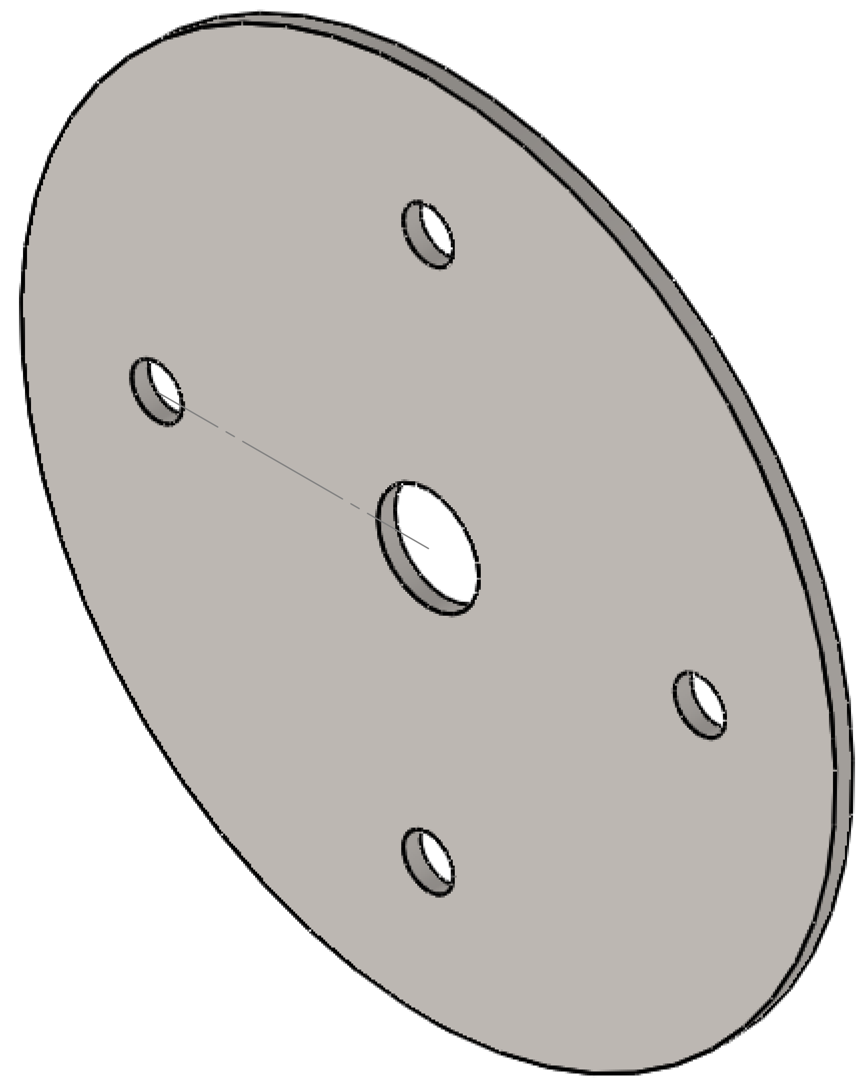

UNLESS OTHERWISE SPECIFIED: DIMENSIONS ARE IN MILLIMETERS SURFACE FINISH: TOLERANCES: LINEAR: ANGULAR:	FINISH:			DEBURR AND BREAK SHARP EDGES	DO NOT SCALE DRAWING	REVISION
	NAME	SIGNATURE	DATE		TITLE:	
DRAWN	SRK		04/06/22		Wheel Hub	
CHK'D	JB		04/21/22			
APPV'D						
MFG						
Q.A				MATERIAL: Plain Carbon Steel	DWG NO. Wheel Assem 02	A2
				WEIGHT:	SCALE:1:1	SHEET 1 OF 1

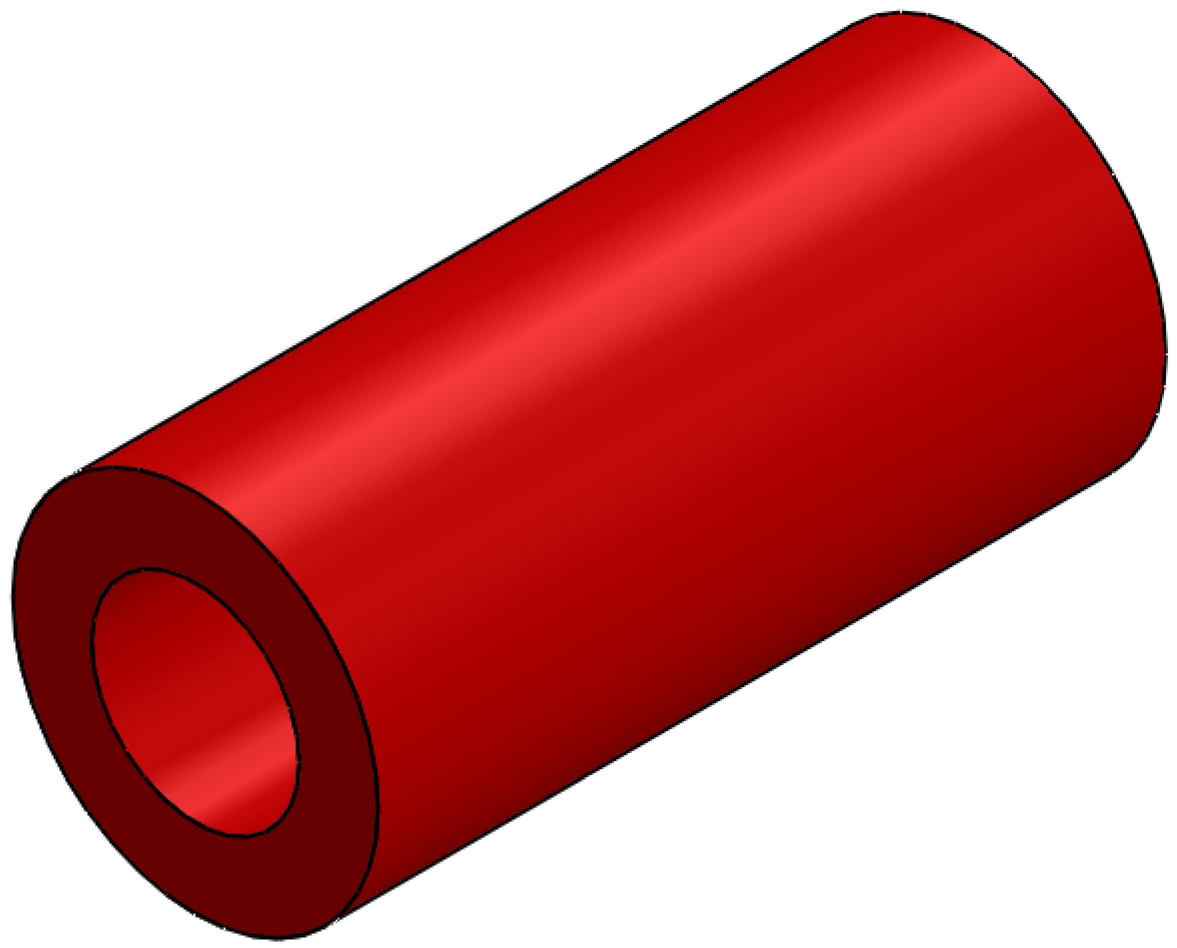

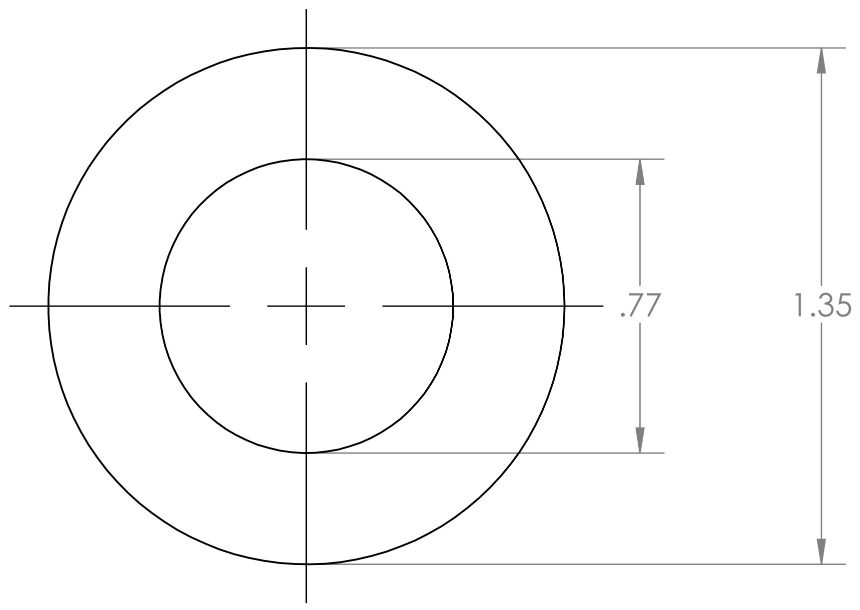

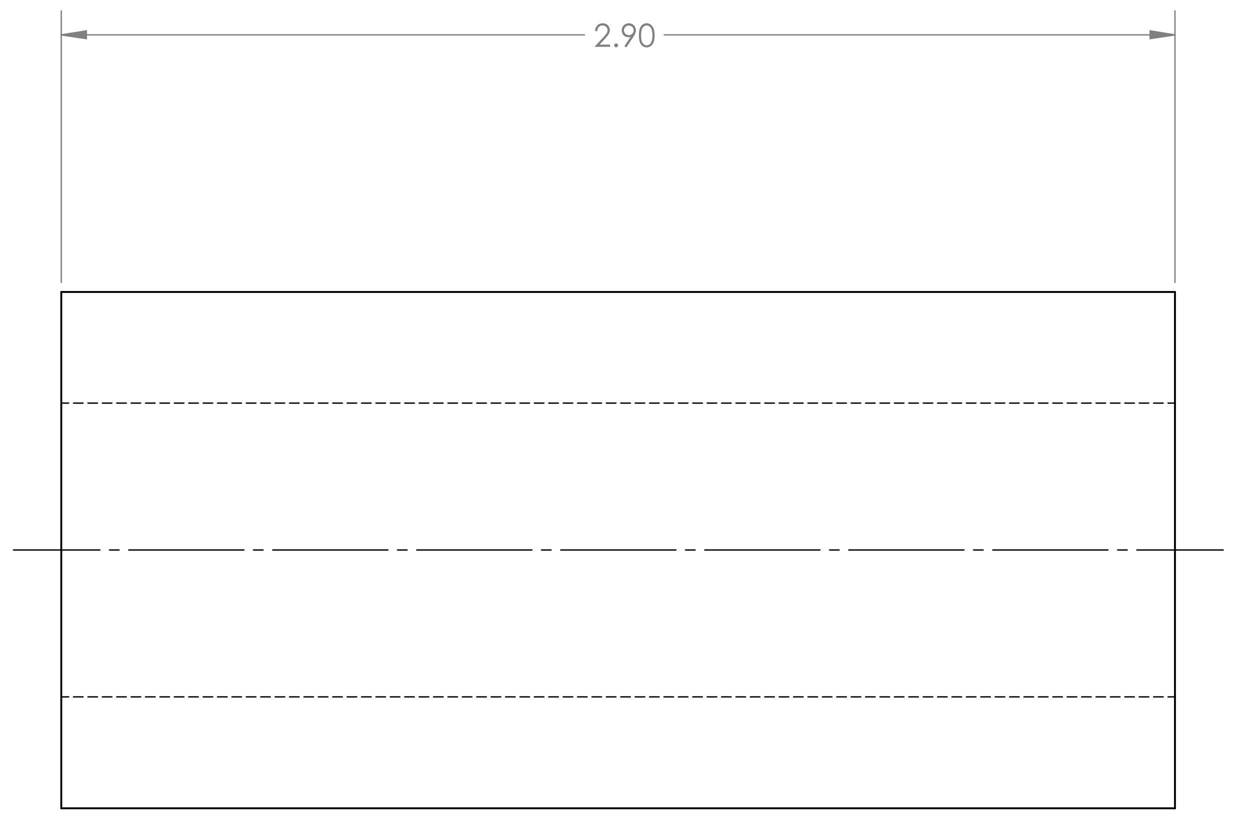

UNLESS OTHERWISE SPECIFIED: DIMENSIONS ARE IN MILLIMETERS SURFACE FINISH: TOLERANCES: LINEAR: ANGULAR:			FINISH:			DEBURR AND BREAK SHARP EDGES	DO NOT SCALE DRAWING	REVISION
	NAME	SIGNATURE	DATE				TITLE: Shaft Collar	
DRAWN	CZ		04/06/22					
CHK'D	JB		04/21/22					
APPV'D								
MFG								
Q.A				MATERIAL: ABS			DWG NO. Wheel Assem 03	A2
				WEIGHT:			SCALE:2:1	SHEET 1 OF 1